Creative Design and Data Science Center

Annual Report

Achievements in **FY2022**

Akita International University

CreDDS Center - Concept / Purpose / Projects

[Denomination] Creative Design and Data Science Center (CreDDS-C)

[Establishment] April 1, 2022

[Concept]

Established as part of AIU's 4th Medium Term Plan (2022~2027), which aims to transform AIU's research, education and public engagement in the context of the pedagogic aspirations of Applied International Liberal Arts (AILA).

Intended to be a central driver of innovative research, education and public engagement under the Institute for Applied International Liberal Arts (AILA Institute, est. March 2022).

Will serve AILA Pedagogy from Levels 100~400 (undergraduate) and beyond (postgraduate).

Will have a synergistic mutually supportive relationship with the Active Learning Center and the Center for Collaborative Research and Outreach with all three centers providing the impetus for the transformations anticipated under AILA.

[Purpose]

Designing and executing projects to nurture inspiring leaders who subscribe to the AILA ideals of integrating profound thought with decisive action in a transnational, transdisciplinary context.

Meeting future needs of society and challenges facing the earth's environment while consolidating on AIU's strengths built up thus far contributing to pedagogic excellence and local-global partnerships.

Integrating transformative technology with the essence of humanity to create caring societies and resilient communities which will contribute to furthering universal values of sustainability and inclusion.

Adding value (environmental, social and economic) through innovative solutions by coupling evidence with insight to achieve the above through the medium of "propulsive projects".

[Projects]

CreDDS Center Projects will integrate evidence with insight through the medium of "propulsive projects", designed to add environmental, social and economic value.

A propulsive project is defined as one which leads to a cluster of affiliated projects whose mutually synergistic relationship with each other could lead to an exponential increase in the above value propositions.

The above projects are to be designed with both a "bird's eye" and a "worm's eye" view, namely, they will seek solutions to global grand challenges which have acute local impacts on communities and the environment.

The project entry point will be challenges faced by local communities but in seeking solutions, the projects will explore collaborative national and transnational partnerships with institutions in AIU's international collaborative ecosystem (ICE).

CreDDS Center Report

Achievements in FY2022

Contents

Current Researchers and Staff Members

Director

Select Professor: Dr. Akitoshi SEIYAMA (Doctor of Science)
Research Field: Medical Science, Biomedical Engineering, Data Science

Coordinator

Associate Professor: Dr. Norikazu TAWARA (Ph.D., Economics)
Research Field: Labor and Search Theory, Economic Dynamics
Incentives and Markets

Visiting Researcher

Dr. Sayaka OKAHASHI (Ph.D.)

Dr. Satoshi SASAYAMA (Doctor of Medical Science)

Dr. Tatsuro MIURA (Doctor of Human Health Sciences)

Research Coordinator

M.A. Travis SENZAKI (Master of Asian Studies)
Area Responsibility: International Collaboration

Dr. Noriko NARISAWA (Doctor of Area Studies)
Research Field: Anthropology, Social Research, African Studies

Staff (Concurrent Office: Research and Community Outreach Services)

Yoko ABE (Director)

Yoshinori SAKAMOTO (Head)

Yuka OKURA

Visiting Researcher
Dr. Sayaka OKAHASHI (Ph.D.)

Present affiliation and position

National Center for Geriatrics and Gerontology
Center for Gerontology and Social Science
Senior Research Fellow

Research field and importance of collaboration

Dr. Okahashi aims to realize ideal community-based comprehensive care. To achieve this goal, she is conducting observational and interventional studies that contribute toward solving the issues for older adults, such as preventing the adverse prognosis of dementia and improving the quality of life of individuals with dementia, those who need care, and their families.

As practice, through developing a Virtual Reality and Augmented Reality technology, Dr. Okahashi is conducting research to observe how physical and mental functions and the level of care needs change in individuals with dementia and their families. Thereby, Dr. Okahashi is planning to develop care programs for individuals with dementia and their caregivers, verify their effectiveness, and examine measures for social implementation. The research field, concept and technology described above are important for our CreDDS programs, especially for the “Healthy Aging” program.

Visiting Researcher
Dr. Satoshi SASAYAMA (Doctor of Medical Science)

Present affiliation and position

Graduate School of Medicine Kyoto University, Human Health Sciences
Advanced Medical Data Intelligence, Laboratory of Information Systems
Associate Professor

Research field and importance of collaboration

Dr. Sasayama aims to build a ubiquitous community home health care and nursing care cooperation system. He is developing a system that realizes smooth sharing of information between healthcare professionals and patients and their family members supporting home medical care. Further, he is constructing a bacterial database, an e-Learning system in the field of health science, and creating interactive teaching materials.

As practice, Dr. Sasayama is engaging in development of "electronic contact notes for

home health care" using tablet terminals that are easy for the elderly to handle. Thereby, he is now practicing to provide his technology to make a close relationship between medical staffs at core hospitals and patient's families in Kyoto Prefecture. The research field, concept and technology described above are important for our CreDDS programs, especially for “Healthy Aging” program.

Visiting Researcher
Dr. Tatsuro MIURA (Doctor of Human Health Sciences)

Present affiliation and position

National Hospital Organization Kyoto Medical Center
Division of Clinical Laboratory Science
Part-time Laboratory Scientist

Research field and importance of collaboration

Dr. Miura is working on analyses of various data and construction of sensor systems related to health sciences. At Kyoto Medical Center, he is engaging in measuring physiological function and biochemical tests for patients as a clinical laboratory staff member, while at Kyoto University School of Medicine, he has developed a noninvasive optical monitoring system for blood glucose concentration of diabetic patients. In addition, he has participated in the national projects, including those organized by the Ministry of Land, Infrastructure, Transport and Tourism, and the Ministry of Internal Affairs and Communications, and has engaged in developing biosensor systems and evaluating volunteers' physiological function using the sensor systems. His research field, concept and technology are important for the promotion of our CreDDS programs, especially for the boundary area between “Health & Human Well-being” and “Lifelines, Transport & Settlement System”.

Advanced Biomedical Engineering
12: 81–90, 2023.

Original Paper

DOI:10.14326/abe.12.81

Development of an Electric Pegboard (e-Peg) for Hand Dexterity Improvement and Cognitive Rehabilitation: A Preliminary Study

Sayaka Okahashi,[*, **, ***, #] Kenta Sakamoto,[†, ††] Fumitaka Hashiya,[†††] Keisuke Kumasaka,[‡] Taro Yamaguchi,[‡‡] Akitoshi Seiyama,[**, ***] Jun Utsumi[‡‡]

Abstract Fine motor dysfunction and cognitive impairments commonly develop after stroke, which greatly impact the daily lives of patients. In current occupational therapy, hand dexterity and cognitive functions are evaluated individually (e.g., by manipulation of small objects with fingers, or a paper-and-pencil test), which is insufficient for therapists to grasp the total ability of combined dexterity and cognition in everyday situations. Additionally, the traditional methods require a tester to measure the completion time manually and tend to be monotonous for patients. These problems would be solved using technology. This study aimed to develop a new electric pegboard (e-Peg) prototype and to investigate preliminary utility in healthy adults. The system judges the peg insertion accuracy based on magnetism and records the time course and scores, which are linked to human object manipulation ability. The e-Peg executes three types of tasks: a basic color matching task (BT), a color comparison task using a pattern sheet (CT), and a visual memory task (MT), with one/two-color sample patterns. Six older and nine younger healthy adults performed the e-Peg tasks, functional tests, and responded to questionnaires. As a result, the number of correct answers in a bicolor symmetrical MT were significantly greater in the younger group than in the older group. The older group required a significantly longer completion time for BT and CT than the younger group. Significant correlations were found between one-color BT/CT and dexterity tests, between bicolor BT/CT and dexterity/cognitive tests, and between a bicolor MT and a cognitive test. Questionnaire results revealed that participants regarded BT/CT as easy/interesting tasks, whereas MT was considered a difficult/challenging task. In conclusion, our e-Peg is potentially a useful rehabilitation device that facilitates many tasks related to hand manipulation and attention/executive functions, and a valuable tool for personalized therapy.

Keywords: electric pegboard, hand dexterity, cognitive functions, occupational therapy, digital rehabilitation device.

Adv Biomed Eng. **12**: pp. 81–90, 2023.

1. Introduction

In the rapid aging society, the number of older patients (≥ 65 years) continues to rise. The number of patients with cerebrovascular disease who received treatment, follow-up, or rehabilitation in Japan was approximately 1.12 million in 2017, and more than 80% were older adults [1]. The average hospitalization time in the recovery phase rehabilitation ward is approximately 70–85 days [2]. Motor and sensory dysfunctions as well as cognitive impairments such as inattention and memory dis-

Received on May 12, 2022; revised on October 21, 2022 and January 23, 2023; accepted on January 24, 2023.

[*] Center for Gerontology and Social Science, National Center for Geriatrics and Gerontology, Aichi, Japan.
[**] Department of Human Health Sciences, Graduate School of Medicine, Kyoto University, Kyoto, Japan.
[***] Creative Design & Data Science Center, Akita International University, Akita, Japan.
[†] Healthtech Business Division, Techlico Inc., Osaka, Japan.
[††] Department of Physical Medicine and Rehabilitation, Kansai Medical University, Osaka, Japan.
[†††] Research Center for Material Science, Nagoya University, Aichi, Japan.
[‡] Department of Rehabilitation, Asaka Hospital, Fukushima, Japan.
[‡‡] Medical Science and Business Liaison Organization, Graduate School of Medicine, Kyoto University, Kyoto, Japan.
[#] 7–430 Morioka-cho, Obu, Aichi 474–8511, Japan.
E-mail: okahashi@ncgg.go.jp

orders are common after stroke [3]. The symptoms greatly impact patients' activities of daily living (ADLs) as well as other leisure, hobby and work activities. Occupational therapy (OT) is conducted in order to improve upper limb movement, hand dexterity, cognitive functions, and ADL abilities in particular.

Conventionally, hand skills and cognitive functions are evaluated separately using test batteries. A tester usually scores using a stopwatch manually. For instance, the Purdue Pegboard Test (PPT) [4, 5], Nine-Hole Peg Test (NHPT) [6], Grooved Pegboard Test (GPT) [7], O'Connor Finger Dexterity Test [8], and Box and Block Test (BBT) [9, 10] are used to examine fine manual dexterity. These are time-based tests used to define performing skills, and their reliability has been established in clinical patients. (such as NHPT for multiple sclerosis [11]; NHPT and PPT for Parkinson's disease [12]). Trail Making Tests (TMT) [13, 14], Digit Span [15], and Symbol Digit Modalities Test [16] are used to examine attention, working memory, and perceptual speed. These tests are paper-and-pencil or oral tests that evaluate the number of correct answers and the time required to answer.

Currently, there are few clinical evaluation and exercise methods that encompass a combination of motor and cognitive domains (for example, a PC typing task that copies a sample text or an exercise task using a commercial game like Nintendo Wii^{TM}) in OT, as these are often too difficult to perform for recovering patients with slow rough movements and low attention function, because the existing tasks require moderate- to high-level upper limb and cognitive functions.

These problems could be solved using technology. Recently, some studies reported epochal digital devices. A custom-made electronic pegboard test using an infrared sensor and microcontroller based on the NHPT [17] and a prototype of an electronic version of the GPT [18] have been developed. These electronic pegboards automate precise time calculation, but they were based on traditional pegboards and only focused on hand manipulation assessments.

Accordingly, the present study aimed to develop a novel electric pegboard (e-Peg) prototype and investigate its utility in healthy adults. This paper proposes a e-Peg system that facilitates three easy to moderate cognitive level tasks, and reports the results of preliminary evaluation experiments.

2. Materials and methods

2.1 The e-Peg system

2.1.1 Experimental apparatus

The e-Peg system comprises a main body that is 50 mm high, 180 mm wide, and 200 mm deep, with 16 (4 × 4) hall sensor-incorporated holes on a top board that fit pegs. The system weighs 650 g including accessories consisting of 8 red and 8 blue color pegs (φ15 × 50 mm) with neodymium magnet (φ8 × 3 mm) at the bottom tip of each peg. The tip of the red peg is N-pole, and that of the blue peg is S-pole (**Fig. 1a**). There is also a liquid crystal display (LCD) screen and 6 navigation buttons for lights and sounds located on the side of the system (**Fig. 1b**). An examiner conducts an e-Peg task by operating these buttons while confirming messages displayed on the LCD screen.

Each hole is illuminated in red or blue color after reading the task pattern from a built-in SD memory card programmed by an examiner in advance. When an examinee inserts the peg with the same color of the lit hole, the system judges this as correct based on magnetism. It also emits two kinds of sounds, "pee" for a correct answer and "poo-poo-poo" for an incorrect answer. A short melody is

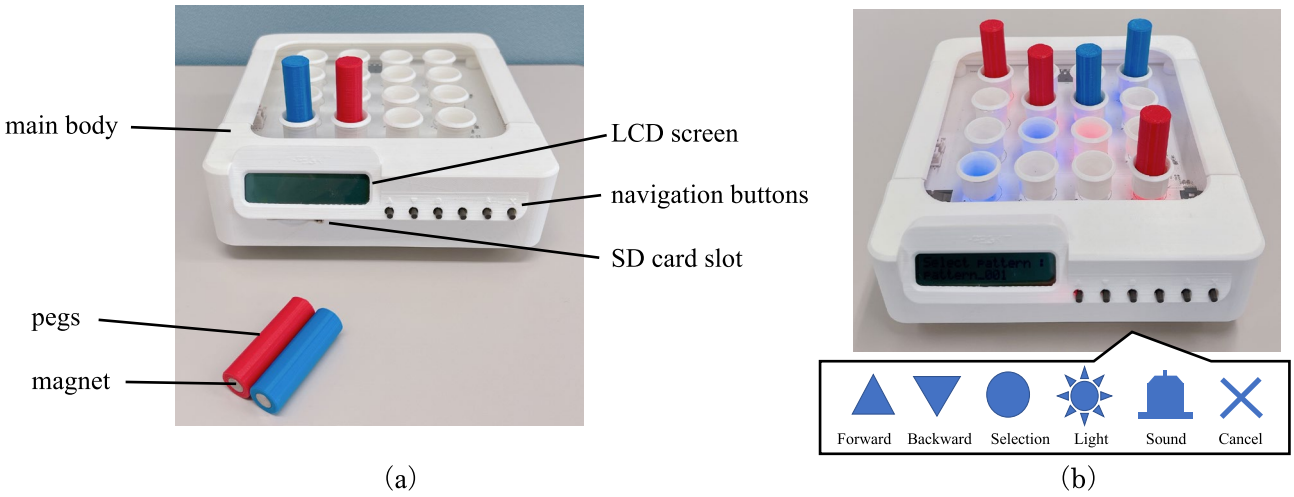

Fig. 1 The e-Peg system.
(a) the main body with lights "off" and pegs; (b) the main body with lights "on" and illustrated navigation buttons.

played upon each task completion and green lights are also illuminated. The block diagram and software flowchart are shown in **Fig. 2**. The electrical circuit diagram is shown in **Supplementary Fig. 1**.

Log data is recorded automatically in a comma separated value (CSV) format on the SD memory card (See **Supplementary Table 1**). The parameters included the peg holes operated, correct/incorrect determination, and the elapsed time after task initiation. The e-Peg housing and pegs were created with a 3D printer (Replicator +, MakerBot Industries, LLC.) using ABS filament based on a blueprint designed by HILLTOP Corporation (Kyoto, Japan).

2.1.2 Task setting

Three types of e-Peg tasks were created as follows:

- A basic task (BT): The examinee inserted a peg with the same color as that of the hole lighting. Eight holes remained lit in red or blue until the task was completed, and response sounds were produced to indicate the match between the peg and hole (**Fig. 3a**).
- A comparison task (CT): The examinee inserted a peg into a relevant hole based on the color and position on a printed design sheet placed in front of the e-Peg system. Sounds were produced during the task, although the holes were not lit (**Fig. 3b**).
- A memory task (MT): The examinee memorized the colors and positions of the lights on the main body by observing it for 5 seconds, after which he/she inserted the colored pegs into the matching holes. Response sounds were produced during the task performance, although the holes were not lit (**Fig. 3c**).

The examinees were required to manipulate the pegs individually as quickly as possible for each task condition under the instruction of an occupational therapist. In the case where a participant responded incorrectly and took over 10 seconds to insert the next peg, the examiner verbally explained that the participant could not provide any more answers and then switched on the LED lights to present the answers.

2.1.3 Sample patterns

Twelve e-Peg sample patterns were created. Six patterns (**Fig. 4, a–f**) were selected for use in this study. Eight of the sixteen holes were lit, giving a light ratio of 50%. Two elements, light color and symmetry, were considered to set difficulty levels: pattern a was composed of a one-color asymmetrical pattern; patterns b, c and d were bicolor symmetrical patterns; and patterns e and f were bicolor asymmetrical patterns.

2.2 Data collection

The preliminary evaluation experiments aimed to exam-

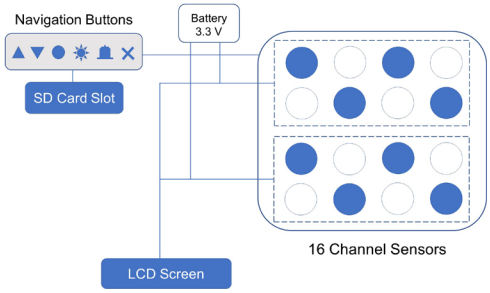

(a) Block diagram

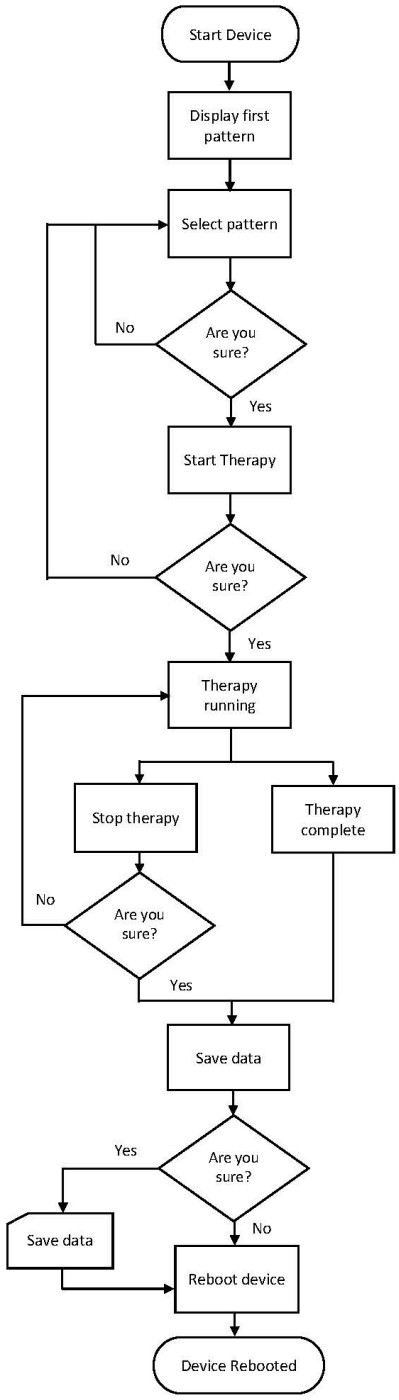

(b) Software flowchart

Fig. 2 The e-Peg system design.

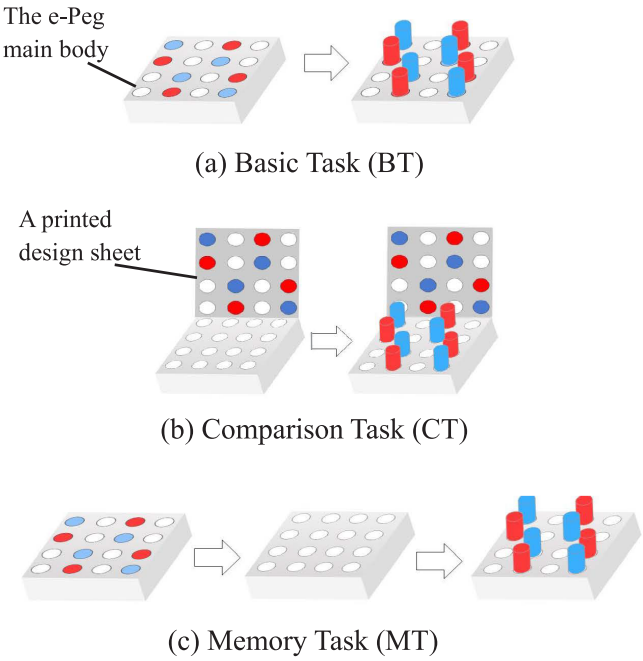

Fig. 3 Three types of e-Peg tasks.
Presented from an examinee's point of view.

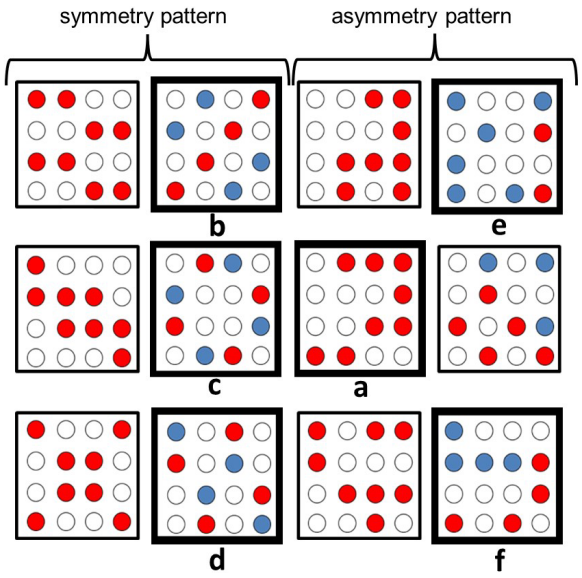

Fig. 4 Sample patterns.
The 6 patterns with bold borders were adopted in this study, presented from an examinee's point of view.

ine the following: 1) comparison of e-Peg performance by age group, 2) relationship between e-Peg scores and functional assessment, and 3) subjective evaluation.

2.2.1 Participants

Six older and eleven younger healthy adults participated in this study. Written informed consent was obtained from all participants and the study was approved by the Ethics Committee at Kyoto University Graduate School and Faculty of Medicine (R2005-1). All participants were right-handed. The inclusion criteria were as follows: people who 1) could operate the e-Peg while sitting for more than 30 minutes; 2) could communicate with the examiner in Japanese; 3) were generally independent in their ADLs at home; 4) scored more than 24 points on the Mini-Mental State Examination (MMSE); and 5) did not have any serious disease (e.g., cerebral nerve system or orthopedic disease of the upper limbs with sequela).

2.2.2 The e-Peg test and a questionnaire

The participants sat in a chair with the soles of their feet placed on the floor. They were seated at one-fist width from the edge of a desk measuring 70 cm high, 159 cm wide, and 69 cm deep in a silent room. The height of the desktop was adjusted based on the participants' elbow positions when their arms were down and their elbows were bent at 90 degrees. The e-Peg main body was placed in front of each participant. The eight red and eight blue pegs were set upright alternately on a wooden setting board (SAKAI Medical Co., Ltd.) placed on the right side of the main body (**Fig. 5**). The participants performed the e-Peg task with the dominant right hand in the following order: BT (using patterns a and b), CT (using patterns a and c), and MT (using patterns b, d, e and f). The number of correct answers and completion time were used to calculate e-Peg score.

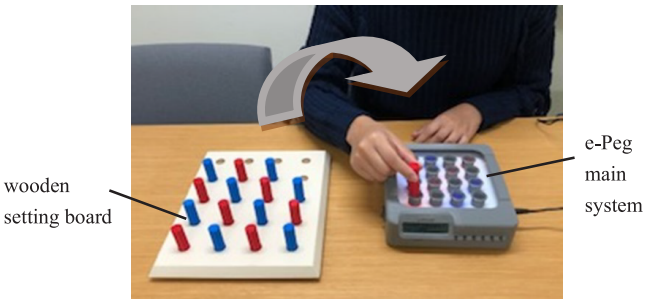

Fig. 5 Scene of the experiment.

A five-point scale questionnaire was conducted after the e-Peg tasks to evaluate subjective user-friendliness, interest level, and difficulty level of each task.

2.2.3 Upper limb/ cognitive function tests

The grip and pinch strength were used to measure upper limb muscle power; the BBT and PPT were used to evaluate hand dexterity. Attention and executive function were assessed by the TMT. MMSE was conducted for older adults as a general cognitive screening.

The BBT standardized by Mathiowetz et al. [9] in

1985 is an elaborate test in which a person is required to move a maximum number of 25-mm cubic blocks from one box to another within 60 seconds [9, 10]. The PPT developed by Joseph in 1948 is a finger and upper limb manipulability test [4] that requires a person to pick up pins and fill in peg holes starting from the topmost hole; the test may be executed using one hand or both hands within 30 seconds. The TMT requires participants to link numbers (1–25) in ascending order (in part A: TMT-A), or numbers (1–13) and Hiragana characters ("a"–"shi") alternately in ascending order (in part B: TMT-B) with a single stroke of a pencil without error as quickly as possible. This test assesses task transition and attention switching [13, 14].

2.3 Data analysis

Comparisons between the two groups were performed using Wilcoxon's rank sum test for the demographic data and the e-Peg scores. Spearman's correlation was performed to determine the association between e-Peg scores and dexterity or cognitive scores. Differences were reported significant if $p < 0.05$. Analyses were conducted using JMP Pro 16.2 (SAS Institute Inc.).

3. Results

3.1 Demographic data

The results obtained from a total of 15 healthy adults (six older and nine younger) are reported as below. The data of two young adults were excluded due to equipment failure. Dexterity (BBT, PPT) with a dominant hand and cognitive function (TMT-A and -B) were significantly better in the younger group than in the older group (**Table 1**).

Six out of eight e-Peg task performance scores are reported below. The abbreviated task names and comments are shown in **Table 2**. The MT scores using two patterns (pattern b which was a practice task and pattern f having plural empty values) were excluded from data analysis.

3.2 The e-Peg performance

Both age groups marked the full number of correct answers in BT/CT, but the number of correct answers were significantly greater in the younger group than in the older group in a MT using a bicolor symmetrical pattern (**Fig. 6a**). The older group required a significantly longer time to perform both BT and CT than the younger group (**Fig. 6b**).

3.3 Relationship between e-Peg score and dexterity/cognitive tests

There were significant negative correlations between one-color BT/CT and dexterity tests. There were significant correlations between bicolor BT/CT and dexterity/cognitive tests. A significant negative correlation between bicolor MT-1 and cognitive test (TMT-B) was also

Table 2 Abbreviated task names and comments.

Task name	sample pattern used	characteristic
one-colored BT	a	symmetry
bicolored BT	b	asymmetry
one-colored CT	a	symmetry
bicolored CT	c	asymmetry
bicolored MT-1	d	symmetry
bicolored MT-2	e	asymmetry

Table 1 Demographic data of the participants.

Participants	Older group ($n = 6$)	Younger group ($n = 9$)	p-Value
Age (years)	80.2 ± 5.1	21.2 ± 2.2	**
Gender (male/female)	3/3	4/5	–
Hand laterality (R/L)	6/0	9/0	–
Grip strength (R) (kg)	26.3 ± 13.6	33.8 ± 10.3	n.s.
Pinch strength (R) (kg)	5.4 ± 3.2	4.9 ± 0.9	n.s.
BBT score (R)	56.7 ± 5.5	67.8 ± 11.0	*
PPT score (R)	12.3 ± 1.2	15.9 ± 2.3	**
TMT-A	53.6 ± 14.6	30.0 ± 6.4	**
TMT-B	85.7 ± 17.1	38.0 ± 10.1	**
MMSE	28.8 ± 1.2	–	–

Data are expressed as mean ± SD. Wilcoxon's rank sum test ($n = 15$), *: $p < 0.05$, **: $p < 0.01$, n.s.: not significant. BBT: Box and Block Test; PPT: Purdue Pegboard Test; TMT: Trail Making Test; MMSE: Mini-Mental State Examination.

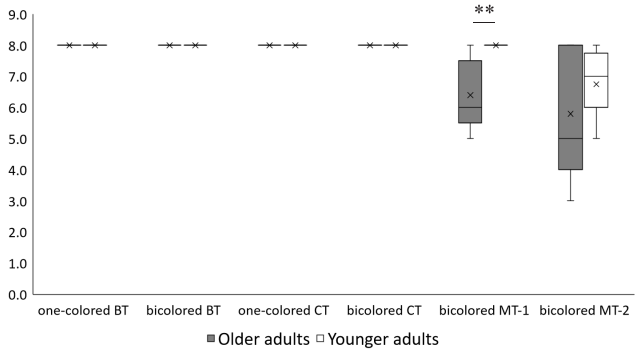

(a) Number of correct answers

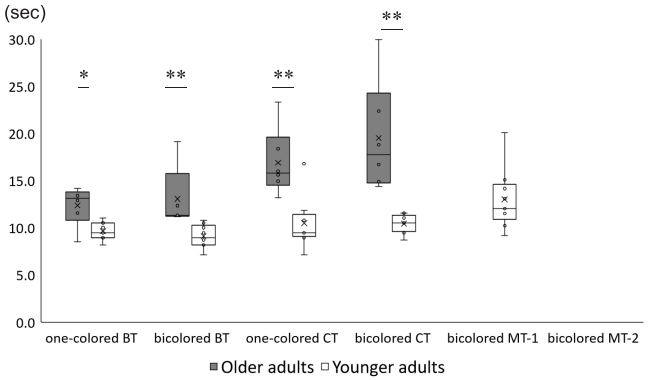

(b) Completion time

Fig. 6 e-Peg performance.
Wilcoxon's rank sum test ($n = 15$), *: $p < 0.05$, **: $p < 0.01$. The completion time was obtained from the tasks performed perfectly by all participants in each age group.

found (**Table 3**).

3.4 Subjective evaluations

Sixty-seven percent of older and 100% of younger participants answered that the e-Peg system was easy-to-use (**Fig. 7a**). The system was also judged to be interesting by 67% (older) and 78% (younger) of participants for BT, by 50% (older) and 78% (younger) for CT, and by 83% (older) and 100% (younger) for MT (**Fig. 7b**). The task level was judged to be easy for BT/CT by 67% (older) and 100% (younger), and difficult for MT by 67% (older) and 56% (younger) of participants (**Fig. 7c**).

4. Discussion

4.1 Comparison of e-Peg performance by age group

The e-Peg scores in the older group were significantly lower than those in the younger group in five out of six tasks. As previous studies described decreases in hand/finger muscle strength, manipulation, walking ability, and information processing speed with age [19–21], the age difference in e-Peg scores could have been caused by dexterity/attention span decline due to increase in age. Additionally, Walters et al. [22] conducted an eye tracking study during commonly used dexterity tests such as NHPT and GPT, and reported "a greater number of corrective saccades and lesser time gazing at the pegboard holes in older compared with young adults". Therefore, our result may reflect the age-related oculomotor characteristics which are related to visual attention. In our next study, we plan to investigate the relationship between eye movements and each e-Peg task performance in different age groups.

The median number of correct answers in the bicolor asymmetrical MT was the lowest among all tasks in each group. Rajsic et al. [23] examined visual working memory when 18 healthy university students and hospital staff memorized the type and number of objects, and reported that their performance was higher for a symmetrical condition than for an asymmetrical condition. Asymmetrical tasks would require more attention/memory during color and location memorization than other tasks.

Table 3 Correlations between e-Peg score and dexterity/cognitive tests.

	BBT	PPT	TMT-A	TMT-B
one-colored BT	-0.78^{**}	-0.70^{**}	0.42	0.42
bicolored BT	-0.70^{**}	-0.81^{**}	0.56^{*}	0.60^{*}
one-colored CT	-0.80^{**}	-0.65^{**}	0.48	0.43
bicolored CT	−0.42	-0.58^{*}	0.69^{**}	0.67^{**}
bicolored MT-1	0.29	0.48	−0.50	-0.66^{*}
bicolored MT-2	−0.16	0.04	−0.06	0.01

Spearman's rank correlation analysis ($n = 15$), *: $p < 0.05$, **: $p < 0.01$.
BT: a basic task; CT: a comparison task; MT: a memory task; BBT: Box and Block Test; PPT: Purdue Pegboard Test; TMT: Trail Making Test. The time required was used as the score in BT and CT; the number of correct answers was used as the score in MT.

4.2 Relationship between e-Peg score and functional assessments

There were significant negative correlations between one-color BT/CT and dexterity tests, and bicolor BT/CT had significant correlations with dexterity tests and TMT. The TMT subjects examinees to a cognitive load via task transition and attention switching [13]. Grubert et al. [24] reported that the element of attention required was qualitatively different during a one- and a two-color number searching task. These results suggest that the bicolor tasks reflected an examinee's hand manipulation and switching attention.

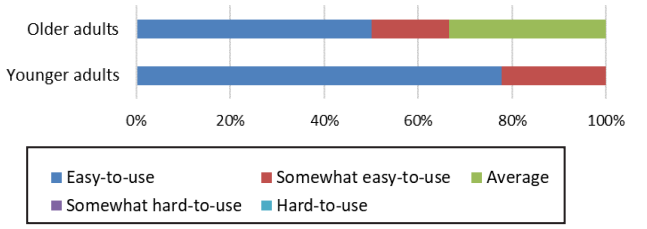

(a) Usability

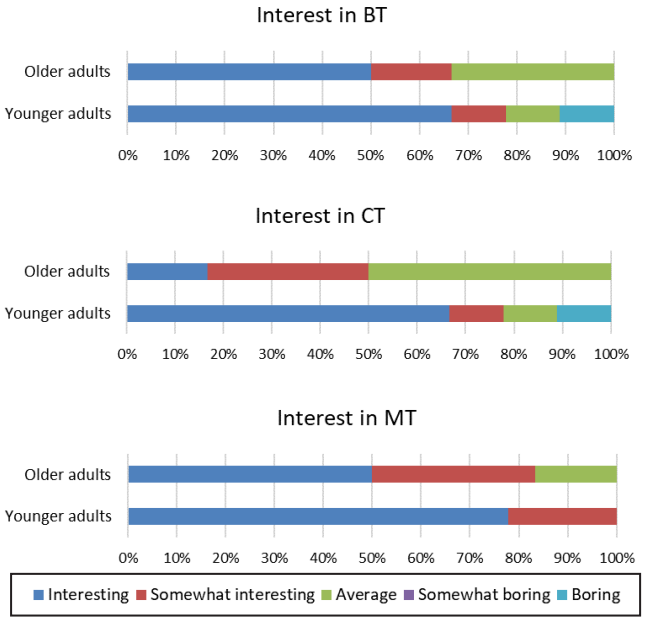

(b) Interest

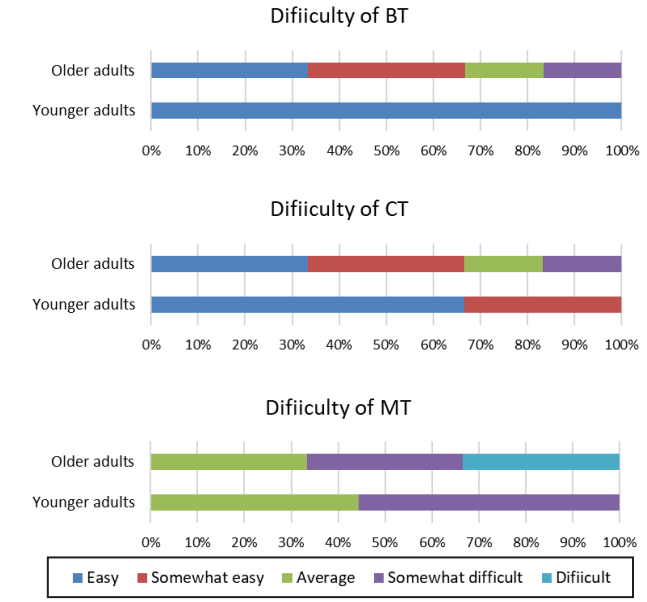

(c) Difficulty

Fig. 7 Subjective evaluations of e-Peg tasks. Older adults ($n = 6$), younger adults ($n = 9$).

There was a significant negative correlation between a bicolor symmetrical MT and TMT-B. The result suggests that the MT reflects an examinee's visual working memory and executive function when memorizing the two-color pattern and placing each colored peg in its appropriate position.

4.3 Usability, interest, and difficulty

The e-Peg system was judged to be easy-to-use by the majority of participants. One reason would be that our peg size, which was approximately 15 mm in diameter, was designed with reference to daily necessaries such as chopsticks and personal seals. The system was judged to be interesting by 50–78% of participants for BT/CT and by more than 80% for MT. The task level was judged to be easy by 67–100% of participants for BT/CT, and difficult by more than 50% of participants for MT. Csikszentmihalyi [25] reported that people found it interesting when a challenge level was neither too high nor too low for their current ability. Not all participants performed the bicolor MT correctly, which suggests that the difficulty level was appropriate for them.

4.4 Comparison between e-Peg and other analog/digital pegboards

There are three advantages of using e-Peg. First, the system can assess not only a motor task, but also a motor-cognitive dual-task as an all-in-one test. Some similar digital pegboards with precise automated time calculation [17, 18] aimed only at assessing dexterity based on the conventional pegboards. Petrigna et al. [26] have reported that the 25-hole GPT, which involves placement of keyhole-shaped pegs, performed in a dual-task situation is a feasible test to evaluate manual dexterity. A dual-task cognitive condition is a more challenging situation compared to that of motor condition or single task alone.

Second, our e-Peg system is superior to other commercial products such as Rapael Smart Pegboard™ (Neofect USA Inc.) [27] due to automatic correct/incorrect judgement of two-color peg insertion in each hole using magnetism and diversity of the hole lighting presentation according to configurable color patterns via an SD card.

Third, the e-Peg has better size and weight compared to other products (**Table 4**). The compactness is a merit of being usable at home or while traveling.

4.5 Limitations and future directions

These encouraging results were obtained only from our preliminary study, and need to be verified with a large number of participants including different age groups and medical conditions, referring to a study on reliability of PPT in adults after stroke [28].

Patients usually struggle to maintain a high level of

Table 4 Comparison table of size and weight.

		e-Peg	PPT	BBT	Rapael Smart Pegboard™
size (mm)	height	**50**	20	170	32
	width	**180**	300	290	557
	depth	**200**	450	290	353
approximate weight (kg)		**0.65**	1.0	5.0	6.3

motivation for rehabilitation over a 2-month lengthy hospital stay. Popovic et al. [29] reported that feedback-mediated exercise for poststroke rehabilitation of a hemiplegic arm increased patient motivation (such as interest, enjoyment, and perceived competence) and promoted greater improvement of motor function including speed and smoothness compared to no-feedback exercise. Furthermore, physical therapy containing gamification elements helped patients remain engaged in rehabilitation [30]. It is especially important to be able to continue without getting bored in equipment-mediated rehabilitation. The e-Peg would bring pleasure to daily training. The electronic circuit could be upgraded to variations with ingenuity to keep non-experienced users entertained.

5. Conclusion

We have developed a newly electronic pegboard (e-Peg) for evaluating dexterity and cognitive functions using 3 types of tasks with multiple sample patterns. The preliminary study shows that the system has promising potential as a device for fused rehabilitation of hand manipulation and attention/executive function at various difficulty levels.

Acknowledgment

The authors would like to thank all the volunteers who participated in this study. We are grateful to our team members/advisors in the inaugural Healthcare Innovation Design Entrepreneurship Program (HiDEP) organized by the Medical Science and Business Liaison Organization, Graduate School of Medicine, Kyoto University. We also thank Hikari Otsuka, MSc OT, Yuki Watanabe, MSc OT, and Kurumi Fukuda, BSc OT for many productive discussions in our laboratory.

Declaration of interest statement

Sayaka Okahashi, Fumitaka Hashiya, Taro Yamaguchi, and Jun Utsumi hold a patent on the structure and functions of an electrical pegboard system (JP Patent no. 6861439).

Funding

This work was supported by the Office of Society-Academia Collaboration for Innovation, Kyoto University under the 8th Incubation Program and the FY2018 GAP Fund Program, and KAKENHI; Grant-in-Aid for Scientific Research (C) (21K00229).

Data Availability

The data that support the findings of this study are available from the corresponding author upon reasonable request.

References

1. Ministry of Health, Labour and Welfare, JAPAN: the 2018 Edition Annual Health, Labour and Welfare Report. Nikkei Printing Inc, Tokyo, pp. 74–76, 2019. <https://www.mhlw.go.jp/wp/hakusyo/kousei/18/dl/1-01.pdf> [accessed on October 10, 2022] in Japanese.
2. Ministry of Health, Labour and Welfare, JAPAN: Summary of the 2020 annual survey report (prompt report 2). pp. 145–146, 2021. <https://www.mhlw.go.jp/content/12404000/000795302.pdf> [accessed on October 10, 2022] in Japanese.
3. The Japan Stroke Society: Japanese Guidelines for the Management of Stroke 2015. Kyowa Kikaku, Tokyo, 2017.
4. Tiffin J, Asher EJ: The Purdue pegboard; norms and studies of reliability and validity. J Appl Psychol. **32**(3), 234–247, 1948.
5. Lawson I: Purdue pegboard test. Occup Med (Lond). **69**(5), 376–377, 2019.
6. Kellor M, Frost J, Silberberg N, Iversen I, Cummings R: Hand strength and dexterity. Am J Occup Ther. **25**(2), 77–83, 1971.
7. Grooved Pegboard Test User Instructions. (Lafayette Instrument Co., Lafayette, IN, USA) <https://www.advys.be/docs/GroovedPegboardTestManual.pdf> [accessed on September 25, 2022].
8. O'Connor Finger Dexterity Test User's Manual. (Lafayette Instrument Co., Lafayette, IN, USA) <https://www.ncmedical.com/images/pdf/nc70015_oconnor_finger_dexterity_test_020718.pdf> [accessed on September 25, 2022].
9. Mathiowetz V, Volland G, Kashman N, Weber K: Adult norms for the box and block test of manual dexterity. Am J Occup Ther. **39**(6), 386–391, 1985.
10. Desrosiers J, Bravo G, Hébert R, Dutil E, Mercier L: Validation of the box and block test as a measure of dexterity of elderly people: reliability, validity, and norms studies. Arch Phys Med Rehabil. **75**(7), 751–755, 1994.
11. Feys P, Lamers I, Francis G, Benedict R, Phillips G, LaRocca N, Hudson LD, Rudick R: The Nine-Hole Peg Test as a manual dexterity performance measure for multiple sclerosis. Mult Scler. **23**(5), 711–720, 2017.
12. Proud EL, Bilney B, Miller KJ, Morris ME, McGinley JL: Measuring hand dexterity in people with Parkinson's disease: Reliability of pegboard tests. Am J Occup Ther. **73**(4), 7304205050p1–7304205050p8, 2019.
13. Ishiai S: Higher Brain Dysfunction, 2nd ed. Ishiyaku, Tokyo, 2012.
14. Brain function test committee, Japan Society for Higher Brain

Dysfunction: Trail Making Test Japanese version (TMT-J). Shinkoh Igaku Shuppansha, Tokyo, 2019.

15. Lezak MD, Howieson DB, Bigler ED, Tranel D: Neuropsychological Assessment, 5th ed. Oxford University Press, New York, 2012.
16. Smith A: Symbol digit modalities test. Western Psychological Services, Los Angeles, 1982.
17. Acharya KA, Bhat S, Kanthi M, Rao BK: Fine motor assessment in upper extremity using custom-made electronic pegboard test. J Med Signals Sens. **12**(1), 76–83, 2022.
18. Al-Naami B, Al-Naimat F, Almalty A-MRM, Visconti P, Al-Hinnawi A-R: A prototype of an electronic pegboard test to measure hand-time dexterity with impaired hand functionality. Appl Syst Innov. **5**(1), 2, 2022.
19. Torrens-Burton A, Basoudan N, Bayer AJ, Tales A: Perception and reality of cognitive function: Information processing speed, perceived memory function, and perceived task difficulty in older adults. J Alzheimers Dis. **60**(4), 1601–1609, 2017.
20. Ranganathan VK, Siemionow V, Sahgal V, Yue GH: Effects of aging on hand function. J Am Geriatr Soc. **49**(11), 1478–1484, 2001.
21. Abe T, Soma Y, Kitano N, Jindo T, Sato A, Tsunoda K, Tsuji T, Okura T: Change in hand dexterity and habitual gait speed reflects cognitive decline over time in healthy older adults: a longitudinal study. J Phys Ther Sci. **29**(10), 1737–1741, 2017.
22. Walters BH, Huddleston WE, O'Connor K, Wang J, Hoeger Bement M, Keenan KG: The role of eye movements, attention, and hand movements on age-related differences in pegboard tests. J Neurophysiol. **126**(5), 1710–1722, 2021.
23. Rajsic J, Wilson DE: Asymmetrical access to color and location in visual working memory. Atten Percept Psychophys. **76**(7), 1902–1913. 2014.
24. Grubert A, Eimer M: Qualitative differences in the guidance of attention during single-color and multiple-color visual search: behavioral and electrophysiological evidence. J Exp Psychol Hum Percept Perform. **39**(5), 1433–1442, 2013.
25. Csikszentmihalyi M: Beyond Boredom and Anxiety. Jossey-Bass, Hoboken, NJ, 2000.
26. Petrigna L, Pajaujiene S, Iacona GM, Thomas E, Paoli A, Bianco A, Palma A: The execution of the grooved pegboard test in a dual-task situation: a pilot study. Heliyon. **6**(8), e04678, 2020.
27. Neofect: Smart Pegboard <https://www.neofect.com/us/smart-pegboard> [accessed on October 8, 2022].
28. ClinicalTrials.gov: Establishing of the Reliability of the Purdue Pegboard Test in Adults After a Stroke. <https://clinicaltrials.gov/ct2/show/NCT05009108> [accessed on October 8, 2022].
29. Popovic MD, Kostic MD, Rodic SZ, Konstantinovic LM: Feedback-mediated upper extremities exercise: increasing patient motivation in poststroke rehabilitation. Biomed Res Int. **2014**, 520374, 2014.
30. Gamboa E, Ruiz C, Trujillo M: Improving patient motivation towards physical rehabilitation treatments with PlayTherapy Exergame. Stud Health Technol Inform. **249**, 140–147, 2018.

Sayaka Okahashi

Sayaka Okahashi is currently a Senior Research Fellow at National Center for Geriatrics and Gerontology after being an assistant professor at Nagoya University and Kyoto University. She is an Occupational Therapist and received her MS and PhD from Kobe University. Her research interests focus on gerontechnology and program development for care of people with dementia and their family.

Kenta Sakamoto

Kenta Sakamoto joined Teclico Inc. after graduating from Kyoto University Graduate School of Medicine. He is a Research Fellow in the Department of Rehabilitation Medicine at Kansai Medical University. He is an Occupational Therapist and received his Master's degree from Kyoto University. His research interests include development cognitive rehabilitation system using Cross Reality (xR) technology.

Fumitaka Hashiya

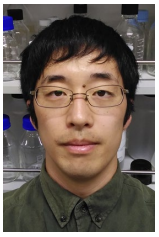

Fumitaka Hashiya is assistant professor of Research Center for Material Science at Nagoya University. He majored in chemical biology and received MS and PhD from Kyoto University in 2019. His current research is RNA therapeutics including mRNA vaccine and siRNA therapy.

Keisuke Kumasaka

Keisuke Kumasaka is currently an Occupational Therapist in Asaka Hospital after working at Kyoto Ohara Memorial Hospital group. He received his degree of Bachelor from the Department of Human Health Sciences, School of Medicine, Kyoto University in 2016. His special fields are stroke/disuse syndrome rehabilitation and mental health support.

Taro Yamaguchi

Taro Yamaguchi is a lecturer, Kyoto University Medical Science and Business Liaison Organization after Sharp Corporation. He has engaged in supporting the creation and growth of startups. He also serves at a Kyoto University startup company. He has Bachelor and Master of Engineering (Osaka University), Master of Business Administration (Kobe University), and Master of Social Public Health (Kyoto University).

Akitoshi SEIYAMA

Akitoshi SEIYAMA received the doctor degree of Science from the Graduate School of Science, Hokkaido University in 1988. He was Professor of Kyoto University, Graduate School of Medicine, Human Health Sciences. Since April/2022, he is a select Professor of Akita International University, a director of Creative Design and Data Science Center. He is developing new technologies to visualize physical and physiological functions of the living body, especially to visualize human brain functions.

Jun UTSUMI

Jun UTSUMI is CEO of TIR Research Consulting LLC on R&D for practical application of pharmaceuticals and medical devices. He obtained PhD from Hokkaido University and MBA from Otaru University of Commerce. After starting business carrier in pharmaceutical research and clinical development at Toray Industries, Inc., he had appointments of professor of Hokkaido University and Kyoto University. He also served consulting experts in Pharmaceuticals and Medical Devices Agency (PMDA) and Japan Agency for Medical Research and Development (AMED), Japan.

Supplementary Fig. 1. An electrical diagram of the e-Peg system.

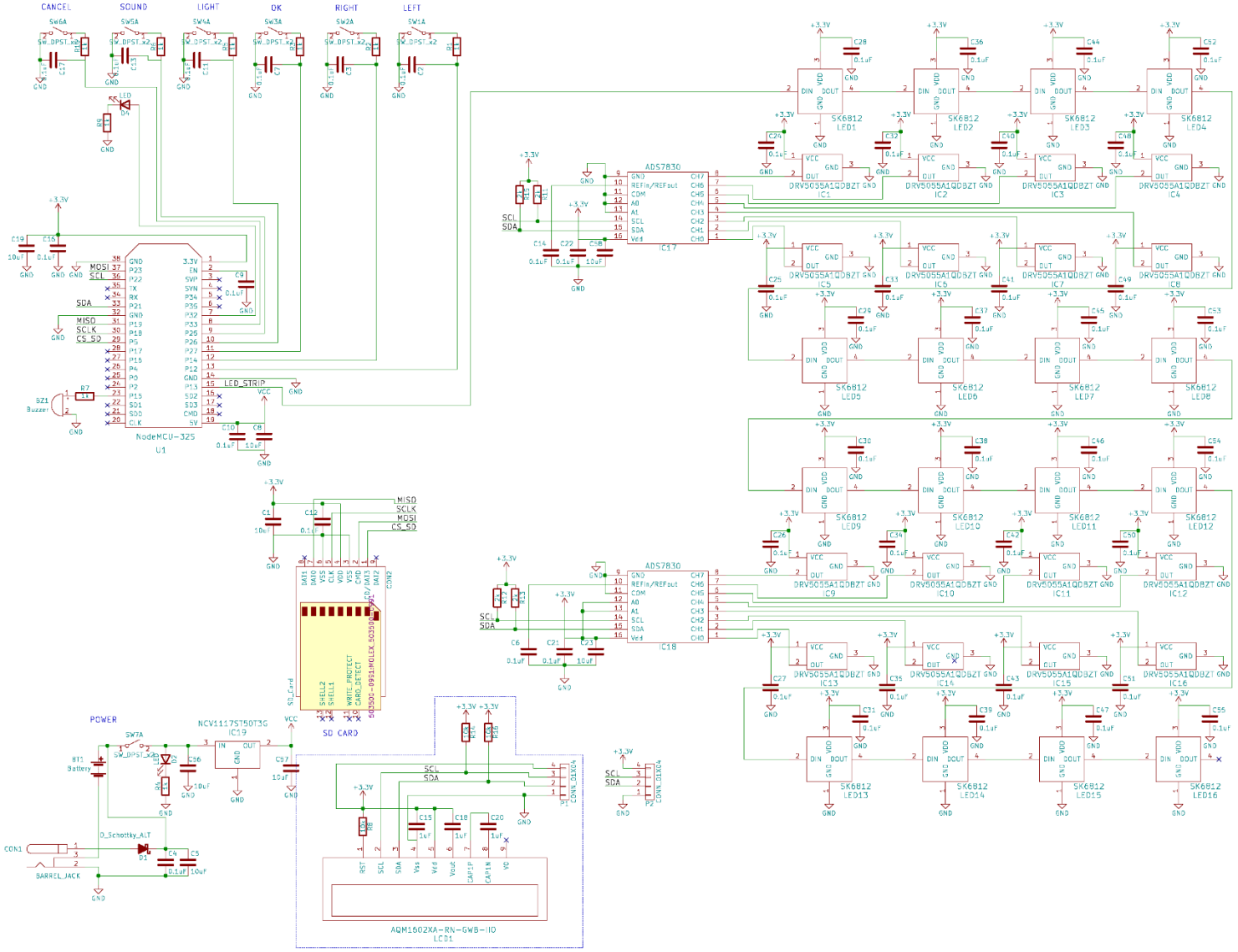

Supplementary Table 1. A sample of log data.

Count	Position	Pattern Colour	Time	OK	NG	BLUE	RED	BUZZER	LED
1	1	0	5.8		X	X		X	X
2	5	B	7.59	X		X		X	X
3	2	B	10.98		X		X	X	X
4	4	R	13.02	X			X	X	X
5	7	R	16.1	X			X	X	X
6	10	R	18.91	X			X	X	X
7	13	R	22.76	X			X	X	X
8	11	0	25.37		X	X		X	X
9	11	0	27.21		X	X		X	X
10	15	B	30.04	X		X		X	X
11	2	B	32.59	X		X		X	X
12	12	B	35.14	X		X		X	X

Count, the order in which a user inserted each peg; Position, the peg hole number (Nos. 1–16) which was registered internally; Pattern Colour, the lighting color in a hole (R, red; B, blue; 0, lights-out); Time (sec), the elapsed time after task initiation, OK/NG, correct or incorrect answer; BLUE/RED, the color of the inserted peg; BUZZER/LED, on or off state of the sound/light switch at that moment. Each e-Peg hole judges “OK (correct)” or “NG (incorrect)”. The corresponding hole judges “OK” only once and keeps the log at the first peg insertion in a task session. In the case of “NG” judgement, the log is kept any number of times.

PLOS ONE

RESEARCH ARTICLE

Importance of two-dimensional gaze analyses in the assessment of reading performance in patients with retinitis pigmentosa

Masako Yoshida[1]*, **Akitoshi Seiyama**[2,3]

1 Yoshida Eye Clinic, Kyoto, Japan, **2** Division of Medical Devices for Diagnoses, Human Health Sciences, Graduate School of Medicine, Kyoto University, Kyoto, Japan, **3** Creative Design & Data Science Center, Akita International University, Akita-City, Akita, Japan

* dolphin118may@gmail.com

Citation: Yoshida M, Seiyama A (2022) Importance of two-dimensional gaze analyses in the assessment of reading performance in patients with retinitis pigmentosa. PLoS ONE 17(12): e0278682. https://doi.org/10.1371/journal.pone.0278682

Editor: Guido Maiello, Justus Liebig Universitat Giessen, GERMANY

Received: April 28, 2022

Accepted: November 22, 2022

Published: December 14, 2022

Data Availability Statement: All relevant data are within the paper and its Supporting Information files.

Funding: The authors received no specific funding for this work.

Competing interests: The authors have declared that no competing interests exist.

Abstract

The causes of reading difficulties in people with peripheral visual field loss are not fully understood. We conducted a two-dimensional gaze analysis on eye movements during reading in patients with retinitis pigmentosa to investigate the causes of reading difficulties in relation to the central visual field using a binocular eye mark recorder (EMR-9). Twenty-seven patients with retinitis pigmentosa whose central visual field narrowed to $\leq 20^{\circ}$ using Goldmann kinetic perimetry (I/4 target) and this present study included eight healthy participants. The participants' visual acuities were corrected to better than +0.4 logMAR. Correlations and multivariate regression analyses were investigated between the number of letters read correctly, the I/4 central visual field, V/4 perifoveal and peripheral visual field, and visual acuity. Multivariate regression analysis revealed that all these parameters played almost equal roles in the number of letters read correctly. In the two-dimensional gaze analysis, the task performance time of patients during reading increased as the I/4 central visual field narrowed. The task performance time was more clearly correlated with the rotation saccade ($r = 0.428$, $p < 0.05$) and the distance of the vertical direction (ΣY) of eye movements ($r = 0.624$, $p < 0.01$), but not with regressive saccade and the distance of the horizontal direction (ΣX). Visual acuity was correlated with the task performance time (-0.436, <0.05) but not with eye movement directionality. Reading difficulties in patients with retinitis pigmentosa result from impaired eye movement directionality. Understanding eye measurements for people with tunnel vision required a two-dimensional gaze analysis. The two-dimensional gaze analysis also showed that the involvement of the perifoveal and peripheral visual fields, visual acuity, and I/4 central visual field was important for reading in people with tunnel vision.

Introduction

Retinitis pigmentosa (RP) is one of the major diseases associated with peripheral visual field loss; it is a hereditary progressive disease that occurs in approximately 1 in 4,000 people. In

many cases, the disease initially affects the rod cells near the macula; therefore, visual field impairment in patients with RP involves isolated scotomas near the macula, expanding and fusing to form a ring-shaped scotoma as the disease progresses. Further progression results in peripheral visual field loss due to the enlargement of the ring-shaped scotoma, leading to the concentric narrowing of the visual field [1]. Therefore, patients with RP struggle in daily life to determine the entire visual field due to the narrowing of their central visual field and have difficulty searching for things and moving due to the loss of the peripheral visual field [1–3]. If the central visual field narrows to a diameter of $\leq 20^{\circ}$, reading may become difficult due to character oversight or line breaks, even though the individual's eyesight is sufficient for reading characters [4, 5].

A countermeasure to reading difficulties includes improving the visibility of characters, such as using a magnifying glass to deal with the deterioration of visual acuity. However, even if visual acuity is normal, narrowing of the central visual field results in reading difficulties because of line breaks resulting in errors or difficulty tracking characters. Furthermore, no effective countermeasures have been established for reading difficulties in people with tunnel vision other than indirect methods such as visual positioning with underlines or a typoscope.

This research area has been the subject of many studies ever since Javal first proposed in 1879 that eye movements in reading were repetitions of fixation and saccade (SC) [6]. There have been reports of gaze measurements of glaucoma patients who first experience a disappearance of hemi-peripheral vision and eventually have impaired foveal vision [7–12]. All these previous studies of eye movements during reading were analyses of latency, amplitude, forward and regressive frequencies, retention frequency, and mean duration, but only for horizontal SCs with adjustments for calibration errors. However, there are no reports of detailed gaze measurements in reading for patients with RP.

We previously used functional magnetic resonance imaging to investigate the eye movement-related brain regions in patients with advanced RP [13]. The impaired SCs in patients with advanced RP were caused by decreased activity in eye movement-related brain regions in the frontal and parietal eye fields due to decreased visual input from the retina. An SC is related to controlling the direction and distance of the line-of-sight movement from the peripheral visual field to the fovea centralis. Therefore, there is a need to analyze the movement direction and distance of the line of sight for eye movements during reading in patients with advanced RP accompanied by peripheral visual field loss and central visual field narrowing.

Patients with advanced RP who visit the first author's Yoshida Eye Clinic often state that they skip the next line or lose track of the beginning of the next line in sentence line breaks. They also state that unintended movements of the viewpoint to another line, even in the middle of a line, cause the individual to lose sight of the part where the next viewpoint is placed, and their reading is interrupted.

Based on the results of functional magnetic resonance imaging studies and the reports of patients with advanced RP, we hypothesized that "directionalization of SCs" would cause reading difficulties in patients with advanced RP who otherwise had normal visual acuity. This study aimed to elucidate the cause of reading difficulties in patients with advanced RP using two-dimensional gaze analysis.

Materials and methods

Participants

This study was approved by the Ethics Committee of Kyoto University Graduate School and Faculty of Medicine, and both written and verbal informed consents were obtained from the participants. Participants were adults up to 65 years of age with sufficient vocabulary and

language skills with at least 12 or more years of education. They included patients with RP and a central visual field that was narrowed to ≤ 20˚ using Goldmann kinetic perimetry (GKP) (I/4 target) and healthy participants. The criteria for inclusion in the study were that the participants had to bitually read books and had no problems conducting this task. During this study, at least one eye was corrected to +0.4 LogMAR or better as a level of visual acuity that could identify characters in reading material. The reliability of the results of gaze analysis was ensured by excluding patients who could not satisfy the calibration criteria of the measuring instrument. In total, 27 individuals (12 men, 15 women) aged 22–64 years (average 42.2 ± 12.7 years) satisfied these conditions. The control group comprised eight healthy adults of a similar age to the patients with RP and had no ophthalmologic abnormalities (four men and four women, aged 25–62 years, average 44.5 ± 13.7 years; see S1 Table).

Analysis of visual function tests

In the case of non-synkinetic movements such as congestion and diversion, the left and right eyes do not always move in a synkinetic manner [14, 15]. The eye movements were assessed simultaneously with both eyes open. The main fixating eye was identified as the eye with a high rate of matching with the line of text. We investigated the visual field (Goldmann kinetic perimetry, GKP), visual acuity, and the number of character reads in 35 fixating eyes in 27 patients with advanced RP and eight healthy participants.

Goldmann kinetic perimetry

The visual function of the participants was evaluated based on the central visual field of the I/4 target of the GKP. The size of the central visual field of the GKP (I/4 target) in the participants was used to divide them into the following four groups: central visual field < 5˚ in one eye (advanced), ≥ 5˚ and < 10˚ (moderate), ≥ 10˚ and ≤ 20˚ (mild), and healthy controls.

It has been reported that peripheral vision affects the fixation/SC pattern during reading [16]. Therefore, we also conducted evaluations of the peripheral visual field using GKP (V/4 target). The areas covered by a radius of 5–10˚ and > 10˚ with a V/4 target were set as the perifovea and periphery, respectively; the area retention rates of the perifoveal and peripheral visual fields of the participant were calculated for each area, with the area retained by healthy individuals as 100%.

Visual acuity test (5-m distance visual acuity and near visual acuity)

We measured LogMAR visual acuity using a 5-m distance vision chart (SC-2000, 4987669605011, NIDEK, Tokyo, Japan) and a 30-cm near vision chart (Yamachi Chart for Near Point Distance, HANDAYA, Tokyo, Japan).

Reading speed

We investigated reading speed under free reading conditions. The number of characters read aloud in 5 min was used as an index of reading ability. The reading material had 22 characters per line and 18 lines per page on white A4 paper, and a plain horizontal Japanese text using both kanji and kana was used. The characters used were in Mincho 20-point font (viewing angle 0.857˚, composition line 0.037˚), which is commonly used in a book. Participants were asked to read aloud with both eyes open at a viewing distance of 40 cm. The experimenter counted the number of characters that could be accurately read for 5 min. It was conducted three times from different parts of the book, and the average value was adopted as the number of characters read.

Analysis of ocular motility

Task and eye movement recording. The line-of-sight measurements were performed in an indoor environment adjusted to an illuminance of 1000 Lx with a fluorescent lamp. The task used a Japanese text of 35 characters per line and 15 lines in a horizontal direction per page, which consisted of both kanji and kana in a 20-point MS Gothic typeface to avoid the effects of low visual acuity on character readability. Participants were instructed to read aloud the horizontal lines of text displayed on the monitor screen at a speed at which they could achieve the task without a time limit.

A head-fixing device with a chin rest was used. The device was placed so that the participants' eye height aligned with the monitor's center. Participants could only move their eyes while reading. The distance between the apex of the cornea and the center of the screen during the test was maintained at 40 cm.

A binocular eye mark recorder (EMR-9 Eye Tracking System; NAC Image Technology, Minato, Tokyo, Japan) was used for the recordings. The sampling rate of the eye-tracking system was 0.1˚ (60 Hz). The calibration function of the EMR-9 eye-tracking system was used to identify nine gaze points on the monitor screen with a viewing angle of 37˚. Calibration was repeated until the instrument calibration criteria were met.

Analyses. The obtained data (see S2 Table) were analyzed using EMR-d Factory, which is included in the EMR-9 eye-tracking system. One line at eye level was analyzed.

Trajectory of fixation. Fixation was defined as the stationary gaze point for 0.1 s or more. The movement angle between fixation was automatically classified and recorded. Any movement in which the movement angle between fixation was within 30˚ above or below the line of characters was defined as parallel SCs (see Fig 1). Parallel SCs in the progressing direction of the line of characters was defined as progression, and opposite to the progressing direction of the line of characters was defined as regression. A movement angle $\geq$ 30˚ from the line of text was defined as the rotation SC. We identified the position of the gaze point by voice information, and the eyes with a higher rate of matching the gaze point with the line of text were judged as the dominant eye.

The analysis items (Fig 1) were the regressive SC, the rotation SC with the line of text as the baseline (0˚) for rotational movement, total eye movement distance by direction (ΣX, ΣY),

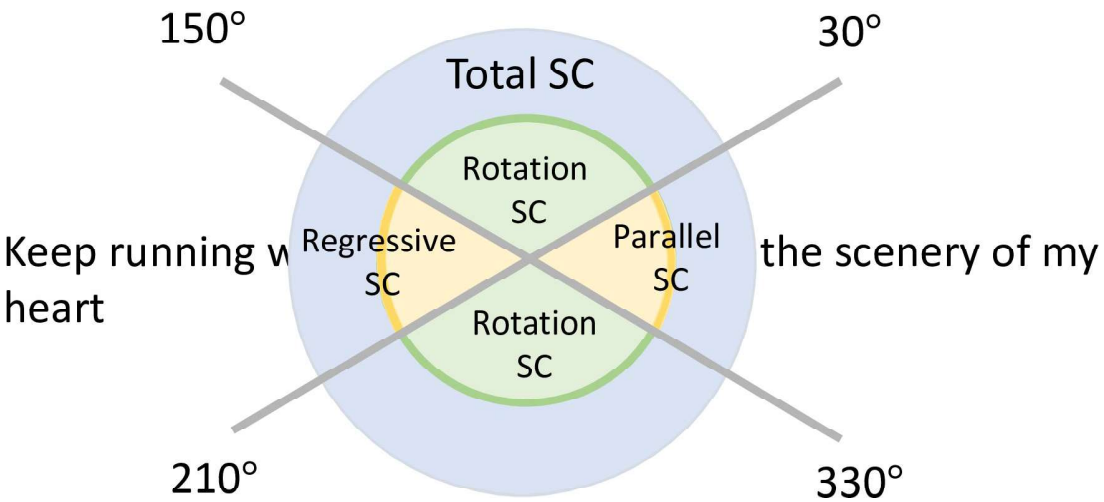

Fig 1. Definition of visual directions in the present study. Abbreviations: SC, saccade. The angle between 30˚ and 330˚and that between 150˚ and 210˚ were defined as the parallel SC. The angles between 30˚ and 150˚ and that between 210˚ and 330˚ were defined as rotation SC.

https://doi.org/10.1371/journal.pone.0278682.g001

and task performance time. The proportions of the regressive SC and rotation SC were calculated with all SCs (including SCs that were parallel to the line of text and SCs with movement in the rotation SC) set as 100%. The correlations between the analysis results for each item and the I/4 central visual field, the V/4 visual field retention rate, visual acuity, and age were investigated.

We evaluated the number of fixations for a given analyzed line (no. of fixation), mean duration of fixation per line (mean duration of fixation), the proportion of regression in all movements between fixation per line (regressive SC), and the proportion of movements in the rotation direction (rotation SC).

Trajectory of eye movement

A quantitative analysis of the trajectory of eye movement was conducted. Here, eye movements in various directions between each fixation were recorded for all the participants. Therefore, instead of the shortest distance between fixation, the eye movement trajectory was divided into units of 0.01 s to precisely measure the total movement distance.

The distance of eye movement (unit viewing angle) was measured separately for the horizontal component (X) and the vertical component (Y). The total movement distance by direction ($\Sigma X = \Sigma(x_i - x_{i-1})$, $\Sigma Y = \Sigma(y_i - y_{i-1})$, and the sum of the total distances ΣTotal (= $\Sigma\sqrt{(x_i - x_{i-1})^2 + (y_i - y_{i-1})^2}$ were calculated.

Cases where the gaze point was not on the screen resulted in the X and Y directions being recognized as out of the measurement range. The data were automatically listed as "error" and "unable to measure eye movement" and excluded from the analysis. The error frequency was used as a reference item because it caused an underestimation of the eye movement distance.

Task performance time (s)

The time (s) required for eye movement across one line, analyzed at eye height, was recorded to evaluate the relationship between eye movement and reading speed. Cases, where lines were skipped were excluded from the analysis target, and measurements were conducted on lines that were read without skipping.

Statistical analyses

The participant's visual field and gaze analysis data are shown in Tables 1 and 2, respectively, using means and standard deviations. The following statistical analyses were performed using statistical software (College Analysis ver. 8.5) [17]. The Kruskal Wallis H test and the Wilcoxon joint test were used for comparative tests between each group, and the significance level was set at 5%. The partial least squares regression was used to contribute to the individual visual field function on the number of letters read correctly. Pearson correlation analysis and linear regression were used for the correlation analysis between data. The strength of the correlation was defined as follows: a correlation coefficient (± r) $\geq$ 0.7 was set as a strong correlation, 0.4–0.69 as a moderate correlation, 0.2–0.39 as a weak correlation, and $<$ 0.2 as no correlation.

Results

Analysis of visual function tests

Table 1 shows visual function according to the central visual field group by GKP (I/4 target) for the fixating eye of the subject. The mean I/4 central visual field for the group was as follows: I/4 central visual field $<$ 5˚ (advanced), 3.6˚ ± 0.84 S.E.; $\geq$ 5˚ and $<$ 10˚ (moderate), 6.7˚ ±

Table 1. Visual function tests in 35 eyes of 35 participants.

	advanced	moderate	mild	Healthy
	n = 9	n = 9	n = 9	n = 8
I/4 central (degree)	3.61 ± 0.84	6.67 ± 0.90	14.56 ± 1.86*	100 ± 0*,+
V/4 perifovea (%)	28.44 ± 6.00	47.78 ± 6.81	85.67 ± 5.05*,+	100 ± 0*,+
V/4 periphery (%)	10.11 ± 3.67#	14.22 ± 4.25#	25.22 ± 4.96#	100 ± 0
Acuity (LogMAR)	0.31 ± 0.33	0.19 ± 0.41	0.12 ± 0.35*,#	'-0.16 ± 0.26*,+
Age (year)	46.89 ± 3.15	42.89 ± 3.79	39.89 ± 3.51	44.50 ± 3.70
Number of letters correctly read	1,026 ± 18	1,623 ± 25	1,780 ± 15*	2,019 ± 16*

The Kruskal Wallis H test and the Wilcoxon joint test were used.

*, $p < 0.05$ vs. advanced, +, $p < 0.05$ vs. moderate

#, $p < 0.05$ vs. healthy

https://doi.org/10.1371/journal.pone.0278682.t001

0.90 S.E.; $\geq 10^{\circ}$ and $\leq 20^{\circ}$ (mild), 14.6° ± 9 S.E.; and healthy group (healthy), 100° ± 0 S.E. There were significant differences between the advanced group and the mild and healthy groups.

The number of characters read aloud for 5 minutes was also significantly smaller at 1,026 characters (± 18 S.E.) for the advanced group than that of the healthy group at 1,980 characters (± 95 S.E.).

The multivariate regression analysis (partial least squares regression) applied to Table 1 (but without age and healthy control) gave the following regression formula with standardized partial regression coefficients:

$$\begin{aligned}&\text{Number of letters read correctly}\\&= 0.217*(\text{I/4 central}) + 0.226*(\text{V/4 perifovea}) + 0.216*(\text{V/4 periphery})\\&\quad - 0.255*(\text{acuity})\end{aligned}$$

The coefficients of determination and residual variance were 0.811 and 19925, respectively.

Further, regression analyses of these parameters and the number of letters read correctly for 27 patients suggested that the V/4 perifoveal ($r = 0.384$, $p < 0.05$) and V/4 peripheral ($r = 0.435$, $p < 0.05$) visual fields, as well as the visual acuity ($r = -0.542$, $p < 0.01$) and I/4 central visual field ($r = 0.514$, $p < 0.01$), were involved in the number of characters read (cf., S2 Fig).

Gaze analysis

During reading in healthy participants, the eye movements were parallel to the line of characters, whereas the eye movement in the patients with RP was often at irregular angles with the line of characters. As the I/4 central visual field narrowed further or the visual field disappeared further, the frequency of error judgments in which the gaze point popped out of the recording screen increased.

For the frequency of movement between fixation, rotation SC increased with the narrowing of the I/4 central visual field. Fig 2 shows the retained visual fields of individuals with highly advanced RP (S4), moderately advanced RP (S12), and healthy individuals (S33); Fig 3 shows

Table 2. Results of the eye movement test using EMR-9.

	advanced	Moderate	mild	healthy
	n = 9	n = 9	n = 9	n = 8
Number of fixations	15.33 ± 1.59	10.67 ± 0.59*	9.67 ± 0.27**	10.0 ± 0.50*
Mean duration of fixations	0.60 ± 0.11	0.51 ± 0.04	0.58 ± 0.04	0.57 ± 0.03
Regressive SC (%)	18.87 ± 3.07	21.83 ± 3.43	18.76 ± 2.67	17.33 ± 2.35
Rotation SC (%)	29.54 ± 9.86	16.51 ± 6.69	11.3 ± 5.13	4.0 ± 2.45*
ΣtTotal (degree)	236.02 ± 11.06	118.15 ± 4.38**	134.05 ± 6.42*	109.88 ± 5.08**
ΣX (degree)	201.86 ± 11.56	100.52 ± 5.75*	111.34±7.39	81.41 ± 3.38**
ΣY (degree)	170.86 ± 8.63	64.73 ± 4.48	58.73 ± 5.33*	48.48 ± 4.88**
Task performance time (s)	10.13 ± 1.96	6.40 ± 0.97**	6.12 ± 0.92**	6.70 ± 0.81*

ΣX (degree); total eye movement distance in the horizontal direction; ΣY (degree); total eye movement distance in the vertical direction.

The Kruskal Wallis H test and the Wilcoxon joint test were used.

*, $p < 0.05$ vs. advanced group

**, $p < 0.01$ vs. advanced group

https://doi.org/10.1371/journal.pone.0278682.t002

the images for the trajectory of fixation as well as the frequency by direction of movement between fixation and the trajectory of eye movement.

Trajectory of eye movement and task performance time

Table 2 summarizes the analysis results of the trajectory of eye movement. The proportion of rotation SC during the fixation trajectory increased inversely to the narrowing of the I/4 central visual field, with a significant ($p < 0.05$) difference between the advanced group (29.54% ± 9.86) and the healthy group (4.0% ± 2.45). Meanwhile, there were no significant differences between groups in the mean duration of fixation and regressive SC.

The eye movement distance was underestimated due to the increased frequency of error (gaze points outside the screen) owing to a narrowed I/4 central visual field. However, there were still significant ($p < 0.05$) differences in all eye movement distances (ΣX, ΣY, ΣTotal) between the advanced and the healthy groups. The task performance time increased with the narrowing of the I/4 central visual field, and there were significant ($p < 0.05$) differences between the healthy group (6.70 s ± 0.81 S.E.) and the advanced group (10.13 s ± 1.96 S.E.).

Individual gaze analysis and visual function of RP patients

Table 3 shows the correlations between the gaze analysis results (trajectory of fixation and trajectory of eye movement) in 27 fixating eyes with a narrowed I/4 central visual field and the task performance time, visual function (I/4 central visual field, V/4 perifoveal visual field, V/4 peripheral visual field, and visual acuity).

Gaze analysis and visual field

The correlation between visual function and gaze analysis results was evident in the vertical direction of eye movements. In the trajectory of fixation, all visual fields were negatively correlated with the rotation SC. On the contrary, there were no correlations between any of the visual fields with parallel regressive SC.

In addition, for the trajectory of eye movement, there was a significant moderate correlation between the I/4 central and V/4 perifoveal visual fields and the eye movement distance in

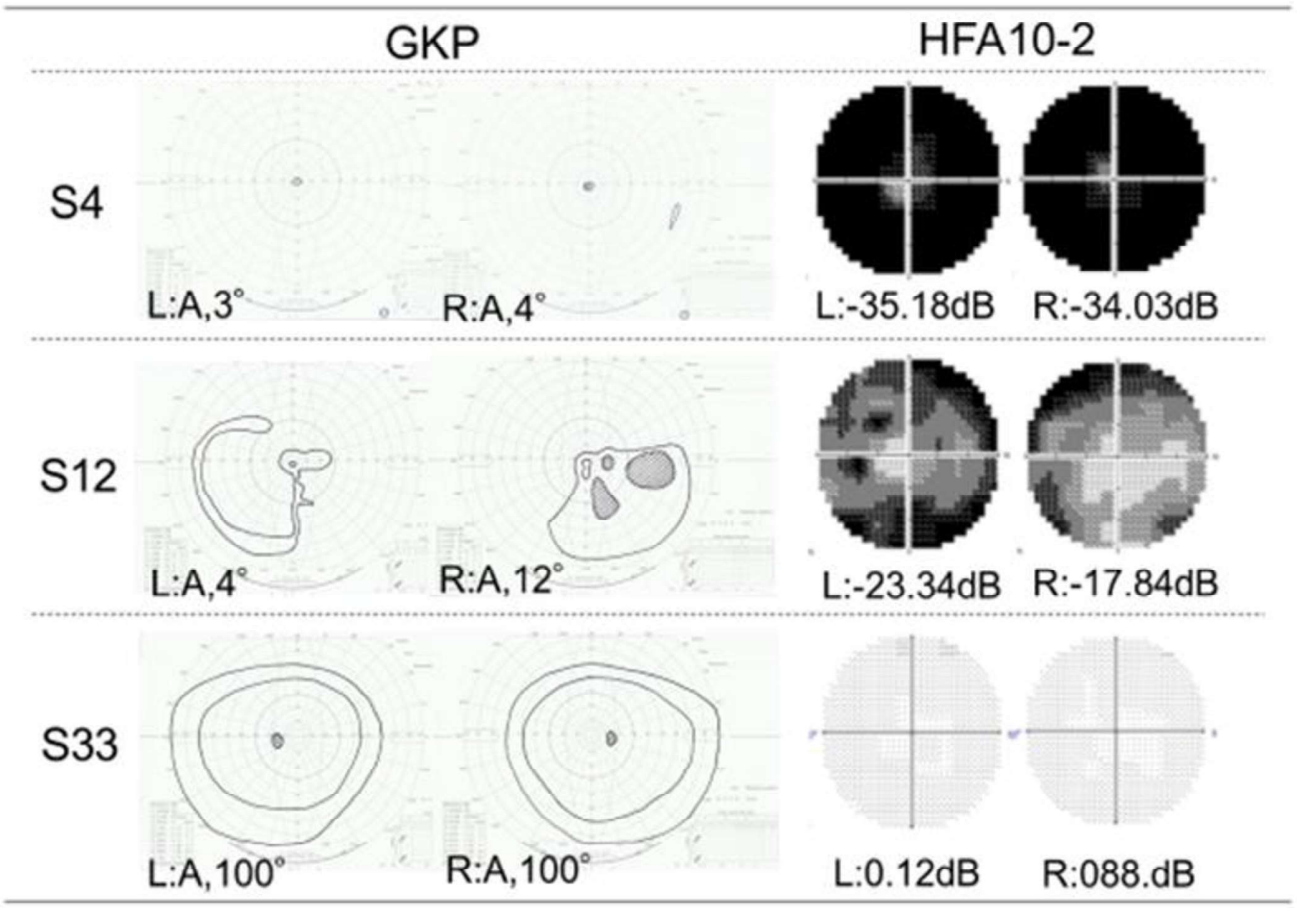

Fig 2. Typical examples of VFs measured using GKP and HFA 10–2. VFs measured using GKP V/4 & I/4 (right) and HFA 10–2 (left). The eye classification and pathology of each subject (S4, S12, and S33) are shown in the S1 Table. Abbreviations: GKP, Goldmann kinetic perimetry; HFA 10–2, Humphrey static perimetry.

https://doi.org/10.1371/journal.pone.0278682.g002

the vertical direction ΣY, but not with the eye movement distance in the horizontal direction ΣX.

All visual fields were significantly negatively correlated with the number of fixations, but there were no correlations between any visual fields and the mean fixation duration.

Visual acuity and gaze analysis

Visual acuity was moderately significantly correlated with total performance time only, while age showed no significant correlation with the ocular motility parameters. The eye movement abnormalities, however, exhibited by the patients in this study did not depend on the age at onset and the duration of onset.

Discussion

In this study, two-dimensional gaze analysis showed, for the first time, that the vertical component that deviated from the line of characters increased with the narrowing of the I/4 central visual field in eye movement during reading in patients with RP.

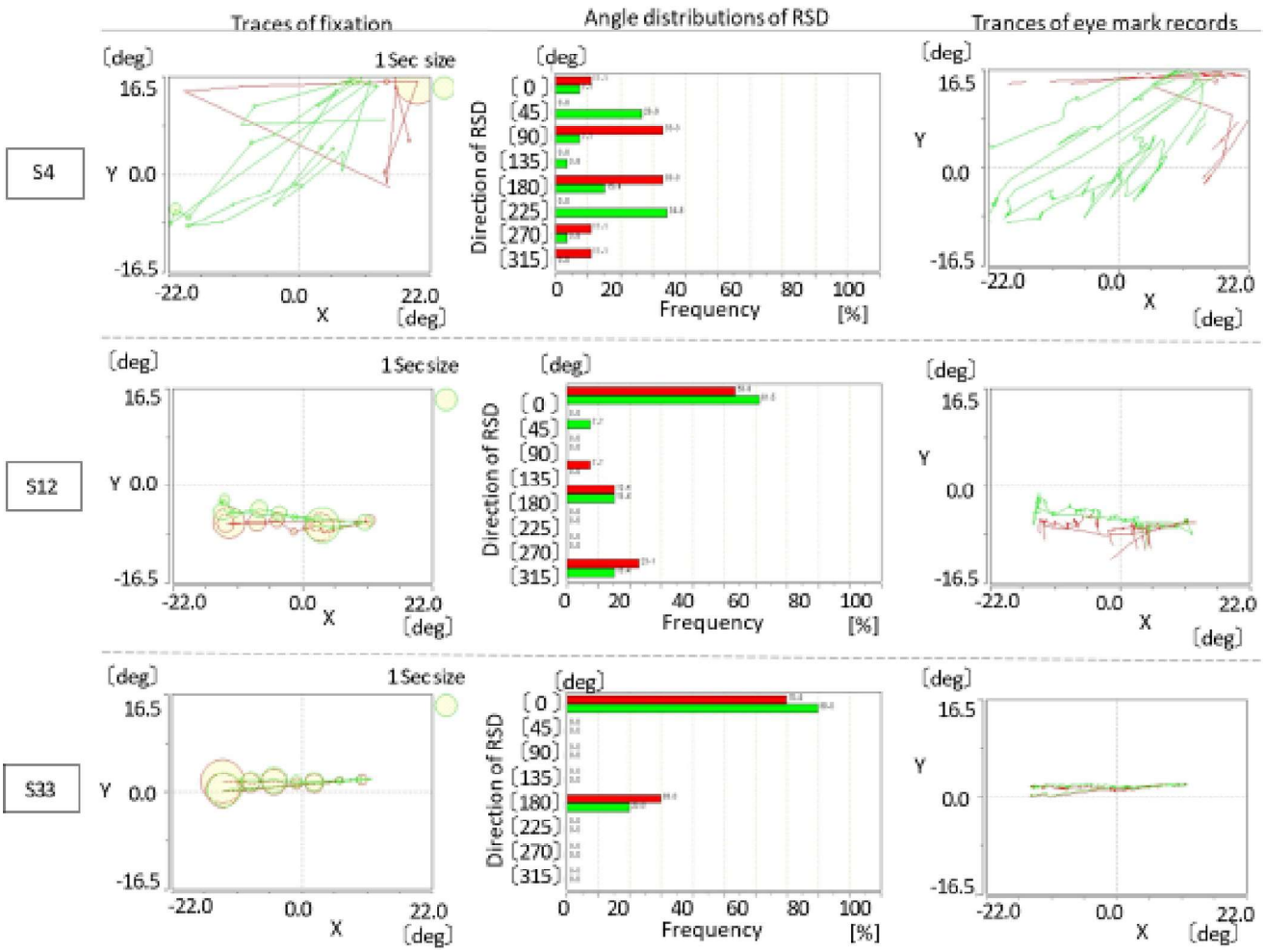

Fig 3. Typical examples of analyses of eye movements during reading. S4 traces for a patient with a visual field of 4˚ in the right eye (the green line) and 3˚ in the left eye (the red line). S12 traces for a patient with a visual field of 10˚ in the right eye (the green line) and 4˚ in the left eye (the red line). S33 traces for a healthy volunteer with a visual field of 100˚ in both eyes (right: the green line, left: the red line. **Left**: Traces of fixation. The size of the circle indicates the length of the residence time at that position. The red lines and circles reflect the movement of the left eye, and the green lines and circles reflect the movement of the right eye. **Middle**: Angle distribution of the rotation SC direction. The red and green bars denote the left and right eyes, respectively. **Right**: Traces of eye movements every 0.01 s. The red and green lines denote the traces of the left and right eyes, respectively. Abbreviations: SC, saccade.

https://doi.org/10.1371/journal.pone.0278682.g003

Reading is a repetition of fixation and SC. Saccades are triggered by position information of the peripheral retina; thus, the loss of the peripheral visual field is not limited to the lack of position information on the peripheral retina, which leads to impairment of the control system for eye movement direction and distance. Makiyama et al. reported that rod and pyramidal cells were damaged in the early stage of RP [18]. Loss of cells in the perifoveal region leads to increased modified SCs, likely increasing eye movement distance. Therefore, gaze analysis during reading in patients with RP requires the analysis of the movement angle between fixation as a means for expressing the deviation from lines of characters and the total eye movement distance as a means for expressing character oversights.

In this study, narrowed I/4 central visual field of patients with RP showed relatively higher correlations between all visual fields and the rotation SC of the trajectory of fixation than those between all visual fields and the regressive SC. Furthermore, there was a relatively stronger

Table 3. Correlation coefficients between parameters of visual function and eye movement analysis.

I/4 central visual field below 20		Analysis of ocular motility							
		Trajectory of fixation				Trajectory of eye movement			Task performance time
		No of FX	FX duration	Regressive SC	Rotation SC	ΣTotal	ΣX	ΣY	
Task performance time		0.385*	0.418*	-0.303	0.428*	0.385*	0.293	0.624**	-
Visual field	I/4 central	-0.459*	-0.026	0.022	0.317	-0.401*	-0.357	-0.448*	-0.486*
	V/4 perifovea	-0.386*	-0.169	0.189	-0.42	-0.397*	-0.373	-0.416*	-0.492**
	V/4 periphery	-0.316	(-)	0.194	-0.234	-0.043	-0.004	-0.248	-0.270
Acuity		0.207	0.125	0.102	-0.003	0.272	0.205	0.199	0.436*
Age		0.116	0.079	0.022	0.212	0.27	0.155	-0.041	0.058

1/4 central, 1/4 central visual field; V/4 perifovea, V/4 perifovea visual field; V/4 periphery, V/4 periphery visual field; Acuity, LogMAR; No of FX, number of fixations; FX duration, mean duration of fixation. We defined the significance levels of the correlation coefficients as follows: a correlation coefficient of ≥ 0.7 was defined as a " strong correlation," that of 0.4–0.69 as a "moderate correlation," that of 0.2–0.39 as a " weak correlation," and that of < 0.2 as "no correlation."

*, $p < 0.05$ vs. advanced group

**, $p < 0.01$ vs. advanced group.

https://doi.org/10.1371/journal.pone.0278682.t003

correlation between all visual fields and the vertical component (ΣY) rather than the horizontal component (ΣX) of the total eye movement distance. These results suggest that abnormalities in the vertical direction may be more prominent in patients with RP and that two-dimensional gaze analysis is necessary for patients with RP.

Additionally, in the one-line fixation trajectory of the gaze task, task performance time had a significant moderate correlation with rotation SC but not with regressive SC. Furthermore, the eye movement trajectory correlated significantly with task performance time for the total eye movement distance in the vertical direction ΣY but not for the total eye movement distance in the horizontal direction ΣX. The data indicate that the decrease in reading speed in patients with advanced RP is partly due to the increase in the vertical component in eye movement.

These results from a two-dimensional analysis of eye movements during reading support our hypothesis that eye movement in rotation directions causes reading difficulties in patients with advanced RP.

All previous studies of eye movements during reading were conducted on glaucoma patients with one-dimensional gaze analyses [7–12]. This time, the increase in movement in rotation directions (i.e., rotation SC) in patients with RP showed the strongest correlation with the V/4 perifoveal visual field, followed by the I/4 central visual field and V/4 peripheral visual field (Table 3). This suggests that even patients with glaucoma, whose disease starts from the peripheral visual field and results in the disappearance of the perifoveal visual field, may exhibit eye movement in rotation directions during reading, similar to patients with RP. However, glaucoma patients who retain peripheral vision may have a lower frequency of eye movements in rotation directions than patients with RP.

Reading involves foveal vision and peripheral vision [16, 19]. Rayner [19] and Ikeda et al. [4] reported that visual information processing in the parafoveal area with a viewing angle of 8˚ is important for determining the landing position of the next gaze point. The results in the present study, where, as with the I/4 central visual field, the V/4 perifoveal visual field was correlated with the extension of the total eye movement distance, suggest the relationship between the foveal vision and peripheral vision.

Ikeda et al. reported that the visual information of the parafoveal area affected the fixation duration [4]. However, the present study did not show any correlation between the visual field

and fixation duration. However, a report indicates that although not accompanied by a decrease in reading speed, the mean duration of fixation, which was correlated with the static visual field indicator HFA10-2, was extended in glaucoma patients [12]. Differences from previous research results may be due to differences in the visual field assessments used. In the future, there is a need to proceed with eye movement analyses on RP cases in the I/4 central visual field $< 5^{\circ}$ group and investigate the correlations between the HFA10-2-based retinal sensitivity distribution and GPK-based viewing angle (I/4 central visual field and V/4 perifoveal visual field) and eye movement.

The number of fixations gave a significant and strongest correlation with the I/4 central visual field and showed a significant but weak correlation with the task performance time. The increase in the number of fixations during reading in tunnel vision is consistent with the findings of the reports by Smith et al. [8, 9] and Murata et al. [12].

According to Morrison and Rayner [20], SC size was determined not by the viewing angle but by the letter spacing. Regarding the number of characters that can be seen and reading speed, Legge et al. [21] reported a decrease in reading speed with four characters or less. Osaka and Oda [22] reported a decrease in reading speed with five characters or less in Japanese with a mixture of kanji and kana characters. The printed reading material (viewing angle 0.857°) and gaze analysis task (viewing angle 1.045°) used in the present study had five consecutive characters with a viewing angle of around 5°. The results in the present study, where the decrease in the number of characters read and extension of task performance time according to the I/4 central visual field was only significant ($p < 0.05$) in the I/4 central visual field of $< 5^{\circ}$ group (advanced), were consistent with the results in the above-mentioned report.

In addition to the foveal viewing angle, several factors, such as visual acuity, contrast sensitivity [9, 23], and working memory [24], have been associated with reading ability. Research using static perimeters by Virgili et al. [5] showed that reading speed in patients with RP was correlated with visual acuity and contrast sensitivity and that the correlation was strongest with a mean retinal sensitivity within 6° of the fovea. Sandberg et al. [25] reported that the reading speed in patients with RP was correlated only with contrast sensitivity, not with the foveal visual field diameter. The gaze analysis task involved a display of easy-to-read Gothic font in 100% contrast to control for the effects of low vision and reduced retinal sensitivity. Multivariant regression and correlation analyses revealed that the visual acuity and I/4 central visual field played major roles in the number of letters read correctly. Further, the involvement of the perifoveal visual field and peripheral visual field were shown during reading of RP patients.

Our study had several limitations. The patients enrolled in this study were relatively young, so our findings cannot be generalized to older patients; thus, further studies that include older individuals are necessary. In addition, the number of patients in the advanced group was small; larger sample sizes are needed to identify significant correlations.

Conclusion

The present study clarified for the first time that reading difficulties in patients with RP are due to SC disorders in mainly vertical rotation SC. This result supports the notion that two-dimensional analysis is required for gaze measurements during reading in patients with RP. Our results also suggest that the involvement of the perifoveal visual field and peripheral visual field, as well as visual acuity and I/4 central visual field, is important for eye movement during reading. These are important findings that could elucidate the need for ophthalmic rehabilitation for patients with RP.

Supporting information

S1 Fig. Typical example of correlation analyses between gaze analyses and visual field. (A) Percentage (%) of the regression saccade (SC) relative to the total SC direction. (B) Percentage (%) of the rotation saccade>30˚ (RSD>30) relative to the total SC direction. (C) Number of fixations. (D) Duration(s) of fixation (> 0.1 s). The data of the 27 patients are presented.
(PPTX)

S2 Fig. Correlation analyses between number of letters correctly read and visual function in 27 patients. The graphs show the relationship between number of letters correctly read vs the I/4 central visual field (A), vs V/4 perifovea (B), vs V/4 periphery (C) and vs acuity (D).
(PPTX)

S1 Table. Analysis of ocular motility in our study population.
(DOCX)

S2 Table. Visual function measured with an eye mark recorder for all participants.
(DOCX)

Acknowledgments

The authors would like to express their deepest appreciation to Natsuki Tsujita and Haruka Nakamura (graduate students at the Graduate School of Medicine Kyoto University, Kyoto, Japan), Dr. Toshikazu Ikoma (Faculty of Health and Medical Sciences, Hokuriku University, Ishikawa, Japan), and Dr. Masashi Yamakawa (Department of Mechanical and System Engineering, Kyoto Institute of Technology, Kyoto, Japan). In addition, we would like to thank Editage (www.editage.com) for English language editing.

Author Contributions

Conceptualization: Masako Yoshida.

Data curation: Masako Yoshida, Akitoshi Seiyama.

Formal analysis: Masako Yoshida, Akitoshi Seiyama.

Investigation: Masako Yoshida.

Methodology: Masako Yoshida.

Project administration: Masako Yoshida.

Resources: Masako Yoshida.

Supervision: Akitoshi Seiyama.

Validation: Akitoshi Seiyama.

Visualization: Masako Yoshida.

Writing – original draft: Masako Yoshida.

Writing – review & editing: Masako Yoshida, Akitoshi Seiyama.

References

1. Grover S, Fishman GA, Brown J. Patterns of visual field progression in patients with retinitis pigmentosa. Ophthalmology. 1998; 105: 1069–1075. https://doi.org/10.1016/S0161-6420(98)96009-2 PMID: 9627658

2. Szlyk JP, Seiple W, Fishman GA, Alexander KR, Grover S, Mahler CL. Perceived and actual performance of daily tasks: relationship to visual function tests in individuals with retinitis pigmentosa. Ophthalmology. 2001; 108: 65–75. https://doi.org/10.1016/s0161-6420(00)00413-9 PMID: 11150266
3. Sugawara T, Hagiwara A, Hiramatsu A, Ogata K, Mitamura Y, Yamamoto S. Relationship between peripheral visual field loss and vision-related quality of life in patients with retinitis pigmentosa. Eye (Lond). 2010; 24: 535–539. https://doi.org/10.1038/eye.2009.176 PMID: 19590526
4. Ikeda M, Saida S. Span of recognition in reading. Vision Res. 1978; 18: 83–88. https://doi.org/10.1016/0042-6989(78)90080-9 PMID: 664279
5. Virgili G, Pierrottet C, Parmeggiani F, Pennino M, Giacomelli G, Steindler P, et al. Reading performance in patients with retinitis pigmentosa: a study using the MNREAD charts. Invest Ophthalmol Vis Sci. 2004; 45: 3418–3424. https://doi.org/10.1167/iovs.04-0390 PMID: 15452044
6. Rayner K. Eye movements in reading and information processing: 20 years of research. Psychol Bull. 1998; 124: 372–422. https://doi.org/10.1037/0033-2909.124.3.372 PMID: 9849112
7. Kanjee R, Yücel YH, Steinbach MJ, González EG, Gupta N. Delayed saccadic eye movements in glaucoma. Eye Brain. 2012; 4: 63–68. https://doi.org/10.2147/EB.S38467 PMID: 28539782
8. Smith ND, Glen FC, Crabb DP. Eye movements during visual search in patients with glaucoma. BMC Ophthalmol. 2012; 12: 45. https://doi.org/10.1186/1471-2415-12-45 PMID: 22937814
9. Smith ND, Glen FC, Mönter VM, Crabb DP. Using eye tracking to assess reading performance in patients with glaucoma: a within-person study. J Ophthalmol. 2014; 2014: 120528. https://doi.org/10.1155/2014/120528 PMID: 24883203
10. Burton R, Smith ND, Crabb DP. Eye movements and reading in glaucoma: observations on patients with advanced visual field loss. Graefes Arch Clin Exp Ophthalmol. 2014; 252: 1621–1630. https://doi.org/10.1007/s00417-014-2752-x PMID: 25074043
11. Kasneci E, Black AA, Wood JM. Eye-tracking as a tool to evaluate functional ability in everyday tasks in glaucoma. J Ophthalmol. 2017; 2017: 6425913. https://doi.org/10.1155/2017/6425913 PMID: 28293433
12. Murata N, Miyamoto D, Togano T, Fukuchi T. Evaluating silent reading performance with an eye tracking system in patients with glaucoma. PLOS ONE. 2017; 12: e0170230. https://doi.org/10.1371/journal.pone.0170230 PMID: 28095478
13. Yoshida M, Origuchi M, Urayama S, Takatsuki A, Kan S, Aso T, et al. fMRI evidence of improved visual function in patients with progressive retinitis pigmentosa by eye-movement training. NeuroImage Clin. 2014; 5: 161–168. https://doi.org/10.1016/j.nicl.2014.02.007 PMID: 25068106
14. Enright JT. Changes in vergence mediated by saccades. J Physiol. 1984; 350: 9–31. https://doi.org/10.1113/jphysiol.1984.sp015186 PMID: 6747862
15. Enright JT. Facilitation of vergence changes by saccades: influences of misfocused images and of disparity stimuli in man. J Physiol. 1986; 371: 69–87. https://doi.org/10.1113/jphysiol.1986.sp015962 PMID: 3701657
16. Hochberg J. Components of literacy: speculation and exploratory research. In: Levin H, Williams JP, editors. Basic studies on reading. New York: Basic Books; 1970. pp. 74–89.
17. Fukui M. College analysis, ver. 8.5. https://www.heisei-u.ac.jp/ba/fukui/analysis.html/ (downloaded on 2022.07.16).
18. Makiyama Y, Ooto S, Hangai M, Takayama K, Uji A, Oishi A, et al. Macular cone abnormalities in retinitis pigmentosa with preserved central vision using adaptive optics scanning laser ophthalmoscopy. PLOS ONE. 2013; 8: e79447. https://doi.org/10.1371/journal.pone.0079447 PMID: 24260224
19. Rayner K. The perceptual span and peripheral cues in reading. Cogn Psychol. 1975; 7: 65–81. https://doi.org/10.1016/0010-0285(75)90005-5
20. Morrison RE, Rayner K. Saccade size in reading depends upon character spaces and not visual angle. Percept Psychophys. 1981; 30: 395–396. https://doi.org/10.3758/bf03206156 PMID: 7322819
21. Legge GE, Pelli DG, Rubin GS, Schleske MM. Psychophysics of reading—I. Normal vision. Vision Res. 1985; 25: 239–252. https://doi.org/10.1016/0042-6989(85)90117-8 PMID: 4013091
22. Osaka N, Oda K. Effective visual field size necessary for vertical reading during Japanese text processing. Bull Psychon Soc. 1991; 29: 345–347. https://doi.org/10.3758/BF03333939
23. Burton R, Crabb DP, Smith ND, Glen FC, Garway-Heath DF. Glaucoma and reading: exploring the effects of contrast lowering of text. Optom Vis Sci. 2012; 89: 1282–1287. https://doi.org/10.1097/OPX.0b013e3182686165 PMID: 22885786
24. Osaka N, Osaka M, Kondo H, Morishita M, Fukuyama H, Shibasaki H. The neural basis of executive function in working memory: an fMRI study based on individual differences. Neuroimage. 2004; 21: 623–631. https://doi.org/10.1016/j.neuroimage.2003.09.069 PMID: 14980565

25. Sandberg MA, Gaudio AR. Reading speed of patients with advanced retinitis pigmentosa or choroideremia. Retina. 2006; 26: 80–88. https://doi.org/10.1097/00006982-200601000-00013 PMID: 16395143

Neuroscience Research 186 (2023) 43–50

Contents lists available at ScienceDirect

Neuroscience Research

journal homepage: www.sciencedirect.com/journal/neuroscience-research

Characterization of forehead blood flow bias on NIRS signals during neural activation with a verbal fluency task

Akitoshi Seiyama [a,b,*], Tatsuro Miura [a,b], Yuji Sasaki [a], Sayaka Okahashi [a,b,c], Nami Konishi [d], Monte Cassim [a,e]

[a] Human Health Sciences, Graduate School of Medicine, Kyoto University, 53 Kawahara-cho, Shogoin, Sakyo-ku, Kyoto 606-8507, Japan
[b] Creative Design & Data Science Center, Akita International University, Yuwa, Akita 010-1292, Japan
[c] Department of Social Science, National Center for Geriatrics and Gerontology, 7-430, Morioka-cho, Obu, Aichi 474-8511, Japan
[d] Department of Nursing, Kyoto Tachibana University, 34 Yamada-cho, Oyake, Yamashina-ku, Kyoto 607-8175, Japan
[e] Akita International University, Yuwa, Akita 010-1292, Japan

ARTICLE INFO

Keywords:
Near infrared spectroscopy
Forehead scalp blood flow
Cerebral blood flow
Modified Beer-Lambert Law
Hemodynamic separation method
Verbal fluency task

ABSTRACT

The major problem of near-infrared spectroscopy (NIRS) for brain activity measurement during verbal fluency task is the overlapping forehead scalp blood flow (FBF) on the target cerebral blood flow (CBF). There could be among-individual differences in the influence of FBF on CBF. We investigated effects of FBF on CBF by comparing signals obtained through a laser Doppler flowmeter (LDF) and NIRS using the modified Beer-Lambert Law (MBLL). Among 25 healthy individuals, 7 participants showed a strong correlation between LDF and NIRS signals (r_s >0.500). There were no significant differences according to age or sex. Subsequently, we applied the hemodynamic separation method to the values calculated using the MBLL ($\Delta[\text{oxy-Hb}]_M$): to separate the concentration of oxygenated hemoglobin in the forehead ($\Delta[\text{oxy-Hb}]_F$) and cerebral cortex ($\Delta[\text{oxy-Hb}]_C$). First, we found that the influence of $\Delta[\text{oxy-Hb}]_F$ on $\Delta[\text{oxy-Hb}]_C$ in the high r_s group was almost twice as large as that in the low r_s group. Second, presence of sex and age differences in the influence of $\Delta[\text{oxy-Hb}]_F$ on $\Delta[\text{oxy-Hb}]_C$ were suggested. Based on the results, we discuss the factors affecting FBF and the resulting variations in NIRS signals.

1. Introduction

During the last three decades, near-infrared spectroscopy (NIRS) has become a powerful tool for noninvasive and continuous examination of cognitive (Agbangla et al., 2017), emotional (Bendall et al., 2016), and psychiatric (Chou et al., 2020) brain function. However, since NIRS involves the emission of near-infrared light from the scalp surface into the intracranial region via the skull, forehead scalp blood flow (FBF) could have interference effects on the calculated NIRS signals, including changes in the concentrations of oxygenated, deoxygenated, and total hemoglobin (Δ[oxy-Hb], Δ[deoxy-Hb], and Δ[total-Hb], respectively) (Takahashi et al., 2011; Kirilina et al., 2012). This interference is especially large for continuous-wave NIRS based on the analytical algorithm of the modified Beer-Lambert law (MBLL). To minimize the effect of FBF on NIRS signals, various approaches based on the NIRS system have been proposed, including spatially resolved spectroscopy (Yamada et al., 2009), frequency-domain spectroscopy (Fantini and Sassarolin, 2020), and time-resolved spectroscopy (Milej et al., 2020), as well as analytical algorithms, including independent component analysis (Kohno et al., 2007), wavelet analysis (Tsunashima et al., 2009), and diffuse optical tomography (Tian and Liu, 2014).

Recently, Yamada et al. (2012) proposed a method for separating conventional NIRS signals into functional and systemic components, even when the task involves motion, with the assumption of differences in hemodynamic responses in the microcirculation between the cerebral and outer cerebral regions during task performance (hemodynamic separation method, HDSM). Initially, their definition was based on the separation of the functional and systemic blood flow components during neural activation.

However, the aforementioned studies focused on clarifying the cerebral blood flow (CBF), rather than the FBF, during task performance. Since there are differences in changes in the FBF during task performance across individuals (Drummond, 1997; Liu et al., 2018), it is important to separately consider the FBF and CBF, as well as to characterize FBF in individuals, to facilitate elucidation of human brain function under various conditions.

* Corresponding author at: Creative Design & Data Science Center, Akita International University, Yuwa, Akita 010-1292, Japan.
E-mail address: aseiyama@gl.aiu.ac.jp (A. Seiyama).

https://doi.org/10.1016/j.neures.2022.09.012
Received 11 April 2022; Received in revised form 1 September 2022; Accepted 25 September 2022
Available online 30 September 2022

Verbal fluency tasks (VFTs) are commonly used to investigate prefrontal cortical function in humans, especially cognitive function in the elderly (Appell et al., 1982; Storandt et al., 1984). They comprise two types of tests; namely, the letter fluency test (LFT) and word fluency test (WFT). In the LFT, each participant is asked to generate as many words as possible orally within 60-s using three letters each as the first syllable (e.g., /a/, /s/, /p/). In the WFT, the participants are asked to generate as many words as possible orally within 60-s according to three categories (e.g., animal, fruit, and fish). The LFT and WFT mainly involve the frontal and temporal cortices, respectively (Martin et al., 1994). Moreover, compared with the WFT, the LFT is less affected by the participants' educational history, especially within the first 30-s of task performance (Crow, 1998; Ito and Hatta, 2002). Therefore, the LFT has been recently used for differential diagnosis coupled with functional NIRS monitoring of the bilateral prefrontal cortices, including the dorsolateral Brodmann's area 9, 46 (BA 9, 46), ventrolateral (BA 44, 45), and frontopolar (BA 10), as well as the superior temporal cortical surface regions (Takizawa et al., 2014; Husain et al., 2020). Changes in the oxygenated Hb concentration (Δ[oxy-Hb]) are used as a functional indicator of brain activation since they are strongly correlated with increased cerebral blood flow (CBF) accompanying brain activation. Therefore, Δ[oxy-Hb] is considered as a reliable indicator of CBF (Malonek et al., 1997; Strangman et al., 2002). However, several studies have reported that changes in the FBF during the VFT overlap in the cortical Δ[oxy-Hb] calculated using the MBLL, which causes overestimation of the stimulus-induced changes in the cortical Δ[oxy-Hb] (Takahashi et al., 2011; Kirilina et al., 2012). This is a crucial problem in the application of NIRS to aid psychiatric diagnoses, given that the "integral and centroid values" (horizontal and vertical axes, respectively) are used in the judgments of neural status. The integral value is defined as "the size of the hemodynamic response during the 60-s activation task period" while the centroid value serves as an index of time-course changes throughout the task, with the periods representing the timing of hemodynamic responses (Takizawa et al., 2014; Husain et al., 2020).

Furthermore, the regulation of facial blood flow differs across regions (Liu et al., 2018); moreover, FBF is regulated by both sympathetic and parasympathetic nerves. Specifically, sympathetic nerve regulation is dominant for the eyelids, cheeks, and chin region as a vasodilator and the nose and ear regions as a vasoconstrictor (Drummond, 2012). Therefore, we hypothesized that the effects of FBF on CBF differ across individuals.

This study aimed to evaluate changes in FBF and the influence of FBF on functional CBF in participants while performing VFT. Specifically, we aimed to discuss the factors affecting FBF while performing a VFT, the influences of FBF on CBF, and sex and age differences in the effects of FBF on CBF regulation while performing a VFT.

2. Materials and methods

2.1. Participants

This study was approved by the Kyoto University Graduate School and the Faculty of Medical Ethics Committee; moreover, it adhered to the tenets of the Declaration of Helsinki. We included 25 healthy right-handed Japanese volunteers who provided written informed consent before participation. There were 11 men (mean age ± standard deviation [s.d.] = 45.5 ± 12.6 years, 26–66 years) and 14 women (42.2 ± 15.9 years, 23–67 years). The participants were divided into five groups according to age, i.e., participants in their 20 s (24.5 ± 1.6; four women and two men), 30 s (36.8 ± 4.5; two women and two men), 40 s (41.5 ± 1.5; two women and four men), 50 s (56.0 ± 1.8; two women and two men), and 60 s (64.6 ± 2.8; three women and two men).

2.2. Verbal fluency tasks

A single trial LFT was used to examine stimulus-induced brain activation in each subject. In the LFT, each trial comprised a 30-s pre-task control period, a 60-s task period, and a 70-s post-task control period. During the control period, the participants were requested to repeatedly verbalize five Japanese vowels (/a/, /i/, /u/, /e/, and /o/). During the task period, the participants were requested to verbalize as many words as possible that begin with one Japanese character (hiragana, indicating a syllable) shown on a computer screen at 20-s intervals (three characters per 60-s task period). At the start, the characters /ko/, /ka/, and /si/ were shown on the screen. These are the most frequently used sounds at the beginning of Japanese words, as indicated in the Japanese dictionary, Sanseido Shin Meikai Kokugo Dictionary.

2.3. Multimodal NIRS measurements

We performed simultaneous measurements using a 19-channel NIRS (FOIRE-3000, Shimadzu, Japan) and a laser Doppler flowmeter (LDF) (FLO-C1, Omega Flow, Japan) at 0.07-s sampling intervals. The NIRS was used as a master instrument; additionally, LDF signals (see below) were input through analog input channels of the NIRS. Changes in the concentrations (expressed as arbitrary units [a.u.]) of oxygenated (Δ[oxy-Hb]) and deoxygenated Hb (Δ[deoxy-Hb]) using three NIR light wavelengths (780, 805, and 830 nm) (Hori et al., 2017). We used seven emitter and seven detector optodes (Fig. 1A). The emitter and detector distances were set 3 cm apart in a 2-by-7 array (Oonishi et al., 2014). The areas between each emitter and detector pair were defined as measurement channels. The channels were assumed to correspond to cortical regions located 2–3 cm beneath the scalp surface (Seiyama et al., 2004). We placed the optode-set on the forehead, with the lowest optode-line being placed along the T4-Fpz-T3 line of the International EEG system. This arrangement allowed measurements of changes in the Hb concentrations in the bilateral prefrontal cortex (PFC), frontopolar cortex, and anterior regions of the superior and middle temporal cortices.

We attached one LDF probe to the left (or right) temple centered between the corner of the left (or right) eye and the base of the left (or right) ear. The FLO-C1 allowed measurement of the velocity (velocity [LDF]. Subsequently, we calculated the number of red blood cells (RBCs) simultaneously in a tissue (mass [LDF]) and the mass flow of RBCs (flow [LDF]) as the product of the RBC number and velocity (see Fig. 1C). The distance between the incident and detecting optical fibers was 500 μm; further, the mean optical depth from the tissue surface was approximately 1 mm, which allowed measurement of hemodynamic parameters only in the skin or scalp area (Kashima et al., 1994).

2.4. Signal processing

2.4.1. NIRS signal analysis using the modified Beer-Lambert Law (MBLL)

First, we estimated changes in the concentrations of Hb species ($\Delta[\text{oxy-Hb}]_M$, $\Delta[\text{deoxy-Hb}]_M$, and $\Delta[\text{total-Hb}]_M$ (= $\Delta[\text{oxy-Hb}]_M$ + $\Delta[\text{deoxy-Hb}]_M$)) from control conditions based on the MBLL (Seiyama et al., 1988; Wray et al., 1988) using the extinction coefficient of chromophores reported by Matcher et al. (1995). We processed the subsequent NIR signals as follows: a moving average with a time window of 4.2-s was applied to remove short-term motion artifacts in the analyzed data. Based on the report by Takizawa et al. (2008), we set pre- and post-task baselines as the mean across the last 10-s and 5-s of the pre-task and post-task periods, respectively. We performed linear fitting based on the data of the two baselines.

2.4.2. NIRS signals analyzed using the hemodynamic separation method (HDSM)

The NIRS signals analyzed using the MBLL method were further separated to the functional and forehead components according to the

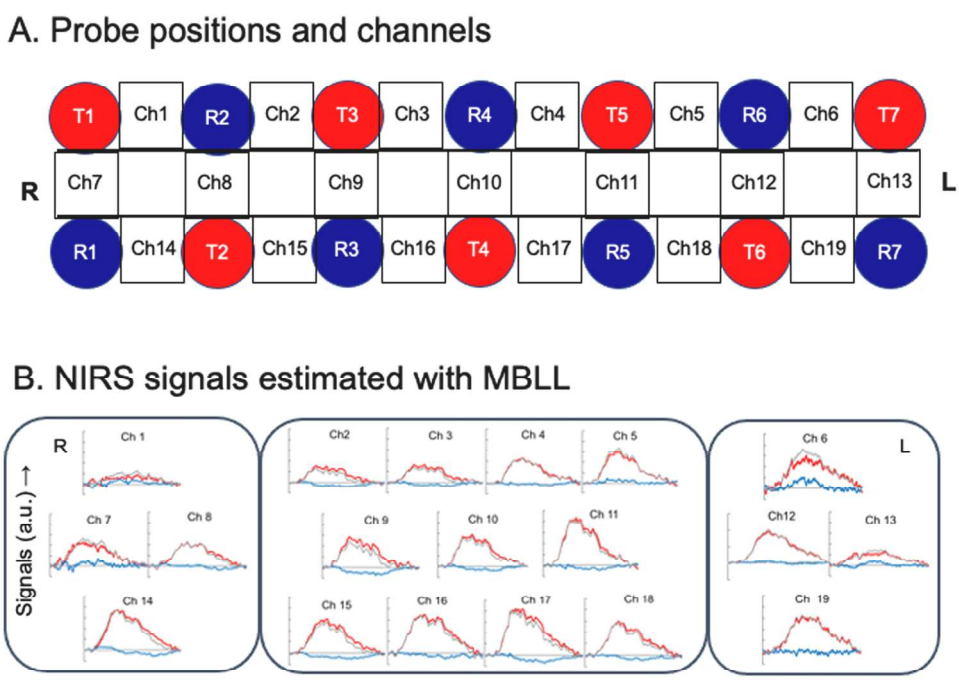

Fig. 1. NIRS probe positions. NIRS signals estimated using the MBLL and LDF signals along a typical common time course. (A) Probe positions of incident (red) and detection (blue) lights as well as measurement channels (white). (B) A typical example of NIRS parameters estimated using the MBLL, with concentration changes in oxy-Hb (Δ[oxy-Hb]$_M$, red line), deoxy-Hb (Δ[deoxy-Hb]$_M$, blue line), and total-Hb (Δ[total-Hb]$_M$, green line) in the R-VPC (Chs 1, 7, 8 and 14), FPC (Chs 2, 3, 4, 5, 9, 10, 11, 15, 16, 17, and 18), and L-VPC (Chs 6, 12, 13 and 19). The vertical axis denotes changes in the Hb parameters (Δ[Hb]$_M$) [ranging from − 0.05–0.15 arbitrary units]). Horizontal axis denotes time (s), where the control, task, and post-task periods are 0–10, 10–60, 60–120-s. (C) Changes in the forehead blood flow parameters measured using a laser Doppler Flowmeter (LDF), where Flow(LDF), Velocity (LDF), and Mass(LDF) denote the erythrocyte flow rate, erythrocyte velocity, and number of erythrocytes within 1-mm tissue depth, respectively. Time course is similar to that shown in (B).

method of Yamada et al. (2012). In brief, we used a fNIRS package provided by the National Institute of Advanced Industrial Science Technology (downloaded 2015). The functional components of NIRS signals due to the change in CBF (Δ[oxy-Hb]$_C$ and Δ[deoxy-Hb]$_C$) and the systemic components of NIRS signals those in the FBF (Δ[oxy-Hb]$_F$ and Δ[deoxy-Hb]$_F$) were estimated assuming the presence of following relations: Δ[deoxy-Hb]$_C = k_c \bullet \Delta$[oxy-Hb]$_C$ where k_c (a constant functional parameter) $= -0.6$ and Δ[deoxy-Hb]$_F = k_f \bullet \Delta$[oxy-Hb]$_F$ where essentially $0 < k_f$ (a constant systemic parameter) < 1 (cf. Supplementary Fig S1) but we also counted cases of $k_f = 0$ and ≥ 1 (cf., Supplementary Fig S2) taking account of the systemic fluctuation originated by arterial system and congestion in vascular beds, respectively.

The 19 channels were clustered into three groups; further, we synthesized the NIRS signals in each cluster (see Fig. 1A and B). The first cluster of 11 channels was approximately located at the frontopolar and dorsolateral PFC. The second and third clusters comprised four channels approximately located at the left and right ventrolateral PFC (L-VPC and R-VPC, respectively). Channels containing artifacts, including apparently large motion artifacts and/or low signal-to-noise ratios, were not included in the analyses. The synthesized Δ[oxy-Hb] was used as an index of brain functional activation and quantified using two visual spatiotemporal indices; namely, the integral and centroid values (Takizawa et al., 2014). The integral values of the Δ[oxy-Hb]$_M$, Δ[oxy-Hb]$_C$, Δ[oxy-Hb]$_F$ (i.e., integral Δ[oxy-Hb]$_M$, integral Δ[oxy-Hb]$_C$, and integral Δ[oxy-Hb]$_F$) were the area under the curve of Δ[oxy-Hb] during the task period; moreover, they were indices of the magnitude of the hemodynamic response. The centroid values [unit, second (s)] are indicated by a perpendicular line from the centroid time, which yielded half of the integral values of Δ[oxy-Hb]$_M$, Δ[oxy-Hb]$_C$, or Δ[oxy-Hb]$_F$ throughout all the task periods.

2.5. Statistics

We performed correlation analyses among the time courses of NIRS signals (Δ[oxy-Hb]$_M$, Δ[oxy-Hb]$_C$, Δ[oxy-Hb]$_F$) and the standardized LDF signal using Spearman's rank-order correlation coefficients. A correlation coefficient (r_s) ≥ 0.500 indicated the presence of a significant correlation. The centroid and integral values were expressed as the mean $\pm$ standard deviation (s.d.). We used the Wilcoxon t-test with Bonferroni correction after Friedman's χ^2 r-test to compare NIRS signals before and after HDSM (i.e., Δ[oxy-Hb]$_M$, Δ[oxy-Hb]$_C$, Δ[oxy-Hb]$_F$). The Kruskal Wallis H-test and joint Wilcoxon test were used to analyze differences according to age. The Mann-Whitney U-test was used to compare sex and age differences. Statistical significance was set at $p < 0.05$. Cohen's d was calculated to determine the effect size.

3. Results

3.1. Separation of hemoglobin in the forehead scalp and cerebral cortex

Fig. 1 A shows the positions of the optical probes and channels (see Methods, the section regarding multimodal fNIRS measurements). Fig. 1B shows typical examples of the time course of changes in NIRS parameters (i.e., Δ[oxy-Hb]$_M$, Δ[deoxy-Hb]$_M$, and Δ[total-Hb]$_M$)

estimated using the MBLL method. Additionally, Fig. 1C shows the hemodynamic LDF parameters [Velocity (LDF), Mass (LDF), and Flow (LDF)] in the forehead simultaneously measured with LDF. For functional analyses, Δ[oxy-Hb]$_M$ in 11 channels in the PFC (i.e., channels 2, 3, 4, 5, 9, 10, 11, 15, 16, 17, and 18 in Fig. 1A) were target signals; moreover, we examined correlations between the Δ[oxy-Hb]$_M$ and the LDF signals to estimate the effect of the forehead hemodynamic change on the cerebral hemisphere. Among the LDF parameters, flow (LDF) showed the highest correlation with Δ[oxy-Hb]$_M$ (averaged values of correlation coefficient (r_s) from the 11 channels was 0.735) (Fig. 3A). The integral value of Δ[oxy-Hb]$_M$ during the task period (i.e., Δ[oxy-Hb]$_M$) was 512 (a.u.).

To separate Hb parameters in the cortex (Δ[Hb]$_C$; i.e., Δ[oxy-Hb]$_C$, Δ[deoxy-Hb]$_C$, and Δ[total-Hb]$_C$) and those in the forehead scalp (Δ[Hb]$_F$; i.e., Δ[oxy-Hb]$_F$, Δ[deoxy-Hb]$_F$, and Δ[total-Hb]$_F$) from those estimated using the MBLL method (Δ[Hb]$_M$; i.e., Δ[oxy-Hb]$_M$, Δ[deoxy-Hb]$_M$, and Δ[total-Hb]$_M$), we applied the HDSM on the Δ[Hb]$_M$. Figs. 2A and 2B shows typical examples of the time courses of Δ[Hb]$_C$ and Δ[Hb]$_F$, respectively. Results of the separation of Δ[oxy-Hb]$_M$ to Δ[oxy-Hb]$_C$ and Δ[oxy-Hb]$_F$ in 25 participants using HDSM are summarized in Table 1. Each parameter was significantly separated.

To clarify the method, we compared the NIRS parameters and the forehead scalp blood flow parameters measured using LDF, which reflect the hemodynamic parameters in the surface of the forehead (~1 mm from the skin surface). The r_s value between flow (LDF) and Δ[oxy-Hb]$_F$ or that and Δ[oxy-Hb]$_C$ were 0.762 or 0.399, respectively (see Figs. 3B and 3C). Changes in Δ[oxy-Hb]$_C$ and Δ[oxy-Hb]$_F$ during the VFT (i.e., integral Δ[oxy-Hb]$_C$ and integral Δ[oxy-Hb]$_F$) were 85.2 and 426.8, respectively; additionally, the ratio of integral Δ[oxy-Hb]$_F$ to integral Δ[oxy-Hb]$_C$ was ca. 5.0.

Table 2 shows the correlation coefficients (r_s) between the FBF measured with the LDF (Flow [LDF]) and NIRS signals. First, we separated the high r_s group (n = 7), where $r_s > 0.500$ (Δ[oxy-Hb]$_M$ vs. Flow [LDF]), and the low r_s group (n = 18), where r_s was below 0.500. We defined the former and latter as the high- and low-FBF-influenced groups, respectively (1st row in Table 2). Subsequently, we analyzed Δ[oxy-Hb]$_F$ and Δ[oxy-Hb]$_C$ in each group (2nd and 3rd row in Table 2). In both groups, the values of r_s were in the order of Δ[oxy-Hb]$_F$ > Δ[oxy-Hb]$_M$ > Δ[oxy-Hb]$_C$.

NIRS signals are usually obtained using the MBLL method. However, these signals contain Hb in both the cerebral cortex and forehead scalp. To obtain accurate NIRS signals from the cerebral cortex and to allow accurate diagnosis, it is important to separate Hb in the cerebral cortex and forehead scalp. Table 3 shows the relationship between the integral NIRS values before (i.e., MBLL only) and after HDSM. The ratio of integral Δ[oxy-Hb]$_C$ to integral Δ[oxy-Hb]$_M$ in the low r_s group (mean value of 0.683) was almost twice larger than that in the high r_s group (mean value of 0.326). Contrastingly, the ratio of integral Δ[oxy-Hb]$_F$ to integral Δ[oxy-Hb]$_C$ in the low r_s group (mean value of 1.84) was almost half of that in the high r_s group (mean value of 3.84).

3.2. Sex differences in hemoglobin in the forehead scalp and cerebral cortex

Figs. 4A and 4B show the distribution of integral Δ[oxy-Hb]$_M$ (closed circle; i.e., before HDSM) and integral Δ[oxy-Hb]$_C$ (open circle; i.e., after HDSM) of 11 male respondents and 14 female respondents, respectively. Although there were no significant sex differences in the distributions of integral Δ[oxy-Hb]$_M$ (p = 0.309) and integral Δ[oxy-Hb]$_C$ (p = 0.118), there were large effective size (d) values for integral Δ[oxy-Hb]$_M$ and integral Δ[oxy-Hb]$_C$ (d = 0.468 and d = 0.655, respectively).

Before HDSM, men had a larger distribution of integral Δ[oxy-Hb]$_M$ (range: −78.9 to 521.0) than women (range: −16.7 to 185.0). However, after HDSM, women had a larger distribution of integral Δ[oxy-Hb]$_C$ (range: −71.2 to 56.6) than men (range: −8.3 to 85.2) (see discussion).

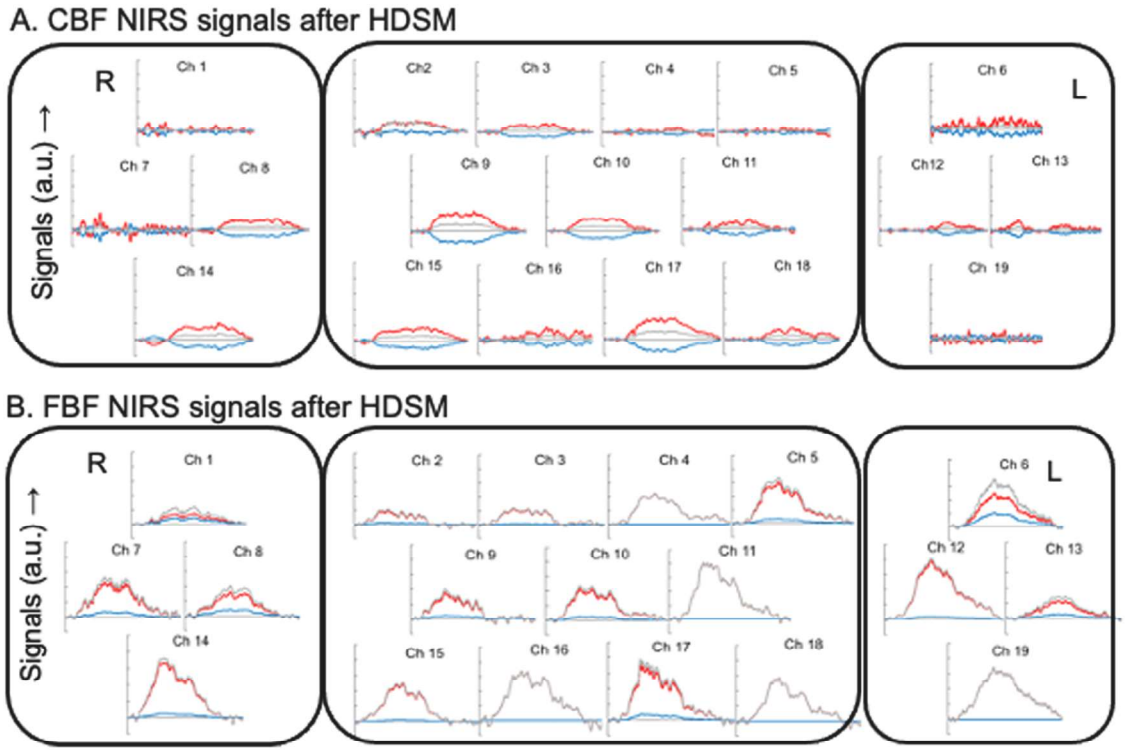

Fig. 2. Time courses of NIRS signals of CBF and FBF after HDSM application. (A) A typical example of Δ[Hb]$_C$ obtained after the HDSM. (B) A typical example of Δ[Hb]$_F$ obtained after HDSM application. The ranges and units in the vertical and horizontal axes are similar to those in Fig. 1B. Fig. 1B shows the original data (Δ[Hb]$_M$) before HDSM application. The right, middle, and lefts clusters are the same as those in Fig. 1B [R-VPC (Chs 1, 7, 8, and 14), FPC (Chs 2, 3, 4, 5, 9, 10, 11, 15, 16, 17, and 18), and L-VPC (Chs 6, 12, 13, and 19)].

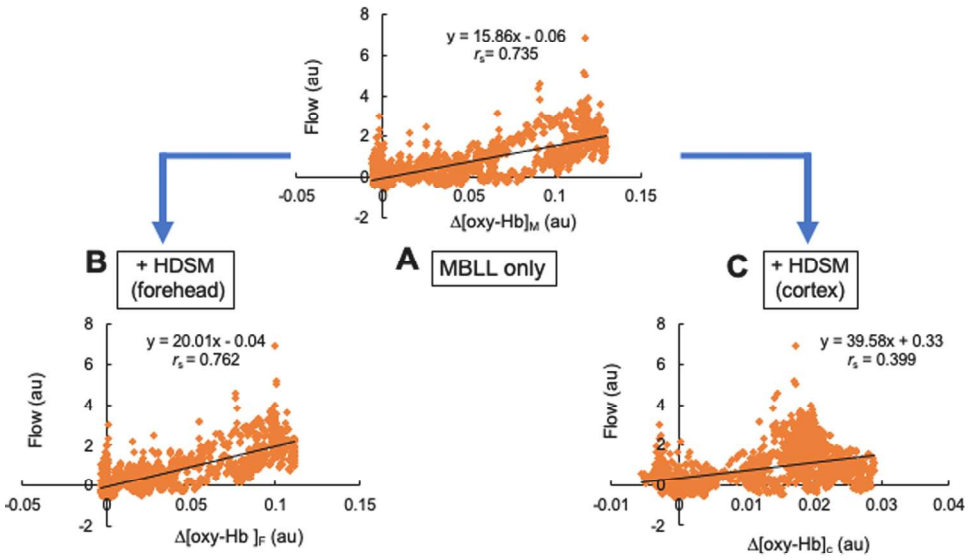

Fig. 3. Correlation analyses between time course changes in NIRS signals and Flow (LDF) measurements. Typical example of correlation analyses between NIRS and LDF signals before [A, Δ[oxy-Hb]$_M$ vs. Flow(LDF)] and after HDSM application [B, Δ[oxy-Hb]$_F$ vs. Flow (LDF); C, Δ[oxy-Hb]$_C$ vs. Flow(LDF)]. Original data are shown in Fig. 1B and 1C for Δ[oxy-Hb]$_M$ vs. Flow(LDF) while those for Δ[oxy-Hb]$_F$ vs. Flow(LDF) and Δ[oxy-Hb]$_C$ vs. Flow(LDF) are shown in Figs. 2B and 2A, respectively. Flow(LDF) was similar to that shown in Fig. 1C.

Table 1
Separation of Δ[oxy-Hb]$_M$ to Δ[oxy-Hb]$_C$ and Δ[oxy-Hb]$_F$ using HDSM.

Parameter	Mean	SD
Δ[oxy-Hb]$_M$	98.06 **	120.9
Δ[oxy-Hb]$_F$	78.76 *	101.4
Δ[oxy-Hb]$_C$	23.28^{++}	32.8

**, $p < 0.01$; Δ[oxy-Hb]$_M$ vs Δ[oxy-Hb]$_C$ (n = 25)
* , $p < 0.05$; Δ[oxy-Hb]$_M$ vs Δ[oxy-Hb]$_F$ (n = 25)
$^{++}$, $p < 0.01$; Δ[oxy-Hb]$_C$ vs Δ[oxy-Hb]$_F$ (n = 25)

Table 2
Correlation coefficients between time course changes in Flow (LDF) and NIRS signals.

Time course in	High r_s Group (n = 7)	Low r_s Group (n = 7)
Δ[oxy-Hb]$_M$	0.677 ± 0.089	0.287 ± 0.154
Δ[oxy-Hb]$_F$	0.682 ± 0.084	0.317 ± 0.131
Δ[oxy-Hb]$_C$	0.362 ± 0.190	0.225 ± 0.138

Data are expressed as mean values ± SD. The high r_s group showed a correlation coefficient $r_s > 0.500$ between time course changes in Flow(LDF) and Δ[oxy-Hb]$_M$ obtained using the MBLL method. Δ[oxy-Hb]$_F$ and Δ[oxy-Hb]$_C$ denote Δ[oxy-Hb] in the forehead scalp and cortex, respectively, after HDSM.

Table 3
Relationship between integral values of NIRS signals before (MBLL only) and after HDSM.

Ratio of integral Δ[oxy-Hb]	High r_s Group (n = 7)	Low r_s Group (n = 18)
Δ[oxy-Hb]$_C$ to Δ[oxy-Hb]$_M$	0.326 ± 0.24	0.683 ± 1.01
Δ[oxy-Hb]$_F$ to Δ[oxy-Hb]$_C$	3.84 ± 3.30	1.84 ± 1.07

Data are expressed as mean values ± SD. Δ[oxy-Hb]$_M$ denote the integral values of Δ[oxy-Hb] obtained using the MBLL method. Δ[oxy-Hb]$_F$ and Δ[oxy-Hb]$_C$ denote the integral values in the forehead scalp and cortex, respectively, after HDSM.

Among women, all values of integral Δ[oxy-Hb]$_C$ showed a left shift from those of integral Δ[oxy-Hb]$_M$ (the values became small). Contrastingly, the values among men were within the range of 0–100 (see the direction of arrows in the Figure (Figs. 4A and 4B)) (see discussion).

3.3. Age differences in hemoglobin in the forehead scalp and cerebral cortex

Fig. 5 shows an age-based comparison of the scatter plots of the centroid (vertical axis) and integral values (horizontal axis) of Δ[oxy-Hb] before HDSM (Fig. 5A) and after HDSM (Fig. 5B), where participants were classified as follows according to age: 20 s (n = 5), 30 s (n = 4), 40 s (n = 6), and 50–60 s (n = 5 for women and n = 4 for men). In the 50–60 s cohort, men and women were divided given the presence of menopause and post-menopause in women. In each group, the centroid values (i.e., Centroid Δ[oxy-Hb]$_M$ in Fig. 5A and Centroid Δ[oxy-Hb]$_C$ in Fig. 5B) showed no remarkable differences according to age groups as well as before and after HDSM. However, there were two remarkable findings regarding integral Δ[oxy-Hb]$_M$ and integral Δ[oxy-Hb]$_C$ as follows.

First, although we had observed two exceptions in men (see Fig. 4A and the above section) in all age cohorts, the integral Δ[oxy-Hb]$_C$ after removing the Δ[oxy-Hb]$_F$ in 23 participants were smaller than those of integral Δ[oxy-Hb]$_M$ ($d > 0.599$) (see discussion). Second, the distribution of integral values for the 20 s group was larger than those for other age cohorts, both before and after HDSM (see discussion).

4. Discussion

It is important to identify stimulus-induced neural activation by NIRS based on functional hyperemia (neurovascular coupling) and changes in Δ[deoxy-Hb] (Malonek et al., 1997; Strangman et al., 2002). Under conditions of suppressed scalp blood flow, simultaneous NIRS measurements and functional magnetic resonance imaging (fMRI) revealed that balances between Δ[oxy-Hb] and Δ[deoxy-Hb] were dependent on hemodynamic conditions in the cerebral microcirculation (Seiyama et al., 2004). Stimulus-induced neural activation under normal conditions is characterized by an increase in Δ[oxy-Hb] and a small decrease in Δ[deoxy-Hb]; contrastingly, an increase in both Δ[oxy-Hb] and Δ[deoxy-Hb] characterize the congestion condition. In the case of blood flow interference in the extracortical regions, Yamada et al. (2012) proposed HDSM for separating CBF and FBF (referred to as functional and systemic components, respectively). They assumed that during task performance, CBF showed an increase in Δ[oxy-Hb] and a decrease in Δ[deoxy-Hb] according to the normal hemodynamic response. Contrastingly, the FBF showed an increase in both Δ[oxy-Hb] and Δ[deoxy-Hb] due to passive dilation and changes in vascular bed compliance in the extracortical regions. To clarify this method, we compared CBF

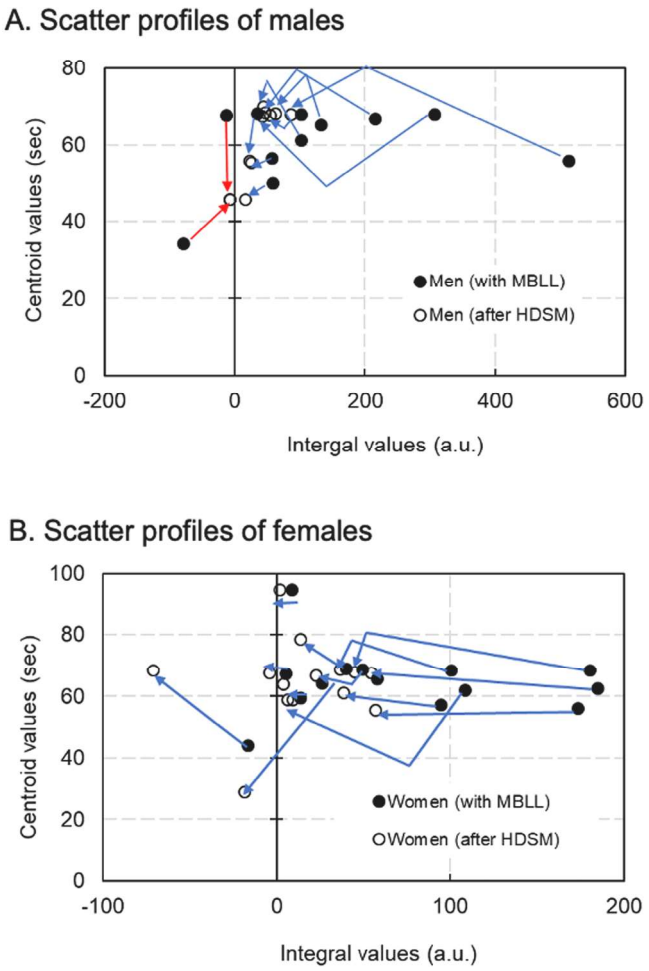

Fig. 4. Sex differences in NIRS parameters before (MBLL only) and after HDSM application. A comparison of scatter plots of the centroid (vertical axis) and integral values (horizontal axis) of Δ[oxy-Hb]. The arrows denote the directions of changes in parameters before (black circles) to after (white circles) HDSM application. The blue and red arrows show the left- and right-shifts of the parameters, respectively. (A) Scatter plot of Centroid $\Delta[\text{oxy-Hb}]_M$ and Integral $\Delta[\text{oxy-Hb}]_M$ for men (i.e., before HDSM) are shown using closed circles while those after HDSM (i.e., Centroid $\Delta[\text{oxy-Hb}]_C$ and Integral $\Delta[\text{oxy-Hb}]_C$) are shown using white circles. (B) Scatter plot of Centroid $\Delta[\text{oxy-Hb}]_M$ and Integral $\Delta[\text{oxy-Hb}]_M$ for women (i.e., before HDSM) are shown using closed circles while those after HDSM (i.e., Centroid $\Delta[\text{oxy-Hb}]_C$ and Integral $\Delta[\text{oxy-Hb}]_C$) are shown using white circles.

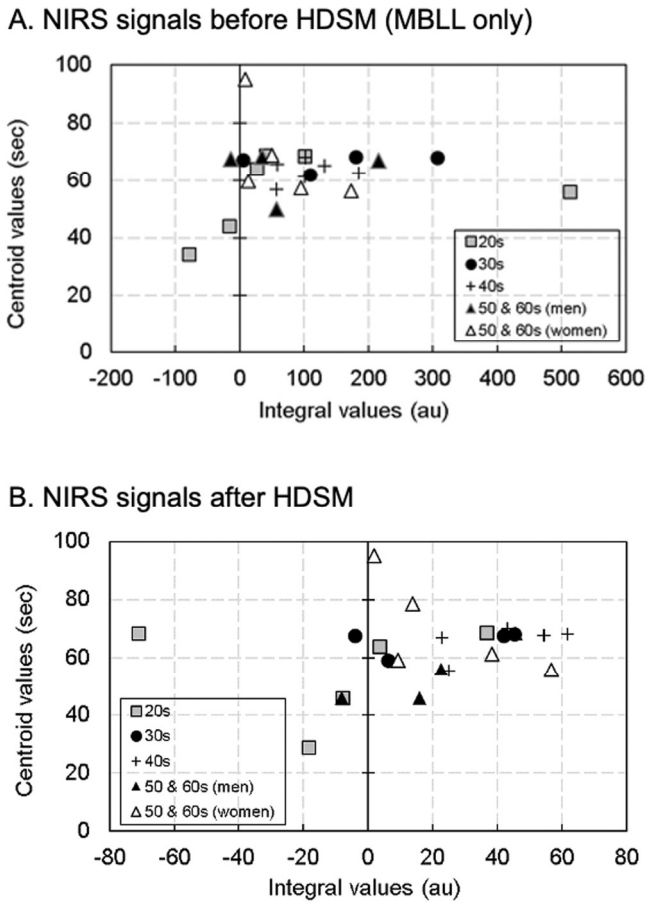

Fig. 5. Age differences in NIRS signals before (MBLL only) and after HDSM Comparison of scatter plots of the centroid (vertical axis) and integral values (horizontal axis) of Δ[oxy-Hb] before (A) and after HDSM (B) are shown.

parameters measured using NIRS and FBF parameters measured using LDF, which reflects the hemodynamic parameters on the forehead surface (~1 mm from the skin surface).

Table 2 and Fig. 3 indicate that the r_s values were in the order of $\Delta[\text{oxy-Hb}]_F > \Delta[\text{oxy-Hb}]_M > \Delta[\text{oxy-Hb}]_C$. Table 3 shows the contribution of integral $\Delta[\text{oxy-Hb}]_F$ to integral $\Delta[\text{oxy-Hb}]_C$ in the high r_s group was almost twice larger than that in the low r_s group. This suggests that the effect of the FBF on NIRS signals in the high r_s group is more than twice as large as that in the low r_s group. There has been scarce research on the influence of FBF on CBF since it was first developed for measuring human brain functions (Hoshi and Tamura, 1993; Kato et al., 1993; Villringer, 1993). However, a previous study (Chihara et al., 1998) during the early stages of NIRS development indicated the requirement of caution in its application. The FBF changes could be attributed to several reasons. Specifically, the FBF in the forehead is influenced by physiological, physical, and experimental/instrumental factors, which result from the autonomic function of cardiac and respiratory oscillations, vasomotor action, pressure and gravitational influences, and optode contact error (cf., Yamada et al., 2012).

Fig. 2 shows a typical example of NIRS signals after HDSM (the estimated as CBF and FBF are shown in Figs. 2A and 2B, respectively), whose original NIRS signals obtained with MBLL are shown in Fig. 1B. The NIRS signals in the R-VPC and L-VPC are remarkably reduced or disappear after HDSM (Fig. 2A), while those shown in Fig. 2B show large amplitude and similar shape to the LDF signals, especially to flow(LDF), shown in Fig. 1C.

It should be noted that the influences of FBF on NIRS signals obtained using the MBLL method differ across individuals and tasks; moreover, they may vary within the same participant and among experiments. Further, it is unlikely that there is a constant influence of FBF during the experiments, except in rare cases. Therefore, the influence of the FBF should be minimized as possible. Our results suggest that judging from the correlation analyses ($\Delta[\text{oxy-Hb}]_F > \Delta[\text{oxy-Hb}]_M > \Delta[\text{oxy-Hb}]_C$, see Fig. 3 and Table 2), the HDSM can separate the FBF and CBF in NIRS signals obtained using the MBLL method as expected, although it should be noted that in the present study, we adopted the HDSM proposed by Yamada et al. (2012), which was based on several assumptions, including that a linear negative relationship exists between changes in cerebral oxy-Hb and cerebral deoxy-Hb, and that capillaries mainly generate the functional component of NIRS signals, while arteries and veins generate the systemic component; however, the assumptions themselves required further evaluations.

In our study, all participants performed the VFT at the same level. The task outcome of men and women were 17.8 ± 5.5 and 17.9 ± 5.6, respectively, and there were no significant differences among generation. As for NIRS signals, the integral $\Delta[\text{oxy-Hb}]_M$ and its distribution (s.d.) showed lager values in men (129 ± 164) (Fig. 4A, closed circle) than

those of women (73 ± 69) (Fig. 4B, closed circle), and after HDSM those difference became small, the integral $\Delta[\text{oxy-Hb}]_C$ and its distribution were 34 ± 29 for men (Fig. 4A, open circle) and 14 ± 34 for women (Fig. 4B, open circle). Although there was still no significant difference in NIRS signals (i.e., integral $\Delta[\text{oxy-Hb}]_C$) between men and women, the effect size between sex difference changed from a medium value ($d = 0.47$) for the integral $\Delta[\text{oxy-Hb}]_M$ ($U = 61$, $p = 0.390$) to a relatively large value ($d = 0.65$) for the integral $\Delta[\text{oxy-Hb}]_C$ ($U = 50$, $p = 0.076$). This result suggests that the presence of sex differences in the VFT-induced changes in FBF and CBF, although further investigation with increasing in number of participants is required.

As for sex difference in the VFT-induced CBF change, an fMRI study conducted by Gauthier et al. (2009) have reported that during VFT tasks, men showed larger neural activation, reflecting the increase in CBF, than women in the left inferior temporal gyrus, cerebellum, anterior and posterior cingulate cortices, right superior frontal gyrus, dorsolateral PFC, lingual gyrus, and anterior cingulate cortices, regardless of the performance. This indicates the presence of strong relationships among neural circuits mediating cognitive, emotional, physiological, and behavioral responses, and that their functional changes induce changes in $\Delta[\text{oxy-Hb}]_C$ (Villringer et al., 1993).

On the other hand, sex difference in the VFT-induced FBF change could be attributed to the following several factors as follows. Difference in the thicknesses of the head and face soft tissue (men larger than women) (Mori et al., 2003; He et al., 2021) could explain the larger value of k_f in women (0.38 ± 0.14) than in men (0.17 ± 0.12) ($U = 44$, $p < 0.01$, see also Supplementary Figs. 1 S and 2 S). Furthermore, the relatively smaller value of FBF and its distributions ($U = 48$, $p = 0.357$, $d = 0.62$) in women (64 ± 54) than in men (127 ± 140) could be explained by a smaller number of perfused facial microvessels in women than in men (Mayrovitz and Regan, 1993) and the differences in hematological variables such as hematocrit, RBC volume, blood volume and hemoglobin concentration in the peripheral circulation (Diaz-Canestro et al., 2022).

In addition to the aforementioned factors, since the task was performed while sitting in a chair, our findings could have been affected by sex differences in the overall body size; length from the heart to the forehead (Smulyan et al., 2001); and vascular compliance (Winer et al., 2001), especially in venous compliance, since the smooth muscles of veins and venules are thinner than those of arteries and arterioles. For men with large bodies, the large distance from the heart and forehead vessels results in a large increase (and thus large deviation) of blood flow in the external carotid artery to the forehead microvessels. Moreover, women have lower venous compliance than men (Winer et al., 2001), which results in lower transmural pressure (Huxley and Wang, 2010) for a given increase in venous volume as well as a quicker increase in hydrostatic pressure (Shore et al., 1995). These sex differences could affect the influence of FBF on CBF and the interpretation of NIRS signals. Therefore, it is important to separate the FBF from the CBF.

Compared with the other age cohorts, the 20 s age cohort showed a tendency of large deviation in the values of integral $\Delta[\text{oxy-Hb}]_M$(97 ± 212 of 20 s vs 98 ± 84 of over 30 s, $U = 38$, $p = 0.242$ and $d = 0.01$)and still in the integral $\Delta[\text{oxy-Hb}]_C$ (4.6 ± 52.8 of 20 s vs 28.7 ± 22.0 of over 30 s, $U = 33$, $p = 0.146$ and $d = 0.77$)(see also Fig. 5). Regarding the large deviations in 20 s, we may be able to consider both organic and functional factors as follows. For organic factors, a magnetic resonance study on participants aged 7–87 years revealed that dynamic changes in neural structure occur during maturation in humans, with the main changes being a non-linear decrease and increase in the frontal grey and white matter density, respectively (Sowell et al., 2003). Further, age-dependent declines of CBF, cerebral blood volume, and oxygen utilization have also been reported (Leenders et al., 1990; Zhang et al., 2010). Since the NIRS signals are less sensitive to the blood flow changes in the white matter (Seiyama et al., 2004; Takahashi et al., 2011; Haeussinger et al., 2011), the deviation of the vascular bed structure in the cerebral cortex among young individuals possibly causes a large deviation in detected NIRS signals due to neurovascular coupling. For functional factors, Nakazato and Shimonaka (1989) reported that both state and trait anxiety decreased with age in a survey of individuals aged 25–92 years. They suggest that anxiety tends to decrease with age, with old age appearing to be the most psychologically stable life period in Japan. Costa et al. (1986) reported similar results based on a random sampling survey of patients aged 23–88 years across the United States. Therefore, we can't deny the possibility that both FBF and CBF among individuals in their 20 s reflect some type of task-related stress as well as stresses resulting from the cognitive function generating verbal expression.

This study has several limitations. We focused on the influence of the FBF on the CBF in individuals during VFT performance; therefore, our findings cannot be generalized to functional NIRS measurements. Future studies should include various cognitive tasks and larger sample sizes.

In conclusion, our findings showed that the influence of the FBF on the CBF differs across individuals. The FBF signal mostly results in CBF overestimation, especially under vertical conditions in the sitting position. Our findings suggest that it is important to separate Hb in the cerebral cortex and forehead scalp to obtain accurate NIRS signals and allow accurate examination of brain function in humans.

Authors contributions

All of authors designed the experiment and discussed present results. A.S., T.M., performed the experiment, analyzed the data. A.S. wrote the manuscript and M.C supervised and corrected paper. All of authors reviewed contents of the manuscript.

Declaration of Competing Interest

The authors declare that there is no conflict of interest.

Data Availability

The data that support the findings of this study are available from the corresponding author upon reasonable request.

Acknowledgments

We would like to thank all the study participants. This work was supported in part by JSPS KAKENHI Grant Number JP21K00229 and donation from Sri Lanka-Japan Collaborative Platform.

Appendix A. Supporting information

Supplementary data associated with this article can be found in the online version at doi:10.1016/j.neures.2022.09.012.

References

Agbangla, N.F., Audiffren, M., Albinet, C.T., 2017. Use of near-infrared spectroscopy in the investigation of brain activation during cognitive aging: a systematic review of an emerging area of research. Ageing Res. Rev. 38, 52–66. https://doi.org/10.1016/j.arr.2017.07.003.

Appell, J., Kertesz, A., Fisman, M., 1982. A study of language functioning in Alzheimer patients. Brain Lang. 17 (1), 73–91. https://doi.org/10.1016/0093-934x(82)90006-2.

Bendall, R.C., Eachus, P., Thompson, C., 2016. A brief review of research using near-infrared spectroscopy to measure activation of the prefrontal cortex during emotional processing: the importance of experimental design. Front. Hum. Neurosci. 10, 529. https://doi.org/10.3389/fnhum.2016.00529.

Chihara, E., Shiga, T., Tanabe, K., Tanaka, Y. 1998. Compression of the photoprobe is effective to reduce Hb signals of the frontal skin in near infrared spectrophotometric cerebral tissue oximetry. Proc. SPIE 3194, Photon Propagation in Tissues III, (1 January 1998); https://doi.org/10.1117/12.301086.

Chou, P.H., Huang, C.J., Sun, C.W., 2020. The potential role of functional near-infrared spectroscopy as clinical biomarkers in schizophrenia. Curr. Pharm. Des. 26 (2), 201–217. https://doi.org/10.2174/1381612825666191014164511.

Costa Jr., P.T., McCrae, R.R., Zonderman, A.B., Barbano, H.E., Lebowitz, B., Larson, D. M., 1986. Cross-sectional studies of personality in a national sample: II. Stability in neuroticism, extraversion, and openness. Psychol. Aging 1 (2), 144–149. https://doi.org/10.1037/0882-7974.1.2.144.

Crow, S.F., 1998. Decrease in performance on the verbal fluency test as a function of time: evaluation in a young health sample. J. Clin. Exp. Neuropsychol. 20 (3), 391–401. https://doi.org/10.1076/jcen.20.3.391.810.

Diaz-Canestro, C., Pentz, B., Sehgal, A., Montero, D., 2022. Sex differences in cardiorespiratory fitness are explained by blood volume and oxygen carrying capacity. Cardiovasc. Res. 118 (1), 334–343. https://doi.org/10.1093/cvr/cvab028.

Drummond, P.D., 1997. The effect of adrenergic blockade on blushing and facial flushing. Psychophysiology 34 (2), 163–168. https://doi.org/10.1111/j.1469-8986.1997.tb02127.x.

Drummond, P.D., 2012. Psychophysiology of the blush. In: Crozier, W.R., de Jong, P.J. (Eds.), The Psychological Significance of the Blush. Cambridge University Press, pp. 15–38. https://doi.org/10.1017/CBO9781139012850.

Fantini, S., Sassarolin, A., 2020. Frequency-domain techniques for cerebral and functional near-infrared spectroscopy. Front. Neurosci. 14, 300. https://doi.org/10.3389/fnins. 2020.00300. eCollection 2020.

Gauthier, C.T., Duyme, M., Zanca, M., Capron, C., 2009. Sex and performance level effects on brain activation during a verbal fluency task: a functional magnetic resonance imaging study. Cortex 452, 164–176. https://doi.org/10.1016/j.cortex.2007.09.006.

Haeussinger, F.B., Heinzel, S., Hahn, T., Schecklmann, M., Ehlis, A.C., Fallgatter, A.J., 2011. Simulation of near-infrared light absorption considering individual head and prefrontal cortex anatomy: implications for optical neuroimaging. PLoS One 6 (10), e26377. https://doi.org/10.1371/journal.pone.0026377.

He, R., Yang, W., Wu, Di, Wang, H., 2021. Age- and sex-related measurements of total craniofacial soft tissue thickness and fat in a central Chinese population. J. Craniofac. Surg. 32 (8), 2626–2630. https://doi.org/10.1097/SCS.0000000000007827.

Hori, S., Mori, K., Mashimo, T., Seiyama, A., 2017. Effects of light and sound on the prefrontal cortex activation and emotional function: a functional near-infrared spectroscopy study. Front. Neurosci. 11, 321, 10.3389/fnins.2017.00321. eCollection 2017.

Hoshi, Y., Tamura, M., 1993. Detection of dynamic changes in cerebral oxygenation coupled to neuronal function during mental work in man. Neurosci. Lett. 150 (1), 5–8. https://doi.org/10.1016/0304-3940(93)90094-2.

Husain, S.F., Yu, R., Tang, T.B., Tam, W.W., Tran, B., Quek, T.T., Hwang, S.H., Chang, C. W., Ho, C.S., Ho, R.C., 2020. Validating a functional near-infrared spectroscopy diagnostic paradigm for Major Depressive Disorder. Sci. Rep. 10 (1), 9740. https://doi.org/10.1038/s41598-020-66784-2.).

Huxley, V.H., Wang, J., 2010. Cardiovascular sex differences influencing microvascular exchange. Cardiovasc. Res 87 (2), 230–242. https://doi.org/10.1093/cvr/cvq142.

Ito, E., Hatta, T., 2002. Development of the verbal fluency test for Japanese. Stu. Inform. Sci. 2002 (15), 81–96. https://doi.org/10.1080/1357650X.2014.917656.

Kashima, S., Ono, Y., Sohda, A., Ohsawa, T., 1994. Separate measurement of two components of blood flow velocity in tissue by dynamic light scattering method. Jpn. J. Appl. Phys. 33, 2123–2127. https://doi.org/10.1143/JJAP.33.2123.

Kato, T., Kamei, A., Takashima, S., Ozaki, T., 1993. Human visual cortical function during photic stimulation monitoring by means of near-infrared spectroscopy. J. Cereb. Blood Flow. Metab. 13 (3), 516–520. https://doi.org/10.1038/jcbfm.1993.66.

Kirilina, E., Jelzow, A., Heine, A., Niessing, M., Wabnitz, H., Brühl, R., Ittermann, B., Jacobs, A.M., Tachtsidis, I., 2012. The physiological origin of task-evoked systemic artefacts in functional near infrared spectroscopy. Neuroimage 61 (1), 70–81, 10.1016/ j.neuroimage. 2012.02.074. Epub 2012 Mar 9.

Kohno, S., Miyai, I., Seiyama, A., Oda, I., Ishikawa, A., Tsuneishi, S., Amita, T., Shimizu, K., 2007. Removal of the skin blood flow artifact in functional near-infrared spectroscopic imaging data through independent component analysis. J. Biomed. Opt. 12 (6), 062111 https://doi.org/10.1117/1.2814249.

Leenders, K.L., Perani, D., Lammertsma, A.A., Heather, J.D., Buckingham, P., Healy, M. J., Gibbs, J.M., Wise, R.J., Hatazawa, J., Herold, S., Beaney, R.P., Brooks, D.J., Spinks, T., Rhodes, C., Frackowiak, R.S.J., 1990. Cerebral blood flow, blood volume and oxygen utilization. Norm. Values Eff. Age Brain 113 (Pt 1), 27–47. https://doi.org/10.1093/brain/113.1.27.

Liu, J., Luo, H., Zheng, P.P., Wu, S.J., Lee, K., 2018. Transdermal optical imaging revealed different spatiotemporal patterns of facial cardiovascular activities. Sci. Rep. 8 (1), 10588. https://doi.org/10.1038/s41598-018-28804-0.

Malonek, D., Dirnagl, U., Lindauer, U., Yamada, K., Kanno, I., Grinvald, A., 1997. Vascular imprints of neuronal activity: relationships between the dynamics cortical blood flow, oxygenation, and volume changes following sensory stimulation. Proc. Natl. Acad. Sci. USA 94 (26), 14826–14831. https://doi.org/10.1073/pnas.94.26.14826.

Martin, A., Wiggs, C.L., Lalonde, F., Mack, C., 1994. Word retrieval to letter and semantic cues: a double dissociation in normal subjects using interference tasks. Neuropsychologia 32 (12), 1487–1494. https://doi.org/10.1016/0028-3932(94)90120-1.

Matcher, S.J., Elwell, C.E., Cooper, C.E., Cope, M., Delpy, D.T., 1995. Performance comparison of several published tissue near-infrared spectroscopy algorithms. Anal. Biochem 227 (1), 54–68. https://doi.org/10.1006/abio.1995.1252.

Mayrovitz, H.N., Regan, M.B., 1993. Gender differences in facial skin blood perfusion during basal and heated conditions determined by laser Doppler flowmetry. Microvasc. Res. 45 (2), 211–218. https://doi.org/10.1006/mvre.1993.1019.

Milej, D., Abdalmalak, A., Rajaram St, A., Lawrence, K., 2020. Direct assessment of extracerebral signal contamination on optical measurements of cerebral blood flow, oxygenation, and metabolism. Neurophotonics 7 (4), 045002. https://doi.org/10.1117/1.NPh.7.4.045002. Epub 2020 Oct 7.

Mori, N., Terajima, M., Tokumari, K., Nakajima, K., Aoki, Y., Hashimoto, S., 2003. Head bioinstrumentation and construction of face standard three-dimensional physical model of modern Japanese adults of both sexes using three-dimensional CT images. Anthropological. Science 111 (1), 35–49. https://doi.org/10.1537/asj.111.35.

Nakazato, K., Shimonaka, Y., 1989. A cross-sectional study of development of anxiety in adult lifespan. Jpn. J. Educ. Psychol. 37 (2), 172–178. https://doi.org/10.5926/jjep1953.37.2_172.

Oonishi, S., Hori, S., Hoshi, Y., Seiyama, A., 2014. Influence of subjective happiness on the prefrontal brain activity: an fNIRS study. Adv. Exp. Med. Biol. 812, 287–293. https://doi.org/10.1007/978-1-4939-0620-8_38.

Seiyama, A., Hazeki, O., Tamura, M., 1988. Noninvasive quantitative analysis of blood oxygenation in rat skeletal muscle. J. Biochem 103 (3), 419–424. https://doi.org/10.1093/oxfordjournals.jbchem.a122285.

Seiyama, A., Seki, J., Tanabe, H.C., Sase, I., Takatsuki, A., Miyauchi, S., Eda, H., Hayashi, S., Imaruoka, T., Iwakura, T., Yanagida, T., 2004. Circulatory basis of fMRI signals: relationship between changes in the hemodynamic parameters and BOLD signal intensity. Neuroimage 21 (4), 1204–1214. https://doi.org/10.1016/j.neuroimage.2003.12.002.

Shore, A.C., Sandeman, D.D., Tooke, J.E., 1995. Capillary pressure, pulse pressure amplitude, and pressure waveform in healthy volunteers. Am. J. Physiol. 268 (1 Pt 2), H147–H154. https://doi.org/10.1152/ajpheart.1995.268.1.H147.

Smulyan, H., Asmar, R.G., Rudnicki, A., London, G.M., Safar, M.E., 2001. Comparative effects of aging in men and women on the properties of the arterial tree. J. Am. Coll. Cardiol. 37 (5), 1374–1380. https://doi.org/10.1016/s0735-1097(01)01166-4.

Sowell, E.R., Peterson, B.S., Thompson, P.M., Welcome, S.E., Henkenius, A.L., Toga, A. W., 2003. Mapping cortical change across the life span. Nat. Neurosci. 6 (3), 309–315. https://doi.org/10.1038/nn1008.

Storandt, M., Botwinick, J., Danziger, W.L., Berg, L., Hughes, C.P., 1984. Psychometric differentiation of mild senile dementia of the Alzheimer type. Arch. Neurol. 1984 41 (5), 497–499. https://doi.org/10.1001/archneur.1984.04050170043013.

Strangman, G., Culver, J.P., Thompson, J.H., Boas, D.A., 2002. A quantitative comparison of simultaneous BOLD fMRI and NIRS recordings during functional brain activation. Neuroimage 17, 719–731. https://doi.org/10.1006/nimg.2002.1227.

Takahashi, T., Takikawa, Y., Kawagoe, R., Shibuya, S., Iwano, T., Kitazawa, S., 2011. Influence of skin blood flow on near-infrared spectroscopy signals measured on the forehead during a verbal fluency task. Neuroimage 57 (3), 991–1002. https://doi.org/10.1016/j.neuroimage.2011.05.012.

Takizawa, R., Kasai, K., Kawakubo, Y., Marumo, K., Kawasaki, S., Yamasue, H., Fukuda, M., 2008. Reduced frontopolar activation during verbal fluency task in schizophrenia: a multi-channel near-infrared spectroscopy study. Schizophr. Res. 99 (1–3), 250–262. https://doi.org/10.1016/j.schres.2007.10.025. Epub 2007 Dec 11.

Takizawa, R., Fukuda, M., Kawasaki, S., Kasai, K., Mimura, M., Pu, S., Noda, T., Niwa, S., Okazaki, Y., 2014. Neuroimaging-aided differential diagnosis of the depressive state. Neuroimage 85 (Pt 1), 498–507. https://doi.org/10.1016/j.neuroimage.2013.05.126.

Tian, F., Liu, H., 2014. Depth-compensated diffuse optical tomography enhanced by general linear model analysis and an anatomical atlas of human head. Neuroimage Pt 1 (0 1), 166–180. https://doi.org/10.1016/j.neuroimage.2013.07.016. Epub 2013 Jul 14.

Tsunashima, H., Yanagisawan, K., 2009. Measurement of brain function of car driver using functional near-infrared spectroscopy (fNIRS). Comput. Intell. Neurosci. 2009, 164958 https://doi.org/10.1155/2009/164958. Epub 2009 Jun 25.

Villringer, A., Planck, J., Hock, C., Schleinkofer, L., Dirnagl, U., 1993. Near infrared spectroscopy (NIRS): a new tool to study hemodynamic changes during activation of brain function in human adults. Neurosci. Lett. 154 (1–2), 101–104. https://doi.org/10.1016/0304-3940(93)90181-j.

Winer, N., Sowers, J.R., Weber, M.A., 2001. Gender differences in vascular compliance in young, healthy subjects assessed by pulse contour analysis. J. Clin. Hypertens. 3 (3), 145–152. https://doi.org/10.1111/j.1524-6175.2001.00704.x.

Wray, S., Cope, M., Delpy, D.T., Wyatt, J.S., Reynolds, E.O., 1988. Characterization of the near infrared absorption spectra of cytochrome aa3 and hemoglobin for the non-invasive monitoring of cerebral oxygenation. Biochim. Biophys. Acta 933 (1), 184–192. https://doi.org/10.1016/0005-2728(88)90069-2.

Yamada, T., Umeyama, S., Matsuda, K., 2009. Multidistance probe arrangement to eliminate artifacts in functional near-infrared spectroscopy. J. Biomed. Opt. 14 (6), 064034 https://doi.org/10.1117/1.3275469.

Yamada, T., Umeyama, S., Matsuda, K., 2012. Separation of fNIRS signals into functional and systemic components based on differences in hemodynamic modalities. PLoS One 7 (11), e50271. https://doi.org/10.1371/journal.pone.0050271. Epub 2012 Nov 19.

Zhang, Y., Peng, Y., Chen, G., Chen, W., 2010. Cerebral blood flow, cerebral blood volume, oxygen utilization and oxygen extraction fraction: the influence of age. J. South. Med. Univ. 30, 1237–1239.

Vol.24 No.4, 2022

原著論文

地震映像視聴時の携帯型 NIRS を用いた情動研究

大塚 日花里[*1] 岡橋 さやか[*1*2*3] 精山 明敏[*3]

Evaluation of Emotional Changes During Earthquake Video Watching: A Wearable NIRS Study

Hikari Otsuka[*1], Sayaka Okahashi[*1*2*3] and Akitoshi Seiyama[*3]

Abstract - Sudden occurrences of disasters often agitate people emotionally and make their planned evacuation activities difficult. However, the biological responses to natural disaster situations have not been investigated. This study aimed to: 1) discover the difference in emotional responses between earthquake video-watching and neutral video-watching conditions, and 2) investigate the relationship between emotional responses during watching an earthquake video and subjective emotion assessment/individual anxiety traits. Healthy young adults (n = 12) watched earthquake and neutral videos, and we measured biological signals and performed emotional assessment. We measured biological signals, such as pulse rate and cerebral blood flow in the dorsolateral prefrontal cortex, using a wearable two-channel near-infrared spectroscopy (NIRS) unit. Autonomic nerve indexes (sympathetic and parasympathetic indexes) were calculated from the NIRS data. Subjective emotion assessment was made using the Self-Assessment Manikin. The State-Trait Anxiety Inventory Questionnaire was also performed. We found that sympathetic nerve activity was significantly lower in the earthquake video-watching condition than during the neutral one. Biological indicators inferred both subjective emotion assessment during watching the earthquake video and individual anxiety traits. Autonomic indices based on 2-channel NIRS data may be able to estimate emotional responses to different stimuli.

Keywords : earthquakes, emotion, autonomic nervous activity, cerebral blood flow, anxiety traits

1. はじめに

地震をはじめとする自然災害発生時には，情動が大きく揺さぶられる中で冷静に避難行動をとることが求められる．災害時に誘発される感情には恐怖や驚き，不安などのネガティブなものが多く[1]，地震発生時の恐怖感は，性別や年齢，体感ダメージの大きさといった要素が関連すると報告されている[2]．強い情動が喚起されると，認知に対する妨害的効果が生じ，落ち着いた思考が困難となることから[3]，災害時の情動反応を捉えることは支援に繋げるうえで重要であると考えられる．

しかし，地震などの自然災害に関連する映像視聴時の脳血流変化を検討した報告はなく，自然災害に遭遇した際の人の情動反応と脳活動の関係の多くは今なお明らかにされていない．また，情動喚起時の脈拍や自律神経活動を測定した研究においては，差し迫った脅威を感じる恐怖や身体の切断に関連する嫌悪感，急激な悲しみで心拍数が減少する一方で，同じ否定的な感情でも怒りや不安，汚染に関連する嫌悪感，驚きでは心拍数が増加すると報告されている[4].

生体反応の観察において，NIRS（Near-Infrared Spectroscopy: 近赤外分光法）を用いると非侵襲的に脳血流変化量を計測できる．生体内を透過できる近赤外光（700～900nm）を頭皮上から脳表に向けて照射し，光路中の組織液中の酸素化ヘモグロビン（oxy-Hb），脱酸素化ヘモグロビン（deoxy-Hb），総ヘモグロビン（total-Hb）量の変化を検出する機器であり，低拘束，簡便といった利点がある[5],[6]．NIRS には，前額部や側頭，頭頂，後頭部の計測が可能な多チャンネルのもの[7]や前額部の左右 2 か所で計測する 2 チャンネルのもの[8],[9]があるが，本研究では軽量でワイヤレス仕様のため対象者の動きを制限することなく計測できる後者のタイプを採用した．

NIRS を用いた情動研究では，ネガティブな映像提示によって前頭前野右外側部で oxy-Hb が増加したという報告[10]や，不快な写真を提示した際に両側の腹外側前頭前野の oxy-Hb が増加したという報告がある[11]．また，情動反応には個人差があり，普段から様々な事象に対する不安の感じやすさが大きい人ほど，安静時に右半球優位の oxy-Hb 変化を示すことが報告されている[12].

そこで，本研究では災害に遭遇した際の情動反応に着目し，地震に関する映像視聴時の自律神経活動や脈拍数，脳血流といった生体指標について 2 チャンネル NIRS を用いて捉え，中性映像視聴時との比較を行い，さらにそれらの生体指標と映像への主観的評価及び不安特性との

*1: 京都大学大学院　医学研究科　人間健康科学系専攻
*2: 国立長寿医療研究センター　老年学・社会科学研究センター
*3: 国際教養大学　デザイン創造・データサイエンスセンター
*1: Department of Human Health Sciences, Graduate School of Medicine, Kyoto University
*2: Center for Gerontology and Social Science, National Center for Geriatrics and Gerontology
*3: Creative Design & Data Science Center, Akita International University

関連を検討することを目的とした．その意義として，地震という特異的な場面の映像を視聴している際や模擬的な地震体験時の生体指標を捉えることは，実際に地震に遭遇した際の人の情動反応の解明の一助となると考える．また，情動反応と元来の不安特性との関連を明らかにすることで，個人に合わせた非常時の支援方法の開発に繋げられると考える．

2. 方法

2.1 対象者

健常若年者 12 名（男性 6 名，女性 6 名，23.2±0.6 歳）を対象とした．本研究の課題遂行に支障をきたすと思われる視力障害や聴力障害，言語理解障害，精神障害の既往歴がなく，事前に地震に対する心的外傷がないことを確認するため，Impact of Event Scale-Revised (IES-R：改訂出来事インパクト尺度日本語版)を実施し，カットオフ値 24 点以下の者を対象とした．

2.2 実施方法

対象者には基本情報の聴取・評価と不安尺度を用いた評価後，NIRS を装着した状態で複数の映像視聴と各映像に対する主観的評価を回答してもらった．最後に，これまでの地震経験に関する質問紙への回答を行ってもらった．基本情報の項目は，年齢，性別，教育歴，職業歴，利き手，Japanese Adult Reading Test (JART)で評価した知的機能（IQ），視力であった．不安尺度には日本版 State-Trait Anxiety Inventory（STAI-JYZ ：新版 STAI）を用いた．STAI は，不安を喚起する事象に対する一過性の不安の反応（状態不安）と定常的な個人の不安傾向（特性不安）の 2 側面を測定できる質問紙である．なお，実験 1 回の所要時間は，説明を含め 60 分程度であった．

本研究は京都大学医の倫理委員会の承認（R2855）を得て実施した．

2.3 実施環境および映像提示，主観的評価

本調査は，広さ約 6 ㎡の静かな一室で実施し，室内の気温は 23.8±0.4℃，湿度は 53.7±4.4%であった．対象者は，スクリーン（縦 107 ㎝×横 182 ㎝）から 240 ㎝離れた椅子に座った状態で映像を視聴した（図１）．このときの視野角は 43.5°であった．対象者の注意が音源に逸れ，スクリーンから目を離すことを防ぐため，対象者の後方にスピーカー（Lenovo Speaker M0620）2 台を設置し，音量の平均を対象者の頭部の位置にて約 60 dBになるよう調整した．はじめに練習として 20 秒間の注視点（+）のある画像（以下，十字画面）とそれに続く 20 秒間の映像（自然の風景）を検者による口頭説明とともに提示し，各映像終了後には Self-Assessment Manikin（SAM）の Valence（感情価），Arousal（覚醒度），Dominance（支配度）の 3 項目について 1~9 の 9 段階で画面（図２）を見ながら回答してもらった．対象者には，感情価は快・不快（1[快]～9[不快]），覚醒度は興奮度（1[小]～9[大]），支配度はインパクトの大きさ（1[小]～9[大]）を示すことと，3 つの各項目は 10 秒間しか提示されないこと，口頭で数字のみ回答することを説明した．また，映像視聴中はなるべく身体や頭を大きく動かしたり声を出したりしないことを伝えた．一回の練習終了後，NIRS を装着してもらい，映像視聴を実施した．本施行の映像視聴の流れについて，図 2 に示す．90 秒間の十字画面に続いて，60～120 秒の地震映像 3 種類と 60 秒の中性映像 2 種類のうちいずれか 1 つが提示され，各映像終了後には，練習同様に SAM の感情価，覚醒度，支配度の 3 項目を 1~9 の 9 段階で回答してもらった．十字画面，映像，SAM の回答は全部で 5 回繰り返した．なお，地震映像 3 種類と，中性映像 2 種類は地震映像同士，中性映像同士が連続しないこととし，さらに地震映像 3 種類は疑似ランダムな順として，対象者は 6 条件（3 の階乗通り）のうちいずれかの動画を視聴することとした．表 1 に示すように，3 つの地震映像には，動画サイトで公開されている東日本大震災時に実際に撮影された映像[13]-[15]を使用し，2 つの中性映像は購入した自然の風景の映像[16]にピンクノイズを付加した．なお，ピンクノイズは地震映像の聴覚刺激の条件を統制する目的と，快や不快などの情動を喚起させない目的にて用いた．

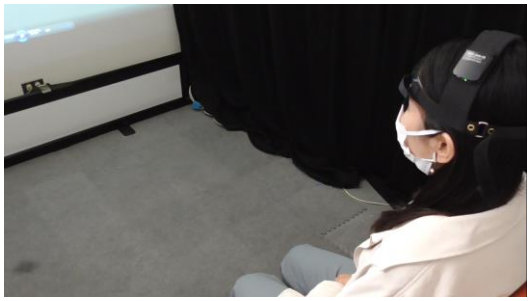

図１ 実験の様子
Fig.1 Experimental Scene

2.4 NIRS 計測

脳血流の計測には 2 チャンネルウェアラブル NIRS（携帯型脳活動計測装置 HOT-2000-VR，NeU 社製）を使用した．本計測装置は，ヘッドセットに左右 1 つずつ設けられている波長 810 ㎚の近赤外光を発光する LED と各 2 つのセンサーユニット（LED から約 1 ㎝と約 3 ㎝の位置）から成る．Real-time scalp signal separating (RT-SSS)と呼ばれる手法[17]により頭皮血流および脳実質の血行動態を捉える LED から約 3 ㎝のセンサーの信号から，頭皮血流の血行動態を捉える LED から約 1 ㎝のセンサーの信号を差し引くことで，右脳と左脳それぞれの総ヘモグロビン量の変化（Δtotal-Hb）を計測・解析し，脳血流変化量を算出する装置である．また，センサーの計測値から推定した脈拍数（回／分）が記録される．

NIRS の 2 つのチャンネルの位置は両側の背外側前頭

前野（国際 10-20 法で左 Fp1～F7，右 Fp2～F8）とした．計測のサンプリングは 100 ミリ秒毎で，高周波のノイズを除去するために 3 秒（30 点）ごとの移動平均を用いて信号の平滑化処理を行った．

(a)

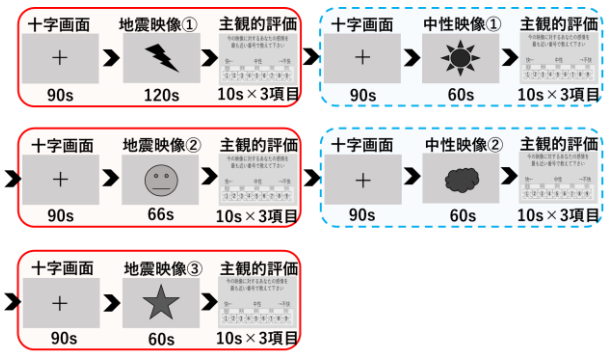

(b)

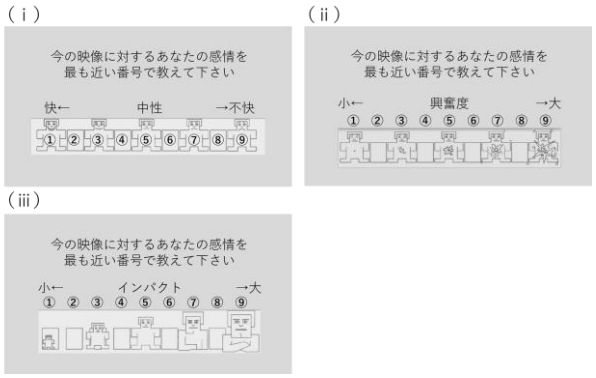

図２　本試行での映像提示の流れの一例と主観的評価を問う画面
Fig.2 An Example of Video Flow in the Main Trial and Subjective Assessment Screenshot
(a) 提示映像の流れの一例，(b) (ⅰ)「感情価」(ⅱ)「覚醒度」(ⅲ)「支配度」．イラストは文献[18]より引用．

表 1 各映像の内容と提示秒数
Table 1 Content and Duration of Each Video

映像	内容	提示秒数
地震①	レストラン内での被災映像[13]	120
地震②	緊急地震速報を伝えるニュース映像[14]	66
地震③	住宅街の屋外での被災映像[15]	60
中性①	自然の風景 1[16]	60
中性②	自然の風景 2[16]	60

2.5　これまでの地震経験に関する質問紙

地震経験に関する質問紙では，対象者がこれまでに経験した中で最も揺れが大きかった地震の最大震度，経験した時期，場所，心情の種類とその程度，自身の行動および行動の適切さとその理由に加え，直近 3 年間で経験した地震で震度 1～震度 2 の発生時について，経験した場所，心情の種類とその程度，自身の行動および行動の適切さとその理由を回答してもらった．なお，この質問紙による回答は，映像視聴時の脳活動に影響を与えないよう，映像視聴後に記入してもらった．

2.6　解析方法

2.6.1　自律神経指標

HOT-2000-VR の脳血流データから RR 間隔を推定し，脈拍変動を求めて自律神経指標を算出した．

具体的には，最初に HOT-2000-VR の右のチャンネルの近赤外光を発光する LED から 1 ㎝ 離れたところに配置されたセンサーユニット 1 で記録される頭皮血流を反映する信号に，前処理として微分と規格化を行った．微分は信号の比較的大きな波のトレンドや大きな動きによるノイズを低減する目的で，次の信号 A(n+1)から現在の信号 A(n)を引いた．規格化は，測定装置や個人間の信号の大きさの違いを揃える目的で(1)式を用いて規格化を行った．

$$\text{規格化} = \frac{\text{信号（時刻 } n\text{）} - \text{信号（全信号の平均）}}{\text{標準偏差}} \quad (1)$$

次に，前処理後の頭皮血流信号をもとに脈波のピークを推定し，ピーク間隔時間（RR 間隔）を算出した．この際，脈波の切痕（心臓の弁の開閉によるピーク）を誤ってピークとして抽出しないよう，規格化信号の高さに閾値を設けた．

自律神経指標の算出には，Toichi らの提案したローレンツプロットの手法を用いた．ローレンツプロットとは，n 番目の RR 間隔を x 座標，n+1 番目の RR 間隔を y 座標として x-y 平面上に順にプロットしていき，楕円状に分布したプロットの広がりの長軸の長さ（L）と短軸の長さ（T）に基づいて交感神経機能指標 CSI（L/T）と副交感神経機能指標 CVI（$\log_{10}(L\times T)$）を算出するものである[19]．

2.6.2　脳血流変化量と Lateral Index

HOT-2000-VR で取得した左右それぞれの Δ total-Hb［測定値］から，傾向変動と周期変動を除去後，さらに移動メディアンフィルタ処理した左右それぞれの値を真の脳活動を反映する Δ total-Hb(L)， Δ total-Hb(R)として求めた．詳細を以下に述べる．

傾向変動は発汗や測定部位の温度上昇といった持続的な変化に伴うノイズ，周期変動は心拍や呼吸変動によるノイズ処理を目的として，(2)式を用いてある時刻 n における残差 y(n)を真の脳活動信号として求めた．ただし，V_{trend} (n)は残差 y(n)が最小になるように近似した 3 次多項式であり，傾向変動を意味する．また，V_{period} (n)は ΔHb_{total} (n) － V_{trend} (n)の周期的変化を取り出した正弦波であり，周期変動を意味する．また，傾向変動と周期変動を除した残差 y(n)の標準偏差が最小となるように，周

期変動は全ての測定時間の 1/2 を周期とした.

$$y(n) = \Delta Hb_{total}(n) - \{ V_{trend}(n) + V_{period}(n) \} \quad (2)$$

さらに対象者の体動や測定不良などによる非周期的なノイズを低減する目的で，移動メディアンフィルタ処理を行い，(3)式を用いて移動平均 t(n)を求めた.

$$t(n) = \text{median} \{ y(n-k), \cdots, y(n), \cdots, y(n+k) \} \quad (3)$$

k は移動メディアンフィルタの項数で，y(n)と t(n)の差の二乗平均が，ノイズの低減と本来の信号 y(n)の歪みの最小化という条件を満たした 200 に設定した．y(n)は(2)式で求めた 0.1 秒ごとの左右それぞれの残差である.

上記のノイズ処理によって得られた t(n)を改めて真の総ヘモグロビン量の変化とし，左右それぞれ Δ total-Hb(L)， Δ total-Hb(R)とした．なお， Δ total-Hb(L)，Δ total-Hb(R)の単位は，総ヘモグロビン濃度の単位（millimol/L: mM）と受光プローブで受光した反射光の光路長の単位（cm）の積であることから，本稿では a.u.（Arbitrary Unit: 任意単位）と表記する.

次に，左右の背外側前頭前野の脳血流の非対称性を示す指標として Lateral Index (LI)を，Ishikawa らの先行研究[12]を参考に，Δ total-Hb(L)，Δtotal-Hb(R)の値から(4)式を用いて求めた.

$$LI = \frac{\{\Delta\text{total L}(n) - \Delta\text{total L}(\min)\} - \{\Delta\text{total R}(n) - \Delta\text{total R}(\min)\}}{\{\Delta\text{total L}(n) - \Delta\text{total L}(\min)\} + \{\Delta\text{total R}(n) - \Delta\text{total R}(\min)\}} \quad (4)$$

Δ total L(n)と Δ total R(n)は 0.1 秒ごとの Δ total-Hb(L)，Δ total-Hb(R)それぞれの値， Δ total L(min)と Δ total R(min)は十字画面から映像視聴終了時までの全ての期間における Δ total-Hb(L)， Δ total-Hb(R)それぞれの最小値である．LI が正のとき，右と比較して左の背外側前頭前野が優位に活動し，LI が負のとき，左と比較して右の背外側前頭前野が優位に活動するということを示す.

2.6.3 統計処理

まず， CSI， CVI， CVI/CSI， Δ total-Hb(L)， Δtotal-Hb(R)， LI，主観的評価（感情価，覚醒度，支配度）それぞれにおいて，3 つの地震映像視聴時の全体と 2 つの中性映像全体の平均値を求めた．なお，5 種類の映像のいずれにおいても各映像視聴時間の中央から前後 60 秒間のデータを対象として自律神経指標，脈拍数及び脳血流変化量を解析した．また，データ表示は，すべて平均±標準誤差で示した.

次に，上記各指標において地震映像と中性映像間での差を調べるため，Shapiro-Wilk 検定でデータの正規性を確認後，対応のある t 検定を行った.

加えて，映像視聴中の生体指標と主観的評価（感情価，覚醒度，支配度）及び STAI の不安特性（状態不安，特性不安）との関連を調べるため，地震及び中性映像視聴時の生体指標のうち CVI/CSI と LI を説明変数として多値ロジスティック回帰分析を行った．CVI/CSI と LI を用いた理由は，説明変数間で相関係数の高い組み合わせが存在する多重共線性の問題を回避するためである．生体指標と主観的評価は 3 つの地震映像の平均値と 2 つの中性映像の平均値を用いた．また，STAI スコアは STAI-JYZ の標準化標本（男・女大学生それぞれ 1088 名及び 1165 名）[20]を用いて，個々の対象者の素点のパーセンタイルを求めた.

解析には IBM SPSS Statistics バージョン 27 と College Analysis Ver.8.4[21]を用い，有意水準は 5%とした．なお，対応のある t 検定の効果量（d）は，d = 0.2 で効果量小，d = 0.5 で効果量中，d = 0.8 で効果量大とされる[22]．また，多値ロジスティック回帰分析で得られた回帰モデルの適合度指標については，最適値からのずれを表す逸脱度（D, 小さいほど有効, $p > 0.05$ 有効），ピアソンの χ^2 統計量（χ^2, 小さいほど有効, $p > 0.05$ 有効）及び最小モデルからのずれを表す尤度比（C, 大きいほど有効, $p < 0.05$ 有効），実測値と予測値の決定係数（R^2）を求めた.

3. 結果

3.1 基本属性

対象者 12 名の教育歴は 16.5±0.3 年，右利き 11 名，左利き 1 名，JART の全検査 IQ は 108.8±1.9 点，視力は左右それぞれ 0.8 以上が 9 名，0.7 が 1 名，0.6 が 2 名で，0.7 以下の者は映像やスクリーン上の文字を認識できることを確認したのち実験を開始した．IES-R は 0.3±0.2 点で，地震の心的外傷によって除外された者はいなかった．STAI のスコアは，状態不安 33.5±1.7 点，特性不安 41.7±3.2 点であった．脈拍数のデータのみ測定の不具合により 1 名を除いた 11 名を解析対象とした.

3.2 自律神経指標，脈拍数，脳血流変化量

各生体指標の結果を図３～５に示す．各図には，対象者毎の地震映像と中性映像視聴時間内の平均値を黒色点でプロットしており，白色点は全対象者の平均値を示している.

各生体指標の平均値（平均±標準誤差）について，CSI は地震条件では 0.94±0.03(a.u.)，中性条件では 1.03±0.06(a.u.)，CVI は地震条件では 5.20±0.13(a.u.)，中性条件では 5.20±0.13(a.u.)で，CVI/CSI の値は，地震条件で 5.60±0.19，中性条件で 5.20±0.29 であった（図３）．また，脈拍数は地震条件では 77.94±3.20 回/分，中性条件では 78.71±3.35 回/分（図４），Δtotal-Hb(L)は地震条件では－0.001±0.01(a.u.)，中性条件では－0.01±0.01(a.u.)，Δtotal-Hb(R)は地震条件では－0.01±0.01(a.u.)，中性条件では－0.01±0.01(a.u.)， LI は地震条件では 0.04±0.06，中性条件では 0.05±0.07 であった（図５）.

映像条件による比較では CSI は地震条件の方が中性条件よりも有意に小さかった（p = 0.046, d = －0.65）．一方で，CVI，CVI/CSI，脈拍数，Δtotal-Hb(L)，Δtotal-Hb(R)，LI については，いずれも有意差はなかった（CVI：p = 0.90, d = －0.04；CVI/CSI：p = 0.08, d = 0.55；脈拍数：p = 0.17, d = －0.44；Δtotal-Hb(L)：p = 0.61, d = 0.15；Δtotal-Hb(R)：p = 0.89, d = 0.04；LI：p = 0.82, d = －0.07）（図３～５）．

3.3　主観的評価

各主観的評価の結果を図６に示す．各図には，対象者毎の 3 つの地震映像の主観的評価の平均値と 2 つの中性映像の平均値を黒色点でプロットしており，白色点は全対象者の平均値を示している．

SAM の 感情価の平均は，地震条件では 6.94±0.20，中性条件では 3.17±0.37，覚醒度は地震条件では 6.17±0.33，中性条件では 2.25±0.20，支配度は地震条件では 6.11±0.40，中性条件では 2.25±0.29 であった（図６）．

条件間での比較では，感情価，覚醒度，支配度のいずれにおいても地震条件の方が中性条件よりも有意に高かった（p < 0.001）（図６）．

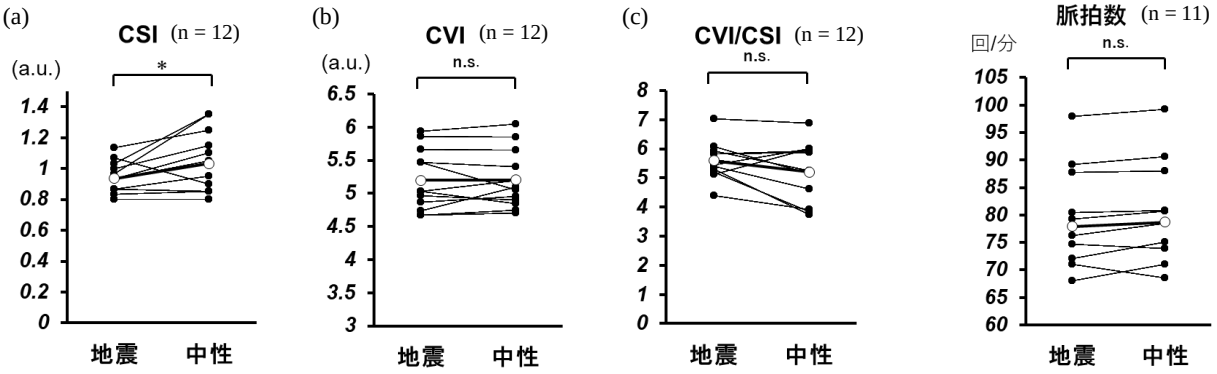

図３　各映像視聴時の自律神経指標
Fig.3 Autonomic Nervous Index during Video Watching
各対象者の平均値（●）と全対象者の平均値（○）を示す．
* p < 0.05, n.s.: not significant

図４　各映像視聴時の脈拍数
Fig.4 Pulse Rate during Video Watching

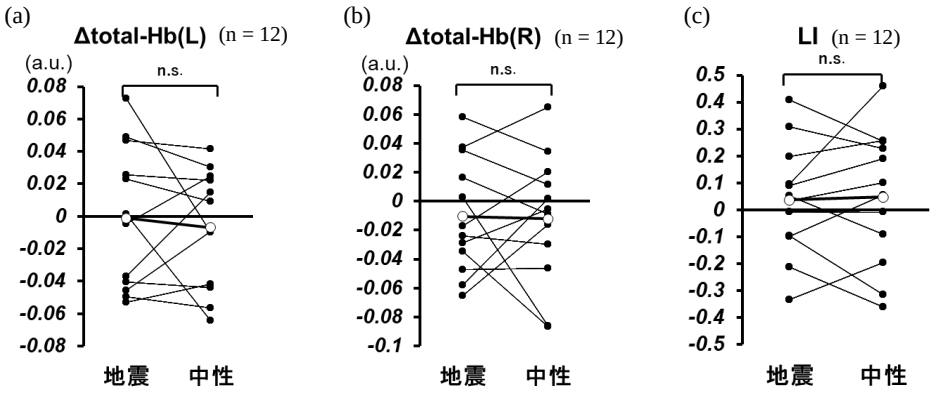

図５　各映像視聴時の脳血流変化量
Fig.5 Cerebral Blood Flow Change during Video Watching

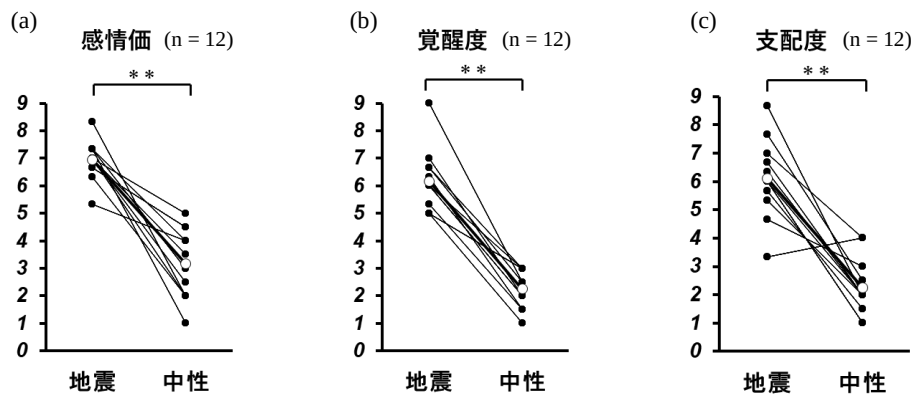

図６　SAM による主観的評価（感情価，覚醒度，支配度）
Fig.6 Subjective Evaluation (Valence, Arousal, Dominance) using SAM
** p < 0.001

3.4　生体指標と主観的評価との関連

地震映像に対する主観的評価（感情価，覚醒度，支配度）を目的変数，地震及び中性映像視聴時の生体指標（CVI/CSI，LI）を説明変数とした多値ロジスティック回帰分析を行った結果を表２に示す．また，回帰分析によって予測した結果の一例（感情価の予測値と実測値の関係）を図７に示す．感情価，覚醒度，支配度の全てを目的変数とした回帰式の適合度について，逸脱度が D = 1.05，p = 1.00，ピアソンの χ^2 が χ^2 = 1.03, p = 1.00，尤度比が C = 0.51, p = 1.00，実測値と予測値の決定係数が R^2 = 0.93 であった．

表２　地震映像に対する主観的評価の多値ロジスティック回帰分析
Table 2 Multiple Logistic Regression Analysis of Subjective Evaluation of Earthquake Video

	説明変数	偏回帰係数	標準誤差	両側確率	オッズ比
覚醒度（ref.感情価）	地震CVI/CSI	-0.20	0.37	0.59	0.82
	地震LI	-0.44	1.21	0.72	0.65
	中性CVI/CSI	0.12	0.22	0.59	1.13
	中性LI	0.33	0.95	0.73	1.38
	切片	0.36	1.49	0.81	
支配度（ref.感情価）	地震CVI/CSI	-0.24	0.37	0.52	0.79
	地震LI	-0.34	1.21	0.78	0.71
	中性CVI/CSI	0.16	0.22	0.47	1.17
	中性LI	0.26	0.96	0.79	1.29
	切片	0.38	1.49	0.80	

ref. 感情価：感情価を基準カテゴリとする．n = 12

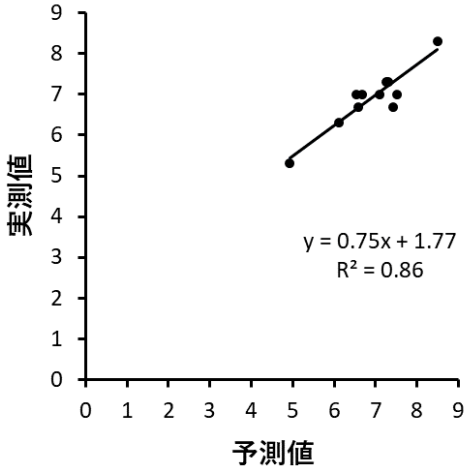

図７　感情価の予測値と実測値の関係
Fig.7 Relationship of Estimated and Actual Values of Valence
図中の回帰式および決定係数（R^2）は，目的変数を感情価とした場合の値．n = 12

3.5　生体指標と不安特性との関連

不安特性（状態不安及び特性不安のパーセンタイル値）を目的変数，地震及び中性映像視聴時の生体指標（CVI/CSI，LI）を説明変数とした多値ロジスティック回帰分析を行った結果を表３に示す．また，回帰分析によって予測した予測値と実測値の関係を図８に示す．状態不安及び特性不安のパーセンタイル値を目的変数とした回帰式の適合度について，逸脱度が D = 96.77, p = 0.00, ピアソンの χ^2 が χ^2 = 84.75, p = 0.00，尤度比が C = 28.35, p = 0.00，実測値と予測値の決定係数が R^2 = 0.91 であった．

表３　不安特性の多値ロジスティック回帰分析
Table 3 Multiple Logistic Regression Analysis of Anxiety Traits

説明変数	偏回帰係数	標準誤差	両側確率	オッズ比
地震CVI/CSI	-1.57	0.34	0.00	0.21
地震LI	-2.27	1.25	0.07	0.10
中性CVI/CSI	0.94	0.24	0.00	2.55
中性LI	1.03	0.85	0.22	2.80
切片	4.81	1.01	0.00	

n = 12

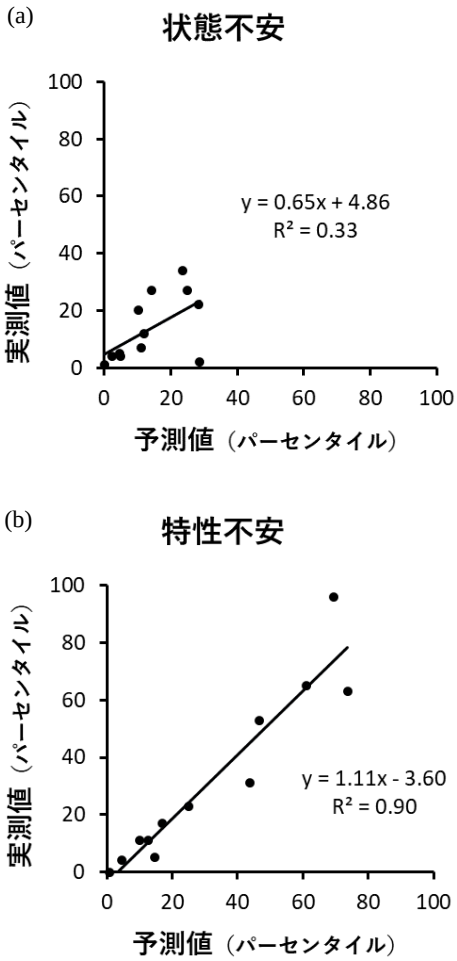

図８　不安特性の予測値と実測値の関係
Fig.8 Relationship of Estimated and Actual Values of Anxiety Traits
図中の回帰式および決定係数（R^2）は，目的変数を(a)状態不安，(b)特性不安とした場合の値．n = 12

3.6　これまでの地震経験に関する質問紙

経験した地震の最大震度は 3 が 1 名，4 が 5 名，5 弱が 3 名，5 強が 1 名，6 弱が 1 名であった．経験した時期は学童・思春期が 6 名で最多であった．場所は自宅の寝室（4 名），居間（3 名）の順に多かった．心情については，驚き（7 名），不安（6 名），緊張・警戒（6 名），恐怖（5 名），動揺・混乱（5 名），心配（5 名）の順に多かった．自身の行動については，丈夫な机やテーブルの下にもぐった（5 名），物が落ちてきそうな場所から離れた（2 名），頑丈なもので頭を守った（2 名）と回答した人がいた一方，驚きや恐怖で身動きできなかった（1 名），特に何もしなかった（3 名）という回答もあった．

直近 3 年間で経験した震度 1～震度 2 の地震については，場所として自宅の居間が 7 名，自宅の寝室が 5 名で全員が自宅で経験していた．心情については，緊張（5 名），驚き（4 名），恐怖（3 名），不安（3 名），心配（3 名）の順に多かった．行動については，特に何もしなかった（8 名），物が落ちてきそうな場所から離れた（3 名）の順に多かった．

4.　考察

本研究の目的は，地震に関する映像視聴時の自律神経活動や脈拍数，脳血流変化量等の生体指標を 2 チャンネル NIRS によって得られたデータに基づいて算出し，中性映像視聴時との比較，及びそれらの生体指標と主観的評価（感情価，覚醒度，支配度）及び不安特性との関連を検討することであった．

まず，地震映像視聴時の方が中性映像視聴時よりも交感神経の活動を示す CSI が有意に低下しており，脈拍数においては，有意差はなかったものの地震条件の方が減少する傾向（d = －0.44，小～中の効果）にあった．先行研究において，不快な聴覚刺激や映像刺激を受けた際は快刺激よりも心拍数が減少するという報告[23],[24]や，差し迫った脅威を感じる恐怖や身体の切断に関連する嫌悪感，急激な悲しみで心拍数が減少するという報告がある[4]．今回の SAM を用いた主観的な評価では地震映像の方が中性映像よりも有意に不快を感じ，覚醒度が高く，支配度が大きいという結果であったことからも，本研究では喚起されたネガティブな情動によって交感神経が低下し，脈拍数も減少傾向となったことが考えられた．

一方，副交感神経指標である CVI では地震条件と中性条件でほとんど差がなかったことに関して，Berntson らは交感神経と副交感神経の活動は非相互的な独立した活動を行う場合があると報告していることや[25]，Kreibig は情動喚起時の自律神経活動に関する文献を調査したレビューにおいて身体の切断に関連する嫌悪感に伴う脈拍数の低下は，副交感神経の影響というより交感神経の離脱によって引き起こされている可能性があると述べている[4]．このことから，本研究の結果もネガティブな情動喚起によって交感神経の独立した低下が生じたものと推測された．

なお，脳血流変化量（Δtotal-Hb(L)，Δtotal-Hb(R)，LI）の指標における地震条件と中性条件の比較では有意差はみられなかった．恐怖の表情を提示した際に右の腹外側前頭前野や補足運動野の oxy-Hb が増加したという Marumo らの報告[26]や，不快な写真提示にて両側の腹外側前頭前野の oxy-Hb が増加したという Hoshi らの報告[11]を支持しなかった．測定部位とした背外側前頭前野は認知制御の関連領域であり，眼窩前頭皮質や背内側前頭前野を介してネガティブな感情を軽減するとされる[27]．また，怒りや軽蔑的な表情，暴力などの脅威となるシーンを見せた際の背側前頭前野の脳活動が大きい人ほど，ネガティブな主観的評価が大幅に低下したことが報告されている[28]．このことから，本研究で提示した情動刺激は背外側前頭前野による制御を必要としない程度の刺激であったことが考えられる．今後はより没入感のある VR（Virtual Reality：仮想現実）映像を用いた臨場感のある地震体験環境を提示することや，模擬的な避難行動などの認知制御を必要とする実験条件下で計測を行うなどの更なる調査が必要である．

次に，生体指標と主観的評価との関連について，生体指標（CVI/CSI，LI）を説明変数とした多値ロジスティック回帰分析により得られた回帰モデルは，実測値と予測値の決定係数（R^2）が 0.93 と高く，感情価，覚醒度，支配度といった主観的評価を自律神経指標や前頭葉脳血流変化量の左右差といった客観的な生体指標で表し得るというデータの基礎的な解釈が得られた．しかし，個々の説明変数の偏回帰係数の有意性は低く，今後対象者数を増やしたうえでの調査が必要である．

生体指標と不安特性との関連について，生体指標（CVI/CSI，LI）を説明変数としたロジスティック回帰分析で得られたモデルにおいても，実測値と予測値の決定係数（R^2）が 0.91 と高く，主観的評価と同様に個人の不安特性を自律神経指標や脳血流変化量の左右差によって表し得るというデータの基礎的な解釈が得られた．さらに，地震映像時と中性映像時の自律神経指標の寄与を示す偏回帰係数で有意性がみられ，自律神経指標の実測値と，回帰式から得られた状態不安と特定不安の予測値では，特定不安に対して極めて高い相関を示した．このことは，状態不安は不安を生じさせる刺激に対して感じる一過性の不安であり，特性不安は個人の安定した不安傾向であること[20]を考慮すると，自律神経指標は個人の元来の不安傾向を規定し得ることが推測された．今後，対象者数を増やすことでこの仮説を検証したいと考える．

最後に，これまでの地震経験に関する質問紙では，震度に関わらず自宅の寝室や居間で地震を経験したと回答した人が半数以上を占めていたことから，次回の研究では自宅内における模擬的な災害体験時の生体反応を捉え

ることも有用と考える．また，同じ災害に被災していても，心的外傷の程度によって情動喚起時の心拍変動や左右の背外側前頭前野の脳血流変化量が異なるという報告もあり[29]，今後は被災時の心情や行動に加えて心的外傷の個人差も含めて調査することが求められる．

Doi らは，情動刺激に対する前頭前野の反応に影響する因子の探索は，情動反応の個人差の原因解明と，病的な精神状態に繋がる危険因子の特定に重要と述べている[30]．また，情動を捉える試みとして，脈拍変動や皮膚温度，会話，身体活動などの客観的な生体認証信号から感情を推定するシステムの開発[31]なども報告されており，今回の結果はこれらの感情推定の試みや個人の情動反応に与える因子の探索の一助となると考える．今後は，上記の課題を踏まえた更なる調査を行い，将来的には緊急時の情動反応をウェアラブル機器を用いて捉え，パニックに陥っている人を冷静な状態に導く支援ツールの開発や，災害時に限らず情動反応の個人差に影響する因子や病的な精神状態に繋がる危険因子の特定などに繋げていきたいと考える．

5. 結論

本研究では，地震及び中性映像を用いた実験を通し，健常若年者を対象に生物学的・主観的な指標を用いて，災害遭遇時の情動反応について検討した．軽量ワイヤレス仕様の 2 チャンネル NIRS で取得したデータに基づく分析から，交感神経指標はネガティブな情動を喚起する地震映像条件下で有意に低下し，両条件の異なる刺激に対する情動反応を捉え得ることが示唆された．一方，脈拍数は地震条件の方が減少傾向であったが有意差はなく，左右背外側前頭前野の脳血流量は条件間で差をみとめなかった．また，情動喚起時の自律神経指標及び脳血流変化量の左右差によって映像に対する主観的感情や個人の元来の不安特性を説明できる可能性が示唆され，地震映像視聴時の生体反応には個人の不安特性が関連することが考えられた．

本研究は少数の対象者による探索的な調査であるため，今後は対象者数を増加させた調査を計画し，さらに VR 技術を用いたより臨場感のある家屋内などの情景提示下での検証が必要である．

利益相反の開示

本論文に関して，報告すべき利益相反関連事項はない．

謝辞

映像作成において京都大学大学院エネルギー科学研究科の石井裕剛准教授，論考において京都大学医学部附属病院医療情報企画部の山本豪志朗准教授，劉暢助教に貴重なご助言を頂き深謝いたします．また，本研究に参加頂きました対象者の方々に御礼申し上げます．本研究は科研費（基盤研究（C），21K00229「実証実験に基づく神経科学と芸術の融合によるバーチャル・アートの創成」）の助成を得たものです．

参考文献

[1] 中村真：大規模災害に伴う感情経験：東日本大震災時に経験した感情の諸側面に関する質問紙調査(1)；宇都宮大学国際学部研究論集，Vol. 36, pp. 125-136 (2013). (Nakamura, M.: Emotional experiences following a large-scale disaster: A questionnaire survey on various aspects of emotions experienced during the Great East Japan Earthquake (1); Research Review, Faculty of International Studies, Utsunomiya University, Vol. 36, pp. 125-136 (2013) (in Japanese)).

[2] Prati, G., Saccinto, E., Pietrantoni, L. and Pérez-Testor, C.: The 2012 Northern Italy Earthquakes: modelling human behavior, Natural hazards (Dordrecht), Vol. 69, No. 1, pp. 99-113(2013).

[3] 北村英哉： 気分状態と情報処理方略（１）－MAGK 仮説をめぐってー，東洋大学社会学部紀要, Vol. 40, No. 3, pp. 61-74(2002). (Kitamura, H.: Mood states and information processing strategies (1) - On the MAGK hypothesis -, Bulletin of the Faculty of Sociology, Toyo University, Vol. 40, No. 3, pp. 61-74(2002) (in Japanese)).

[4] Kreibig, SD.: Autonomic nervous system activity in emotion: a review, Biological Psychology, Vol. 84, No. 3, pp. 394-421(2010).

[5] 松田康宏，小野弓絵：非侵襲生体信号の処理と解析-V, システム／制御／情報, Vol. 62, No. 10, pp. 435-440(2018). (Matsuda, Y. and Ono, Y.: Processing and analysis of non-invasive biological signals-V, Systems/Control/Information, Vol. 62, No. 10, pp. 435-440(2018) (in Japanese)).

[6] 清水公治：非侵襲的脳機能イメージング, 映像情報メディア学会誌, Vol. 64, No. 6, pp. 794-798(2010). (Shimizu, K.: Non-invasive functional brain imaging, Journal of the Institute of Image Information and Television Engineers, Vol. 64, No. 6, pp. 794-798(2010) (in Japanese)).

[7] Shimadzu Corporation：LIGHTNIRS 研究用ポータブル光脳機能イメージング装置，SHIMADZU Excellence in Science（オンライン），入手先 (https://www.an.shimadzu.co.jp/bio/nirs/light_top.htm) (参照 2022-05-06）. (Shimadzu Corporation: LIGHTNIRS Portable Optical Functional Brain Imaging System for Research, SHIMADZU Excellence in Science (online), available from (https://www.an.shimadzu.co.jp/bio/nirs/light_top.htm) (accessed 2022-05-06) (in Japanese)).

[8] NeU：HOT-2000 携帯型脳活動計測装置（オンライン），入手先 (https://neu-brains.co.jp/solution/nirs/hot-2000/) (参照

2022-05-06). (NeU: HOT-2000 Portable Brain Activity Measurement Device (online), available from (https://neu-brains.co.jp/solution/nirs/hot-2000/) (accessed 2022-05-06) (in Japanese)).

[9] DynaSense：近赤外分光法(NIRS)を用いた組織酸素モニタで生体情報の計測 無線データ通信･高機能な携帯型近赤外線組織酸素モニタ装置『PocketNIRS(ポケットニルス)』（オンライン），
入手先 (https://www.dynasense.co.jp/product_hm.html) (参照 2022-05-06). (DynaSense: Tissue oxygen monitoring using near infrared spectroscopy (NIRS) to measure biological information PocketNIRS (Pocket NIRS), a portable near-infrared tissue oxygen monitoring device with wireless data communication and high functionality (online), available from (https://www.dynasense.co.jp/product_hm.html) (accessed 2022-05-06) (in Japanese)).

[10] 藤村優也, 綿貫啓一, 楓和憲, 侯磊, 工藤麻理子, 三宅秀之：動画視聴時のポジティブ・ネガティブ情動の心理尺度に基づく評価と脳活動計測, 日本機械学会論文集, Vol. 82, No. 842, 16-00156(2016). (Fujimura, Y., Watanuki, K., Kaede, K., Hou, L., Kudo, M. and Miyake, H.: Evaluation and brain activity measurement based on psychological scales of positive and negative emotions during video viewing, Proc. of JSME, Vol. 82, No. 842, 16-00156 (2016) (in Japanese)).

[11] Hoshi, Y., Huang, J., Kohri, S., Iguchi Y., Naya M., Okamoto T. and Ono S.: Recognition of Human Emotions from Cerebral Blood Flow Changes in the Frontal Region: A Study with Event-Related Near-Infrared Spectroscopy. Journal of neuroimaging, Vol. 21, No. 2, e94-e101(2011).

[12] Ishikawa, W., Sato, M., Fukuda, Y., Matsumoto, T., Takemura, N. and Sakatani, K.: Correlation between asymmetry of spontaneous oscillation of hemodynamic changes in the prefrontal cortex and anxiety levels: a near-infrared spectroscopy study, Journal of Biomedical Optics, Vol. 19, No. 2, 027005 (2014).

[13] ANNnewsCH：2011 年 3 月 11 日 東日本大震災 仙台空港での地震発生の瞬間～押し寄せる津波【まいにち防災】＊津波映像が含まれています / Great East Japan Earthquake, Tsunami, YouTube（オンライン），
入手先 (https://www.youtube.com/watch?v=mk68bZ701s0) (参照 2022-05-06). (ANNnewsCH: March 11, 2011 Great East Japan Earthquake: Moment of Earthquake at Sendai Airport - Tsunami rushing in [Mainichi Bosai] *Includes tsunami footage / Great East Japan Earthquake, Tsunami, YouTube (online), available from (https://www.youtube.com/watch?v=mk68bZ701s0) (accessed 2022-05-06) (in Japanese)).

[14] NHK：東日本大震災アーカイブス～証言 web ドキュメント～ 3.11 の映像 地震発生直後 14 時 48 分 東京都渋谷区 NHK 放送センター，NHK アーカイブス（オンライン），
入手先 (https://www9.nhk.or.jp/archives/311shogen/summary/area/) (参照 2022-05-06). (NHK: Great East Japan Earthquake Archives - Testimony web document - Video footage of 3.11 Immediately after the earthquake 14:48 NHK Broadcasting Center, Shibuya-ku, Tokyo, NHK Archives (online), Available from (https://www9.nhk.or.jp/archives/311shogen/summary/area/) (accessed 2022-05-06) (in Japanese)).

[15] FNN311：地震発生時 南相馬市 【視聴者提供映像】, YouTube（オンライン），
入手先 (https://www.youtube.com/watch?v=C9n2k2Tnp10) (参照 2022-05-06). (FNN311: At the time of the earthquake, Minamisoma City [viewer-provided video], YouTube (online), available from (https://www.youtube.com/watch?v=C9n2k2Tnp10) (accessed 2022-05-06) (in Japanese)).

[16] Unity Asset Store: Mountain Environment - Dynamic Nature (online), available from (https://assetstore.unity.com/packages/3d/vegetation/mountain-environment-dynamic-nature-191851) (accessed 2022-05-06).

[17] Kiguchi, M. and Funane, T.: Algorithm for removing scalp signals from functional near-infrared spectroscopy signals in real time using multidistance optodes, Journal of biomedical optics, Vol. 19, No. 11, 110505 (2014).

[18] Bradley, M.M. and Lang, P.J.: The International Affective Picture System（IAPS）in the study of emotion and attention, (Coan, J.A. and Allen, J.J.B. ed.), Handbook of Emotion Elicitation and Assessment, New York, Oxford University Press, pp. 29-46(2007).

[19] Toichi, M., Sugiura, T., Murai, T. and Sengoku A.: A new method of assessing cardiac autonomic function and its comparison with spectral analysis and coefficient of variation of R-R interval, Jounal of the Autonomic Nervous System, Vol. 62, No. 1-2, pp. 79-84(1997).

[20] 肥田野直, 福原眞知子, 岩脇三良, 曽我祥子： 新版 STAI マニュアル, 実務教育出版, pp. 35(2017). (Hidano, T., Fukuhara, M., Iwawaki, S. and Soga, S.: New Edition of STAI Manual, Jitsumu Kyoiku Shuppan, pp. 35 (2017) (in Japanese)).

[21] 福井正康：「卒論に最適な」統計・社会システム分析フリーソフト College Analysis Ver.8.4（オンライン），入手先 (https://www.heisei-u.ac.jp/ba/fukui/analysis.html) (参照 2022-05-06).(Fukui, M.: "Ideal for Graduation Thesis," College Analysis Ver. 8.4, a free software for statistical and social system analysis (online), available from (https://www.heisei-u.ac.jp/ba/fukui/analysis.html) (accessed 2022-05-06) (in Japanese)).

[22] 水本篤, 竹内理：研究論文における効果量の報告のために―基礎的概念と注意点―, 関西英語教育学会紀要英語教育研究, pp. 57-66(2008). (Mizumoto, A. and Takeuchi, O.: "For

reporting effect sizes in research papers: Basic concepts and points to note,", Bulletin of the Kansai Society of English Education, Studies in English Education, pp. 57-66 (2008) (in Japanese)).

[23] Bradley, M. M. and Lang, P. J.: Affective reactions to acoustic stimuli, Psychophysiology, Vol. 37, No. 2, pp. 204-215(2000).

[24] Palomba, D., Sarlo, M., Angrilli, A., Mini, A. and Stegagno, L.: Cardiac responses associated with affective processing of unpleasant film stimuli, International journal of psychophysiology, Vol. 36, No. 1, pp. 45-57(2000).

[25] Berntson, G. G., Cacioppo, J. T., Quigley, K. S. and Fabro, V. T.: Autonomic Space and Psychophysiological Response, Psychophysiology, Vol. 31, No. 1, pp. 44-61(1994).

[26] Marumo, K., Takizawa, R., Kawakubo, Y., Onitsuka, T. and Kasai, K.: Gender difference in right lateral prefrontal hemodynamic response while viewing fearful faces: a multi-channel near-infrared spectroscopy study, Neuroscience research, Vol. 63, No. 2, pp. 89-94(2009).

[27] Johnstone, T., Van Reekum, C. M., Urry, H. L., Kalin, N. H. and Davidson, R. J.: Failure to regulate: counterproductive recruitment of top-down prefrontal-subcortical circuitry in major depression, Journal of Neuroscience, Vol. 27, No. 33, pp. 8877-8884(2007).

[28] Goldin, P. R., Manber, T., Hakimi, S., Canli, T. and Gross, J. J.: Neural bases of social anxiety disorder: emotional reactivity and cognitive regulation during social and physical threat, Archives of general psychiatry, Vol. 66, No. 2, pp. 170-180(2009).

[29] Wei, C., Han, J., Zhang, Y., Hannak, W., Dai, Y. and Liu, Z.: Affective emotion increases heart rate variability and activates left dorsolateral prefrontal cortex in post-traumatic growth, Scientific Reports, Vol. 7, No, 1, pp. 16667(2017).

[30] Doi, H., Nishitani, S. and Shinohara K.: NIRS as a tool for assaying emotional function in the prefrontal cortex, Frontiers in Human Neuroscience, Vol. 7, No. 770(2013).

[31] Hayano, J., Tanabiki, T., Iwata, S., Abe, K. and Yuda, E.: Estimation of emotions by wearable biometric sensors under daily activities, 2018 IEEE 7th Global Conference on Consumer Electronics (GCCE), pp. 240-241(2018).

〔2022 年 5 月 9 日受付，8 月 4 日再受付〕

著者紹介

大塚 日花里　（学生会員）

2020 年京都大学医学部人間健康科学科卒業．2022 年京都大学大学院人間健康科学系専攻修士課程修了．現在，同大学博士後期課程在学中．高齢者におけるリモコンの使いやすさの研究，情動喚起時の自律神経指標や脳血流変化量に関する研究に従事．株式会社多聞デイサービス道夢機能訓練指導員(作業療法士)．ヒューマンインタフェース学会学生会員．日本作業療法士協会正会員．修士（人間健康科学）．

岡橋 さやか　（正会員）

2014 年神戸大学大学院システム情報学研究科博士課程修了．2004 年奈良県総合リハビリテーションセンター作業療法士．2011 年名古屋大学医学部助教．2012 年京都大学大学院医学研究科助教．2021 年国立長寿医療研究センター老年社会科学研究部主任研究員，現在に至る．VR を用いたデジタルヘルスケア研究，認知症者と家族介護者に対するアート介入プログラム開発等に従事．ヒューマンインタフェース学会，日本高次脳機能障害学会，日本老年社会科学会会員．博士（学術）．

精山　明敏

1988 年北海道大学大学院理学研究科博士課程修了．愛媛大学医学部医学科（生理学教室）助手，大阪大学医学部医学科（生理学教室）助教授，京都大学医学部人間健康科学科（情報理工医療学講座）教授を経て，現在，国際教養大学特任教授に至る．同大学デザイン創造・データサイエンスセンター　センター長．主に，生体機能の可視化によるヒューマンヘルスサイエンスの研究に従事．日本生理学会学会，医用近赤外線分光法研究会世話人．理学博士．

Acquisition of Research Funds in 2022-2023

Title: Development of shortwave infrared fluorescence molecular imaging for optical diagnostics of human breast cancer

Project/Area Number: 22H03930
Research Category: Grant-in-Aid for Scientific Research (B)
Section: General
Review Section Basic Section: 90110: Biomedical engineering-related
Research Institution: Institute of Physical and Chemical Research
Principal Investigator: Takashi Jin (RIKEN)
Co-Investigator (Kenkyū-buntansha): Akitoshi Seiyama (AIU)
Project Period (FY): 2022-04-01 – 2025-03-31

Title: Creation of "Virtual Art" through the practical fusion experiments of "neuroscience and arts"

Project/Area Number: 21K00229
Research Category: Grant-in-Aid for Scientific Research (C)
Section: General
Review Section Basic Section: 01070: Theory of art practice-related
Research Institution: AIU
Principal Investigator: Akitoshi Seiyama
Co-Investigator (Kenkyū-buntansha): Sayaka Okahashi (NIGG)
Project Period (FY): 2021-04-01 – 2024-03-31

Editor's Postscript

As described in the preface, the Creative Design, and Data Science Center (CreDDS Center) at AIU was established on April 1, 2022 as the newest one of three centers of Akita International University (AIU). This center is new challenge for AIU, because AIU is a famous university as a liberal arts university and for education of foreign language since its establishment in 2004.

Through scientific research, the CreDDS Center will have a synergistic and mutually supportive relationship with other two centers, the Active Learning Center (ALC) and the Center for Collaborative Research and Outreach (CCRO).

Thereby, the CreDDS Center provides the impetus for the transformations anticipated under Institute of Applied International Liberal Arts (AILA) for contribution to Akita Prefecture and world-wide through industry-government-academia collaboration.

March 31, 2023

Director of CreDDS Center
Akitoshi SEIYAMA

The FY2022 CreDDS Center logo shown on the cover *is an image of an elm tree, a popular and long-lived tree in Northern Japan. Because the research papers published in 2022 were mainly related to human brain function, the Editor selected an MRI image from his brain images that resembles an elm tree in the hope that our CreDDS Center will continue to grow like an elm.*

付記：令和4年度の研究実績として載せております論文は、出版社の了承を得て原文を載せています。また、下記のdoiもしくはWebサイトから論文は無料でダウンロードが可能です。

1. Okahashi S, Sakamoto K, Hashiya F, Kumasaka K, Yamaguchi T, Seiyama A, Utsumi J. Development of an Electric Pegboard (e-Peg) for Hand Dexterity Improvement and Cognitive Rehabilitation: A Preliminary Study.

   Advanced Biomedical Engineering Vol. 12 (2023) p. 81-90.

   DOI https://doi.org/10.14326/abe.12.81

   https://www.jstage.jst.go.jp/article/abe/12/0/12_12_81/_article/-char/en

2. Yoshida M, Seiyama A. Importance of two-dimensional gaze analyses in the assessment of reading performance in patients with retinitis pigmentosa.

   PLoS One. 2022 Dec 14;17(12): e0278682. doi: 10.1371/journal.pone.0278682. eCollection 2022.

   https://journals.plos.org/plosone/article?id=10.1371/journal.pone.0278682

3. Seiyama A, Miura T, Sasaki Y, Okahashi S, Konishi N, Cassim M. Characterization of forehead blood flow bias on NIRS signals during neural activation with a verbal fluency task.

   Neuroscience Research. 2023 Jan 186:43-50.

   doi: 10.1016/j.neures.2022.09.012. Epub 2022 Sep 30.

   https://www.sciencedirect.com/science/article/pii/S0168010222002577?via%3Dihub

4. 大塚日花里, 岡橋さやか, 精山明敏. 地震映像視聴時の携帯型NIRSを用いた情動研究

   ヒューマンインタフェース学会論文誌.2022 年24巻4号 239-248

   doi: https://doi.org/10.11184/his.24.4_239

   https://www.jstage.jst.go.jp/article/his/24/4/24_239/_article/-char/ja

Creative Design and Data Science Center
Akita International University
Yuwa, Akita-city, 010-1292 Japan
TEL: +81-18-886-5884
FAX: +81-18-886-5910
Website: https://web.aiu.ac.jp